HETEROGENEOUS - HOMOGENEOUS EFFECTS IN CHEMICAL REACTORS

by

Andrew John Bird

June, 1977

A thesis submitted for the degree of
Doctor of Philosophy of the
University of London and for the
Diploma of Imperial College

Department of Chemical Engineering and Chemical Technology
Imperial College, London. SW7

Heterogeneous-Homogeneous effects in chemical reactors

by

Andrew John Bird

June, 1977

ERRATA

PAGE

24 Replace Eqn (2.5b) by: $$\frac{\mathcal{D}_{zGs}}{\rho}\left.\frac{dg_{fi}}{dz}\right|_{\ell=0} = g_o - g_{fi}$$

98 Replace Eqn (1) by: $$\nabla^2 X_s - \frac{\alpha_s X_s}{\lambda_s} e^{-\gamma_s/Y_s} = 0$$

99 In $F(Y_s) = \ldots$: replace $(\frac{q}{\lambda s})$ by $\sqrt{\frac{q}{\lambda s}}$

120 Fig 6.14 : Correct captions,

Curve (b) λs : 0.01

Curve (c) λs : 0.1

125 Line 13 : Spelling of 'behaviour'

137 Line 16 : Replace Keq by $\frac{A_x}{A_y}$

137 Line 19 : Replace k_y by A_y

ABSTRACT

Effects associated with the presence of gas phase reactions in catalytic packed bed reactors are described. Non-uniqueness of solutions and changes in steady state performance are considered in some depth. A literature review revealed the uncertainty associated with the available heat transfer correlations. Due to parametric complexity steady state behaviour is elucidated using a generalized analysis and four case studies, from which heuristic criteria for the importance of gas phase reactions are proposed.

Under practical operating conditions, a one phase reactor model is adequate for design purposes because film transport resistances are negligible. An initially neglectable reaction, either heterogeneous or homogeneous, only gains prominence if its thermal parameters and those of the main catalytic reaction are very disparate, behaviour more typical of a gas phase rather than a catalytic reaction. Although the case studies did not fulfil the proposed criteria, the oxidation of higher alcohols and hydrocarbons may well exhibit the necessary properties. The modelling of the oxidative dehydrogenation of butene confirmed previous kinetic results and indicated that catalyst preparation temperature was an important variable. The presence of a fluid phase reaction can extend the parameter range for non-uniqueness of solutions and introduces effects specific to a two phase situation.

CONTENTS

Page

Appendices

LIST OF TABLES

LIST OF FIGURES

ACKNOWLEDGEMENTS

I would like to thank the following individuals and organizations

- Dr. J.J. Noble and Professor D.L. Trimm (now of the University of Trondheim, Norway), for their supervision of this project.

- My laboratory and departmental colleagues, for their friendship.

- The Science Research Council and the Safety in Mines Research Establishment (Department of Energy), for financial assistance.

- Helen, for her support and understanding.

NOMENCLATURE

A	Coolant group (-)
Ap	pellet surface area (m^2)
a_v	Specific pellet surface area (m^{-1})
C	Constant
Ci	Concentration of species i ($kmol.m^{-3}$)
Cp	Specific heat ($W\ kg^{-1}K^{-1}$)
$\mathcal{D}$	Diffusivity (m^2s^{-1})
Da	Damkohler number (-)
Dt	Tube diameter (m)
dp	Pellet diameter (m)
d_p'	Equivalent sphere diameter ($\frac{6Vp}{Ap}$) (m)
E	Activation energy ($kcal.mol^{-1}$)
g	Weight fraction (-)
Gs	Superficial mass velocity ($kg\ m^{-2}s^{-1}$)
hp	Contact resistance ($W\ m^{-2}K^{-1}$)
h	Film heat transfer coefficient ($W\ m^{-2}K^{-1}$)
H	Film heat transport group (-)
$(-\Delta H)$	Heat of reaction ($J\ kg^{-1}$)
kf	Gas phase thermal conductivity ($W\ m^{-1}s^{-1}$)
kg	Film mass transfer coefficient (m^2s^{-1})
ko	Arrhenius constant
ks	Solid phase thermal conductivity ($W\ m^{-1}s^{-1}$)
K	Film mass transport group (-)
Ka	Biochemical constant ($mol\ \ell^{-1}$)
K_{eff}	Effective pellet thermal conductivity ($W\ m^{-1}K^{-1}$)
Ks	Biochemical constant ($mol\ \ell^{-1}$)
ℓ	Axial distance (m)
L	Reactor length (m)
Ls	Thermal capacity ratio (-)

$\bar{n}$	Unit normal vector
Nu	Nusselt number (-)
p	Emissivity (-)
Pe	Peclet number ($Gsdp/\mathcal{D}_{eff}$) (-)
Pr	Prandtl number (-)
Prm	Radial mass transport group (-)
Prt	Radial heat transport group (-)
r	Radial distance (m)
R	Gas constant (cal $mol^{-1}K^{-1}$)
	Dimensionless radial distance (-)
R(X,Y)	Rate group
Re	Reynolds number (-)
Re_e	Effective Reynolds number for annulus (-)
Rep	Pellet Reynolds number (-)
Re'_p	Pellet Reynolds number based on dp' (-)
Rp	Pellet radius (m)
Rt	Tube radius (m)
S	Specific reactor interphase transfer area (m^{-1})
Sc	Schmidt number (-)
So	Specific reactor coolant surface area (m^{-1})
T	Temperature (K)
U	Overall heat transfer coefficient (W $m^{-2}K^{-1}$)
v	Volume flow rate (m^3s^{-1})
V	System volume (m^3)
Vp	Pellet volume (m^3)
W	Wash out rate (-)
X	Dimensionless reactant concentration or weight fraction (-)
Y	Dimensionless temperature (-)
z	Dimensionless axial distance (-)
Z	Dimensionless product concentration (-)

Greek Symbols

α	Dimensionless pre-exponential factor (-)
	Pellet hollowing (-)
αrs, αrv	Coefficients used in effective radial conductivity calculations
αw	Wall heat transfer coefficient
β	Dimensionless adiabatic temperature rise
	Pellet length to radius ratio (-)
β_v	Parameter in conductivity equation
γ	Dimensionless activation energy (-)
	Parameter in conductivity equation (-)
ε	Voidage (-)
η	Effectiveness factor (-)
λr	Effective radial thermal conductivity ($W\ m^{-1}K^{-1}$)
λz	Effective axial thermal conductivity ($W\ m^{-1}K^{-1}$)
λs	Dimensionless diffusion group (-)
μ	Dynamic viscosity ($kg\ m^{-1}s^{-1}$)
ρ	Density ($kg\ m^{-3}$)
σ	Stefan-Boltzman constant ($W\ m^{-2}K^{-4}$)
τ	Dimensionless time (-)
ϕ	Parameter in conductivity equation (-)

Subscripts

c	Continuum
eff	Effective
f	Fluid
i	Species i
o	Inlet
r	Radial
s	Solid

t Temperature

z Axial

Superscripts

o Static term

* Steady state

CHAPTER ONE

INTRODUCTION

1. INTRODUCTION

This thesis aims to clarify, elucidate and to some extent quantify the effects that the introduction of a gas phase reaction can have on the behaviour and design of catalytic reactor systems. Motivation for this study comes from reports of gas phase reactions, induced by catalytic products, occurring in the riser space after monolithic combustors (Enga, 1976) and short catalytic beds (Keulks et al., 1972). If such reactions also occur in the bed voids they may restrict the range of design alternatives, complicate the computational procedure or modify the reactor's behaviour.

Clearly, in these circumstances there is a considerable incentive to establish the conditions under which these effects may be exhibited so that such complexity can be avoided. As a first step, the possible effects have been described and defined before proceeding to a detailed consideration of steady state and non-uniqueness phenomena and the conditions under which these occur.

The previous work concerning reactions in the gas and catalyst phases of a reactor is meagre, although catalytic reactor modelling is a well documented area. Holton (1975) developed a set of reactor models for two example heterogeneous-homogeneous systems but did not demonstrate the presence of any homogeneous phenomena or generalize the results. Similarly, the study of systems which exhibit more than one steady state solution (i.e. non-uniqueness or multiplicity phenomena) is a well developed research area but complex reaction schemes and two phase systems, as discussed here, have received little attention.

1.1 Definition of a homogeneous effect

A gas phase reaction may modify the reaction scheme in two ways:

(a) Converting the reactant to another product in parallel with the catalytic reaction (concurrent interaction).

(b) Converting the product of the catalytic reaction to undesired materials (consecutive interaction).

Both types of interaction are exhibited by butene and propene partial oxidation schemes (see Chapter 5).

Such an interaction will be important if either

(a) It seriously complicates or restricts design and optimization of the process. The introduction of an extra kinetic term, and

further balance equations, adds to the numerical complexity of the design problem and may also modify the system's allowable operational range. Or,

(b) It has a greater influence on the progress of the reaction or reactor behaviour than would be suggested by its rate under initial conditions. This could be caused by some novel coupling between the reactions, very different thermal behaviour relative to the catalytic reaction or the induction of multiplicity phenomena. In this way a superficially minor reaction, which might be neglected, may have a profound effect on reactor performance.

The choice of operating conditions available to the reactor designer may be restricted by the presence of a gas phase reaction in the following ways:

a) Limitations placed on the range of physical parameters (e.g. pellet geometry or pellet hollowing) by the need to control the extent of the gas phase reaction.
b) The need to consider residence time variations because of the introduction of a product degradation reaction.
c) Limitations on reactant conversion or operating temperatures caused by the need to avoid conditions under which non-uniqueness could occur.

During the operation of a reactor an initially undetected gas phase reaction could cause:

a) Catalyst deactivation due to an excessive temperature rise. This is most likely to occur when the partial oxidation of a high molecular weight hydrocarbon is being attempted. Over oxidation of reactant or product can then lead to excessive heat release.
b) Changes in reactant conversion and the formation of undesired products. The presence of such by-products may have important implications for the operation of downstream separation operations.
c) Difficulties in process control and start-up because of non-uniqueness of reactor profiles.

This brief description and definition of the possible effects provides the background for the results of the steady state and multiplicity investigations presented here. These studies concentrate on quantifying the system parameter ranges associated with the different

phenomena, so that the above complexities may be avoided.

1.2 Types of coupling

Of the three possible locations, in a catalytic reactor where a gas phase reaction can occur, i.e. the reactor voids, catalyst pores and the riser space, only reactions in the voids will be considered in detail. Clearly, reactions in the riser space do not introduce a coupling phenomena and can be handled by conventional methods. Simple collision theory arguments show that the high surface area to volume ratio of the intrapellet voids precludes the development of a gas phase reaction in this location.

When two reactions are occurring in different phases in contact transfer of heat or mass between the phases can significantly affect the results and complicate the mathematical treatment. This coupling can take the following forms:

1) Thermal: Heat release caused by the catalytic reaction leads to ignition of the homogeneous reaction and further rapid heat release which gives rise to severe thermal gradients.
2) Molecular species: The product or reactant of the catalytic reaction is decomposed homogeneously lowering the selectivity and causing further heat release.
3) Free radical species: A catalytic adsorbed intermediate is released into the gas phase where it initiates a free radical chain reaction. This behaviour is best documented for the case of catalytic oxidation of propene to acrolein. An allyl peroxide, formed on the catalyst surface, desorbs and induces gas phase over-oxidation (Keulks et al., 1973).
4) Complex: For example; carbon, formed in the gas phase, causing catalyst deactivation (La Cava, 1977).

It is apparent that coupling schemes of types (3) and (4) are the more subtle and likely to produce the more pronounced effects. Unfortunately, no quantitative data for these sytems is available even if generalized modelling techniques could be developed.

1.3 Possible reaction schemes

Reaction networks can be divided into consecutive and concurrent pathways which enables the behaviour of the system to be analysed in terms of the elementary steps. In this study examples of both simple types will be considered together with a more complex combined structure.

The four detailed reaction schemes considered in Chapters 4 and 5 are:

a) Nitrous oxide oxidation.
b) Methanol partial oxidation to formaldehyde.
c) Carbon monoxide oxidation.
d) Butene oxidative dehydrogenation to butadiene.

These are the only systems where sufficiently detailed information on the kinetics of the reactions in both phases appears to be available. Propene partial oxidation is potentially a most interesting system for study (see Section 1.2) but only catalytic kinetics are available in the open literature (Cartlidge et al., 1975).

The behaviour of these examples is indicative of the phenomena which could be expected for the oxidation of more complex aldehydes and hydrocarbons, for which only qualitative data is available (Shtern, 1964).

1.4 Outline of thesis

The remainder of the thesis can be divided into two parts dealing with steady state effects and multiplicity phenomena.

Steady state effects are discussed in Chapters two to five. Various reactor models are developed in Chapter two while heat transfer and kinetic parameter evaluation is discussed in Chapter three. These building blocks are then utilized to study three specific examples and generate some more general results regarding the phenomena. Finally, a more detailed study of butene oxidative dehydrogenation is presented in Chapter five.

In Chapter six the influence of gas phase reactions on the multiplicity phenomena occurring in a catalytic reactor is discussed. Quantitative results were obtained using a model embracing a single pellet and its immediate fluid environment.

CHAPTER TWO

REACTOR MODELLING I : MODEL DEVELOPMENT

2. REACTOR MODELLING I - MODEL DEVELOPMENT

The heat and mass transfer phenomena occurring in packed bed chemical reactors are complex and models including all these phenomena would be computationally intractable. In this chapter a set of simplified models is developed to enable the different phenomena to be considered in a convenient fashion. As the complexity of a model increases the number of parameters and consequently the uncertainty associated with the results rises.

2.1 Consideration of reactor model

The mixing and transfer phenomena occurring in a packed bed may be classified as:

1. Axial heat and mass transport caused by backmixing in the fluid phase.
2. Axial solid phase heat transfer.
3. Radial heat and mass transport in the fluid phase.
4. Radial solid phase heat transfer.
5. Fluid-wall and solid-wall heat transfer.
6. Film heat and mass transfer resistances around the solid particles.
7. Intra pellet heat and mass transfer resistances.

Some of these phenomena have been shown to be of negligible importance under most conditions. For those that remain a mathematical description has been formulated in the light of experimental evidence.

It has been well established experimentally and theoretically (Corrie, 1972; Carberry, 1976) that catalyst pellets can be considered as essentially isothermal, with the major resistance to heat transfer residing in the fluid film around the pellet.

Radial mass transfer, caused by fluid mixing in the bed voids, has been successfully described by a dispersion model. Solid and fluid phase radial temperature profiles have been shown to be parabolic over most of the reactor diameter, with a steep drop in temperature within about one pellet diameter of the wall (De Wasch and Froment, 1972). Such a profile is also conveniently described by a dispersion equation together with a resistance lumped at the wall. Axial fluid phase heat and mass transfer caused by fluid backmixing have been similarly correlated by a dispersion equation. Solid phase axial heat transport has

been shown to be important for highly exothermic reactions under transient conditions (Elanashie, 1975; Rhee et al., 1974) or in reactors where heat is lost axially by radiation (Eigenburger, 1972). Since only steady state simulations for axially adiabatic reactors are performed in this study this phenomena is not further considered.

Assimilating these simplifications and the assumptions listed below enables a mathematical model to be formulated (Refer to nomenclature list for symbols and their meaning).

Assumptions:

1. Cylindrical symmetry.
2. Axially constant wall temperature.
3. Negligible pressure drop across the bed.
4. Physical and heat transfer properties are constant throughout the bed.
5. Mass flowrate is radially uniform.

Mass balance on component i:

(a) Fluid phase:

$$Gs \frac{\partial g_{fi}}{\partial \ell} = \frac{\mathcal{D}_r}{r} \cdot \rho_f \frac{\partial}{\partial r} \left(r \frac{\partial g_{fi}}{\partial r}\right) + \mathcal{D}_z \cdot \rho_f \frac{\partial^2 g_{fi}}{\partial \ell^2}$$

$$+ kg.a_v (g_{si} - g_{fi}) + R_f(g_{fi}, T_f) \qquad (2.1)$$

(b) Solid phase:

$$kg.a_v (g_{si} - g_{fi}) = R_s (g_{si}, T_s) \qquad (2.2)$$

Energy balance:

(a) Fluid phase:

$$GsCp \frac{\partial T_f}{\partial \ell} = \frac{\lambda r_f}{r} \frac{\partial}{\partial r} \left(r \frac{\partial T_f}{\partial r}\right) + \lambda z_f \frac{\partial^2 T_f}{\partial \ell^2}$$

$$+ h.a_v (T_s - T_f) + R_{tf} (T_f, g_{fi}) \qquad (2.3)$$

(b) Solid phase:

$$h.a_v (T_s - T_f) = \frac{\lambda r_s}{r} \frac{\partial}{\partial r} \left(r \frac{\partial T_s}{\partial r}\right) + R_{ts} (T_s, g_{si}) \qquad (2.4)$$

where R_f and R_s are the rate of species depletion per unit volume of bed for the two phases. Similarly R_{ts} and R_{tf} are the rate of heat release per unit volume of bed for each phase. Evaluation of R_s and R_{ts} would generally involve the use of effectiveness factors.

The boundary conditions for these equations are

1) Mass balance (for all i)

(2.5a) $\quad 0 \leq \ell \leq L \qquad \left.\frac{\partial g_{fi}}{\partial r}\right|_{r=0} = \left.\frac{\partial g_{fi}}{\partial r}\right|_{r=Rt} = 0$

(2.5b) $\quad 0 \leq r \leq R_t \qquad \left.\frac{\partial g_{fi}}{\partial \ell}\right|_{\ell=L} = 0$

$$D_z \cdot \left.\frac{\partial g_{fi}}{\partial \ell}\right|_{\ell=0} = g_o - g_{fi}$$

2) Energy balance

(2.6a) $\quad 0 \leq \ell \leq L \; : \; \left.\frac{\partial T_f}{\partial r}\right|_{r=0} = 0$

$$-\lambda r_f \cdot \left.\frac{\partial T_f}{\partial r}\right|_{r=Rt} = \alpha w_f (T_f - T_w)$$

(2.6b) $\quad 0 \leq r \leq Rt \; : \; \left.\frac{\partial T_f}{\partial \ell}\right|_{\ell=L} = 0$

$$\lambda z_f \cdot \left.\frac{\partial T_f}{\partial \ell}\right|_{\ell=0} = T_o - T_f$$

(2.6c) $\quad 0 \leq \ell \leq L \; : \; \left.\frac{\partial T_s}{\partial r}\right|_{r=0} = 0$

$$\lambda r_s \cdot \left.\frac{\partial T_s}{\partial r}\right|_{r=Rt} = \alpha w_s \, (T_s - T_w)$$

These equations can be cast into dimensionless form using the nomenclature of Table 2.1 with the dimensionless variables $Z = \ell/L$,

Table 2.1 - Parameters of generalized model

Parameter	Definition	Description
γ_s	E_s/RT_o	Activation energies
γ_f	E_f/RT_o	
β_s	$(-\Delta H)_s g_o/CpT_o$	Adiabatic temperature
β_f	$(-\Delta H)_f g_o/CpT_o$	
Da_s	$ko_s.(g_o\rho_f)^{n-1}L/Gs$	Damkohler numbers
Da_f	$ko_f.(g_o\rho_f)^{m-1}L/Gs$	
H	$h.a_v L/CpGs$	Interphase heat and mass transfer groups
K	$kg.a_v L/Gs$	
Prt_s	$GsCpRt^2/\lambda r_s.L$	Radial heat transfer groups
Prt_f	$GsCpRt^2/\lambda r_f.L$	
Prm	$Pe_r.(\frac{Rt}{L})\ (\frac{Rt}{dp})$	Radial fluid mixing group
Pzm	$Pe_z.(\frac{L}{dp})$	Axial fluid mixing group
Pzt	$L\ GsCp/\lambda z_f$	Axial heat dispersion group
Nu_s	$\alpha w_s.Rt/\lambda r_s$	Wall heat transfer groups
Nu_f	$\alpha w_f.Rt/\lambda r_f$	

$R = r/Rt$, $Y = T/T_o$ and $X = g/g_o$,

whence:

$$\frac{\partial X_{fi}}{\partial Z} = \frac{1}{Prm} \cdot \frac{\partial}{\partial R}\left(R \frac{\partial X_{fi}}{\partial R}\right) + \frac{1}{Pzm} \frac{\partial^2 X_{fi}}{\partial Z^2}$$

$$+ K(X_{si} - X_{fi}) + R_f(X_{fi}, Y_f) \qquad (2.1')$$

$$K(X_{si} - X_{fi}) = R_s(X_{si}, Y_s) \qquad (2.2')$$

$$\frac{\partial Y_f}{\partial Z} = \frac{1}{Prt_f} \frac{\partial}{\partial R}\left(R \frac{\partial Y_f}{\partial R}\right) + \frac{1}{Pzt} \frac{\partial^2 Y_f}{\partial Z^2}$$

$$+ H(Y_s - Y_f) + R_{tf}(X_{fi}, Y_f) \qquad (2.3')$$

$$H(Y_s - Y_f) = \frac{1}{Prt_s} \frac{\partial}{\partial R}\left(R \frac{\partial Y_s}{\partial R}\right) + R_{ts}(X_{si}, Y_s) \qquad (2.4')$$

where $R_f = Da_f . \exp(-\gamma_f/Y_f) . X_{fi}^{n}$

$R_{ts} = \beta_s . Da_s . \exp(-\gamma_s/Y_s) . X_{si}^{m} . \eta$

and $\eta = f(\mathcal{D}_{eff}, dp, Y_s, X_{si})$

With boundary conditions:

(2.5'a) $0 \leq Z \leq 1 : \left.\frac{\partial X_{fi}}{\partial R}\right|_{R=0} = \left.\frac{\partial X_{fi}}{\partial R}\right|_{R=1} = 0$

(2.5'b) $0 \leq R \leq 1 : \left.\frac{\partial X_{fi}}{\partial Z}\right|_{Z=1} = 0$

$$Pzm . \left.\frac{\partial X_{fi}}{\partial Z}\right|_{Z=0} = 1 - X_{fi}$$

(2.6'a) $0 \leq Z \leq 1 :$ $\left.\frac{\partial Y_f}{\partial R}\right|_{R=0} = 0$

$$-\left.\frac{\partial Y_f}{\partial R}\right|_{R=1} = Nu_f\ (Y_f - Y_w)$$

(2.6'b) $0 \leq R \leq 1 :$ $\left.\frac{\partial Y_f}{\partial Z}\right|_{Z=1} = 0$

$$Pzt \cdot \left.\frac{\partial Y_f}{\partial Z}\right|_{Z=0} = 1 - Y_f$$

(2.6'c) $0 \leq Z \leq 1 :$ $\left.\frac{\partial Y_s}{\partial R}\right|_{R=0} = 0$

$$-\left.\frac{\partial Y_s}{\partial R}\right|_{R=1} = Nu_s\ (Y_s - Y_w)$$

This full model is difficult to handle numerically and a more pragmatic approach has been adopted. A number of other models can be generated from this general structure which are easier to manipulate. In this way a matrix of simpler models can be obtained which enable the various transport phenomena to be investigated.

2.2 Simplified models

Mears (1976), Young and Finlayson (1971) and Carberry and Wendel (1963) have all suggested design criteria to help in deciding whether axial dispersion is important. Froment (1972) has, however, suggested that for all practical reactor designs the peclet group is at least an order of magnitude greater than the values associated with axial transport effects. Incorporating this simplification and neglecting film mass transfer in comparison to intrapellet diffusional resistances (Carberry, 1976) yields the most complex model considered in this study, a two-dimensional-two phase plug flow (2D2P) model. McGuire and Lapidus (1965), McGreavy and Cresswell (1969) and De Wasch and Froment (1971) have utilised a similar formulation but with a variety of radial boundary conditions. For $H \to \infty$ $Y_s = Y_f$ and thus equations (2.3') and (2.4') can be combined to give a one phase model, which has been the subject of considerable study (e.g. in standard texts by Smith (1970)

Table 2.2 - Relationship between Models

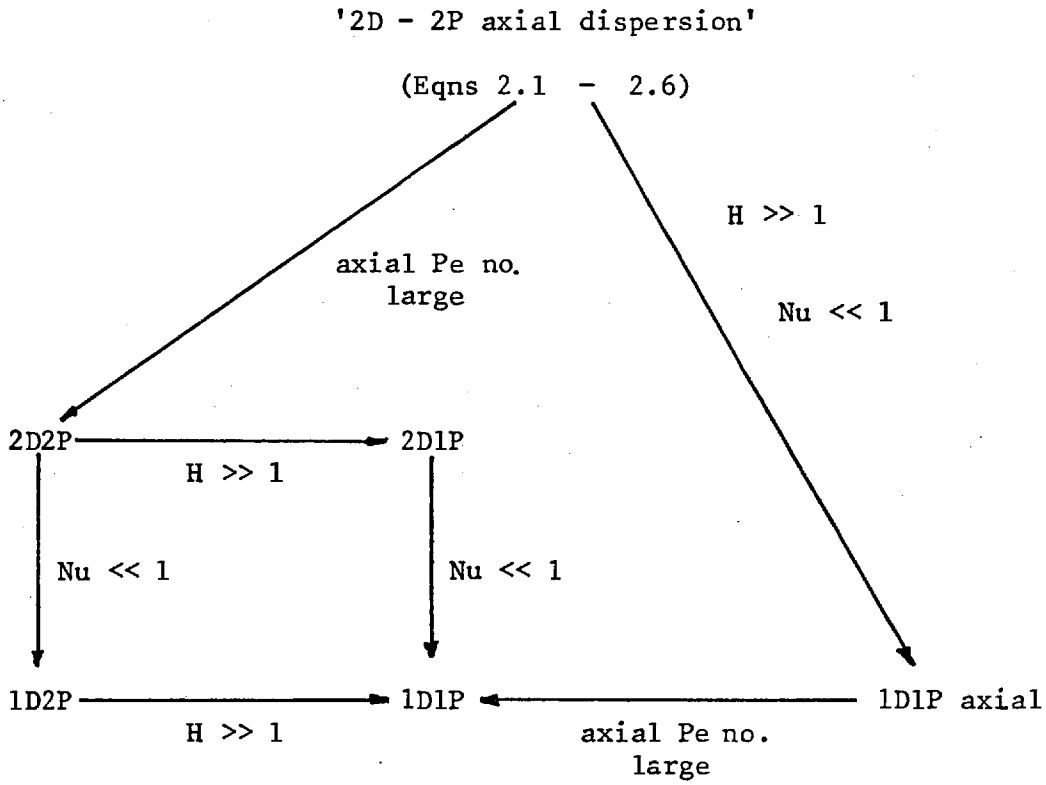

and Aris (1965)).

Alternatively, the radial profile may be approximated by a parabola (Beek, 1962) and an overall transport coefficient utilised to reduce the model to one dimension. This approximation is rigorously correct when Nu is small but the model is often applied under other conditions using a relationship of the form

$$\frac{Prt_s}{A_s} = \frac{1}{Nu_s} + \frac{1}{4}$$

This generates three one dimensional models:

(a) one dimension-one phase ($H \to \infty$), plug flow

(b) one dimension-two phase, plug flow

(c) one dimension-one phase with axial dispersion. This model has been utilized to study the effect of axial dispersion on the selectivity of consecutive reaction schemes.

The two dimensional-two phase plug flow model, developed above, constitutes a set of coupled parabolic partial differential equations. Holton (1975) applied finite difference methods to the solution of this problem. In this study orthogonal collocation techniques have been applied to the solution of this set of equations and the one phase axial dispersion model (a brief description of the technique is given in Appendix 1). This method was chosen because of its lower computational requirements (Finlayson, 1974).

CHAPTER THREE

REACTOR MODELLING II : NECESSARY INFORMATION

3. REACTOR MODELLING II : NECESSARY INFORMATION

This chapter contains a discussion of two of the building blocks necessary for the implementation of the models developed in Chapter two. In view of the parametric sensitivity of the models demonstrated by Holton (1975) a literature review of heat transfer correlations for packed beds has been undertaken and deficiencies in the available data are discussed. In the light of these, some recommendations for further work are proposed. A short section is devoted to the problems of predicting gas phase kinetics in the packed bed environment.

3.1 Heat and mass transfer correlations

Table 3.1 contains a summary of the parameters necessary for the solution of the family of models developed in Chapter two. Excessive over or under design can occur if the parameter estimates are only a few per cent in error (Holton, 1975) (see Table 3.2).

Most modelling studies have utilized the single homogeneous phase approximation and the majority of heat transfer experiments have been similarly interpreted. As it has become necessary and numerically tractable to consider a two phase model some methodology for dividing these continuous phase parameters has been needed. The literature abounds with correlations based on relatively few experimental studies.

3.1.1 Effective radial conductivities

The mechanism of radial heat transfer is complex and a number of processes interact. The 'effective homogeneous phase conductivity' thus includes convective, conductive and radiative contributions. Argo and Smith (1953) associated those processes related in series with the solid phase while those occurring in parallel were associated with the fluid phase. Yagii and Kunii (1957) preferred to divide the effects between static and convective contributions, the latter being correlated using a Reynolds group (see Table 3.3).

De Wasch and Froment (1971), utilizing both these structure models, have obtained expressions for the effective conductivity of each phase which include a contact resistance term, caused by stagnant gas films around the solid contact points. This resistance has a clear physical significance but the available predictive equation (Smith, 1970) correlates the difference between some early experimental results and the

Table 3.1 - Heat and Mass Transfer Parameters

Model	Parameter	
Two dimensional-two phase	a) Wall transfer coefficients	- αw_s
		- αw_f
	b) Radial conductivities	- λr_s
		- λr_f
	c) Radial Peclet group	- Pe_r
	d) Film transfer coefficient	- h
Two dimensional-one phase	a) Wall transfer coefficient	- αw_c
	b) Radial conductivity	- λr_c
	c) Radial peclet group	- Pe_r
One dimensional-one phase Axial dispersion model only	a) Overall heat transfer coefficient	- U
	b) Axial dispersion Pe group	- Pe_z
One dimensional-two phase	a) Overall heat transfer coefficient	- U
	b) Film transfer coefficient	- h

Table 3.2 - Sensitivity of model predictions to parameter values

The changes below correspond to a variation of ± 15% in the parameter and were obtained for a two phase-two dimensional model (Holton, 1975)

Parameter	Effect (%)
h	< 10%
αw_s	< 10%
αw_f	up to 140%
λr_f or λr_s	up to 80%

Table 3.3 - Effective conductivity models

1) De Wasch and Froment, 1971

$$\Lambda r_s = \frac{\beta_v(1-\varepsilon)}{\frac{\gamma}{ks} + \frac{1}{kf/\phi + hp.dp + \alpha rsdp}}$$

$$\Lambda r_f = \varepsilon(kf + \beta_v dp.\alpha rv + \rho_f Cp \mathcal{D}_r)$$

2) Yagii and Kunii, 1957

$$\Lambda r_c = \Lambda r_c^{\,o} + C.RePr$$

$$\Lambda r_c^{\,o} = \frac{\beta_v(1-\varepsilon)}{\frac{\gamma}{ks} + \frac{1}{kf/\phi + dp.\alpha rs}} + \frac{\varepsilon\beta_v.dp.\alpha rv}{kf}$$

where for 1) and 2) $\alpha rs = \sigma\left|\frac{p}{2-p}\right| T^3$

$$\alpha rv = \frac{\sigma T^3}{(1 + \frac{\varepsilon}{2(1-\varepsilon)} \frac{1-p}{p})}$$

3) Argo and Smith, (Smith, 1973)

$$\Lambda r_s = \frac{(1-\varepsilon)\ h'.dp.ks}{2ks + h'dp}$$

where h' is total 'parallel' contributions

$$\Lambda r_f = \varepsilon(kf + \frac{4p\sigma}{2-p} dpT^3 + \frac{CpGsdp}{Pe_r})$$

Table 3.4 - De Wasch and Froment's conductivity model - Parameter values

Parameter	Comment	Value
ϕ	= Fluid film thickness/pellet diameter, related to pellet roughness	
	For catalyst materials (De Wasch and Froment, 1971)	0.0050
γ	= Length of solid path/pellet diameter, related to pellet hollowing	$= 1 - \alpha$
β_v	= Effective void size/pellet diameter	
	Yagii and Kunii (1957) — Solid materials	1.0
	Yagii and Kunii (1957) — hollowed pellets	0.72
hp	Contact resistance	
	Smith, 1970; De Wasch and Froment, 1971	23.2 $W\ m^{-2}k^{-1}$

Schulmann and Voss (1934) equation. It thus includes experimental error and radiation contributions. Fortunately, back calculation using either of the above models with De Wasch and Froment's (1971) data shows that the inclusion of the parameter has little effect on the final result. The contact resistance is also largely independent of temperature, bed voidage (i.e. number of contact points) or pellet material (Smith, 1970) and thus a constant value has been used throughout these calculations.

3.1.2 Wall heat transfer coefficient

Correlations generally relate to the pseudo-homogeneous phase parameter. The separation of the two phase parameters experimentally is difficult, although the inductive heating method of Bhattachryya and Pei (1975) may be applicable.

Hanratty (1954) correlated previous experimental work using only a flow dependent term and noted a considerable difference between beds of cylindrical and spherical pellets. This was attributed to greater fluid mixing near the tube wall for cylindrical pellets. The low conductivity of the packing may explain the absence of a static term. Similar correlations were also proposed by Calderbank and Pogorski (1957) and Yagii and Wakao (1959) for beds of glass and metal spheres. Yagii and Kunii (1960) recorrelated this data using the same structure as their conductivity equation:

$$\alpha w_c = \alpha w_c^o + C\ Rep.\ Pr$$

De Wasch and Froment (1972) also favour this form of correlation. Unfortunately, it is not possible, with the limited data available, to develop general correlations for the two packing dependent terms, αw_c^o and C.

Beek (1962)reviewed the available correlations and suggested, for Rep > 40, the following equations:

$$\text{Cylinders:}\quad \frac{\alpha w_c dp}{kf} = 2.58\ Rep^{1/3}Pr^{1/3} + 0.094\ Rep^{\cdot 8}Pr^{\cdot 4}$$

$$\text{Spheres:}\quad \frac{\alpha w_c dp}{kf} = 0.203\ Rep^{1/3}Pr^{1/3} + 0.220\ Rep^{\cdot 8}Pr^{\cdot 4}$$

as the static contribution was negligible under these conditions. The source of these equations is obscure, their form being related to those

for mass transfer. They however reflect the other correlations quite well and have recently been supported by Smith (1973). Olbrich and Potter (1972) have suggested that Beek's correlation for cylindrical pellets may have no geometric associations, although recent experimental results, reported by Valstar et al. (1975), support the geometric effect.

Having established the continuum phase coefficient some method of subdivision between the two phases is required. Olbrich (1970) has suggested that:

$$Nu_s = 2.12 \text{ for spheres,}$$

$$\text{and } Nu_s \to \infty \text{ for cylinders.}$$

This implies no discontinuity in the temperature profile at the bed wall, in opposition to experimental measurements (Valstar et al., 1975). The higher value for cylinders has been atributed to a larger area of contact, especially in small diameter tubes where such pellets tend to pack with their axes parallel to that of the tube (Olbrich and Potter, 1972).

De Wasch and Froment (1971) suggest that if solid and fluid phase temperatures are not too different then:

$$\alpha w_s = \Lambda r_s / \Lambda r_c \cdot \alpha w_c$$

Holton (1975), using the same reasoning, considered that the Yagii and Kunii (1959) correlation applied to αw_f and obtained αw_s by subtraction. This made $(\alpha w_f / \alpha w_s)$ strongly Reynolds number dependent as it subtracts two correlations of the same basic data. In this study the continuum parameter was divided using the former method.

3.1.3 Effect of pellet hollowing on heat transfer

Hollowing directly affects the effective bed conductivity and thus the relative values of the two phase wall heat transfer coefficients.

For De Wasch and Froment's (1971) model, the major low temperature effect will be a decrease in γ causing a fall in the solid conductivity. Interpenetration, which might increase the number of contact points, is unlikely to be important unless hollowing is quite extreme because of geometric considerations. This is supported by England and Gunn's (1970)

result that hollowing does not change the number of particles per unit bed volume. In any event the contact resistance (hp) is only a weak function of the number of contact points and therefore no modification of the conductivity will occur.

Hollowing will modify the fluid phase conductivity as follows:

(a) Whatever the degree of hollowing the radial peclet number is decreased relative to a bed of solid pellets (Gunn, 1969).

(b) The conductive component will increase but this is of generally minor importance.

(c) The radiation contribution will, however, decrease with increasing voidage.

The overall effect will thus depend on the temperature.

3.1.4 Film heat transfer coefficient

This has been the subject of a thorough analysis by Whitaker (1972), who gave

$$\frac{h\, dp'\, \varepsilon}{kf(1-\varepsilon)} = (0.5\ Rep'^{\frac{1}{2}} + 0.2\ Rep'^{\frac{2}{3}})\ Pr$$

where $dp' = \frac{6.Vp}{Ap}$ and $Rep' = \frac{Gs.dp'}{\mu}\left(\frac{\varepsilon}{1-\varepsilon}\right)$

This equation covers the experimental data, with a maximum scatter of 30%. Barker (1965) questioned the inclusion of a Prandtl number dependence, as most experimenters have studied air. He attributed most of the experimental scatter to a wall effect.

3.1.5 Axial and radial mass dispersion

These phenomena are conveniently correlated by the Peclet group. For solid pellets the radial peclet number (Pe_r) has been correlated by a number of workers (Bernand and Wilhelm, 1950; Fahien and Smith, 1955). The correlation of the latter is used here as it retains a dependence on (dp/Dt).

$$Pe_r = 8.0\ [19.4\ (dp/Dt)^2 + 1]$$

Froment (1972) has however shown that simulation results are insensitive to variations in Pe_r. Axial fluid phase dispersion is similarly described by a constant Pe_z value of 2.0 (Aris, 1965).

Table 3.5 - Effect of operating conditions on heat transfer parameters

T : 1075 K Pellets : cylinders, $\beta = 2$, ks. = 1.11 W m^{-1} k^{-1}

Operating Conditions			2D - 2P					1D - 2P		1D-1P
Gs $kgm^{-2}s^{-1}$	dp m	Dt m	λr_f	λr_s	αw_f	αw_s	$(h.a_v)$ x 10^{-6}	λr_c	αw_c	U
1.10	.003	.05	.79	.64	184.5	148.6	.221	1.43	333.1	135.5
2.10	.004	.04	1.52	.64	267.3	112.3	.213	2.16	379.6	202.0
1.70	.004	1.16	1.48	.64	240.6	103.7	.188	2.12	344.3	14.1
0.50	.006	.06	.95	.64	95.6	64.3	.052	1.59	159.9	91.2
1.70	.004	.05	1.36	.64	234.2	110.0	.188	2.00	344.2	165.7
0.90	.002	.05	.49	.64	168.3	219.2	.352	1.12	387.5	122.7
1.80	.001	.03	.41	.63	302.4	472.6	.141	1.04	775.0	204.0

Table 3.6 - Effect of Geometry, solid conductivity and temperature

(Conditions : Gs : 1.80 $kgm^{-2}s^{-1}$; dp : 0.001 m, Dt : 0.03 m)

			2D - 2P					2D - 1P		1D1P
Geometry	ks	$T_{(K)}$	λr_f	λr_s	αw_f	αw_s	$(h.a_v)$ x 10^{-6}	λr_c	αw_c	U
Cylinders β : 2	1.11	1075	.41	.63	302.4	472.6	.141	1.04	775.0	204.0
Spheres	1.11	1075	.41	.63	136.2	212.8	.141	1.04	349.0	154.4
Cylinders β : 2 α : 2	1.11	1075	.38	.56	313.0	462.0	.175	.94	775.0	190.1
Cylinders β : 2	1.11	383	.25	.63	113.3	286.0	.813	.88	399.3	149.0
Cylinders β : 2	0.7	383	.25	.41	151.3	248.0	.813	.65	399.3	121.4
Cylinders β : 2	0.3	383	.25	.18	232.6	166.6	.813	.43	399.3	89.5

For beds of hollow cylinders the radial peclet number is reduced to 4.7, independent of extent of hollowing or cylinder aspect ratio. The axial peclet number is also reduced, but depends on pellet hollowing thus:

α	.5	.75	.85	0
Pe_z	1.2	1.5	1.2	2.0

(at high Reynolds number)
(England and Gunn, 1970)

3.1.6 Primary information inputs

Of the basic parameters which appear in the above correlations gas phase conductivity and specific heat can be readily estimated using established techniques (see, Reid and Sherwood, 1966).

However, solid phase conductivity and emissivity are less easy to predict. Fortunately, variation of pellet emissivity from 0.5 (Holton, 1975) to 0.9 (Kunii and Furusawa,1972),at 1100K, causes only a 4% variation in the heat transfer parameters, thus circumventing accurate prediction. Solid phase conductivity will lie in the range 0.3 to 1.1 W $m^{-1}K^{-1}$ (Satterfield, 1970) depending on the pellet material, the degree of microparticle fusion and the intrapellet gas. The results in Table 3.6 demonstrate the important effect of variations in this parameter. Unfortunately the predictive methods available (Harriott, 1975) are unreliable and difficult to implement.

3.1.7 Summary

Despite considerable research efforts, it is clear that three main areas of uncertainty exist in the estimation of heat transfer parameters:

(a) A great scatter of pseudo homogeneous-phase wall heat transfer predictions. The correlations proposed by Beek (1962) reflect the general trend quite well but definitive work remains to be done.

(b) The available evidence suggests that the wall coefficient depends on packing geometry but this needs confirmation.

(c) When considering the two phase model further uncertainty is introduced by the difficulties of dividing the radial transport coefficients between the phases. It is clearly diffi-

cult to establish or measure different gas and solid temperature profiles. The presence of thermocouples tends to distort the packing and so some form of transmitting sensor would be required. The inductive heating method, proposed by Bhattachryya and Pei (1975), may enable beds of metal based pellets to mimic reaction conditions.

3.2 Gas phase kinetics

In this section a number of the problems encountered in obtaining relevant gas phase kinetic information are outlined. It was in the light of these problems that the parametric study in Chapter 4 was proposed.

Both molecular and free radical reactions can occur in the gas phase. In this study only gross or mass action kinetic expressions will be used because of the numerical problems involved in integrating free radical reaction schemes.

Where the gas phase reaction proceeds via a degenerate branching scheme (e.g. hydrocarbon oxidation) it may be initiated by very small amounts of radical precursors introducted into the gas phase. The desorption of such materials, present as intermediates of the catalytic reaction, can thus lead to a very rapid increase in the homogeneous rate (Keulks et al., 1972).

Free radical chains can be terminated by either gas/gas or gas/solid collisions and thus the reactor surface to volume ratio and the nature of the surface are vitally important in determining the reaction scheme. The quenching and initiating behaviour of industrial catalyst surfaces is largely unknown (Mulchahy, 1973).

Of the gas phase kinetic equations considered in this study only that for formaldehyde oxidation (Hessam, 1971) is based on a free radical mechanism. The other equations are the results of gross fitting of experimental studies. This approach is necessitated by

(a) The complexity of the free radical schemes for even simple reactants.
(b) The paucity of fundamental radical-radical kinetic data.
(c) The difficulty of discriminating between kinetic schemes experimentally.

This type of result, however, gives little insight into surface to volume ratio effects which are of prime importance when extrapolating from an experimental system to the chemical reactor environment. An estimate of

the rate of gas phase formaldehyde decomposition is obtained in Appendix two from which the difficulty of such an exercise, for even a simple reactant, is apparent.

Clearly it is difficult to quantify the gas phase kinetic rate in the reactor environment, in order to assess the importance of possible reactions. Where the nature of the reactants or reaction suggests that an effect may occur, prudent choice of catalyst support and reactor construction material may minimize any phenomena by increasing chain terminations.

CHAPTER FOUR

STEADY STATE RESULTS

4. STEADY STATE RESULTS

4.1 Introduction

It is apparent that the inclusion of a homogeneous reaction will considerably increase the complexity of the numerical problems involved in the design of a chemical reactor. There is, thus, an incentive to establish the conditions under which the extra reactions are important.

Clearly, any reaction which has a significant rate under inlet conditions would be included in the overall kinetic scheme. Of greater interest are those reactions which have neglectably small initial rates but, by virtue of their thermal characteristics, play a significant part in the conversion of reactants. In this chapter a simple one dimensional-two phase model is employed to try and establish the kinetic conditions under which this type of phenomena occurs. Some attempt is also made to consider the effect of wall and film heat transfer on the phenomena. Finally, detailed modelling results for three kinetic systems are presented to compare the different reactor models and confirm the results of the simpler approach.

4.2 Simplified study of a homogeneous effect

The two phase-one dimensional model, see Table 2.2, used in this study retains a differentiation between the phases but is capable of rapid solution. Under practical industrial conditions the film heat transfer group (H) will lie in the range 50 to 300. The radial heat transfer groups (A_f, A_s) will take values in the range 5 to 15, except where the reactor diameter is large (e.g. sulphur dioxide oxidation) when adiabatic conditions may be approached.

The following areas have been considered:

(a) The range of homogeneous parameters necessary for an effect to be seen.

(b) The modifications caused by introducing a film heat transfer resistance.

(c) The implications of dividing the overall continuum-wall heat transfer coefficient between the two phases in different ways.

For the purposes of this study a homogeneous effect has been defined as a greater than 20% change in one of the observable parameters of the system (i.e. a change in conversion, hotspot temperature, outlet temperature, etc. at least as significant as that due to the uncertainty

Table 4.1 - Parameter ranges

Parameter	Range	Reference
γ_s	less than 40	Wiesz and Hicks (1962)
	14.0 - 28	Van den Bosch and Luss (1977)
	10 - 30 (hydrocarbon oxidation)	Hlavacek (1970)
	10 - 40 (hydrocarbon oxidation)	Firth (1969)
γ_f	20 - 35	Shtern (1964)
	14 - 30	Examples in this study
β_s	1.2 - 0.04	Van den Bosch and Luss (1977)
	1.2 - 0.16	Hlavacek (1970)
β_f	For hydrocarbon oxidation, the homogeneous reaction is unselective and thus $\beta_f > \beta_s$	

Table 4.2 - Kinetic Effect

Primary Reaction	Reaction parameters for 2nd reaction		Damkohler No. for 2nd reaction	
	β	γ	Concurrent	Consecutive
(I)				
Da : .35	.2	10.	.061	.275
	.2	20.	.042	.145
β : 0.2	.2	30.	.024	.08
	.2	40.	.015	.04
γ : 10.0	0.5	40.	.0090	.03
	0.7	40.	.0070	.022
Overall conversion: ∿ 40%	1.0	40.	.0055	.018
(II)	.5	10.	.080	.032
Da : .40	.5	20.	.013	.0015
β : .5	.5	30.	.00096	$.60.10^{-4}$
γ : 10.0	.5	40.	$.70.10^{-4}$	$.33.10^{-5}$
Overall conversion: ∿ 95%	1.0	40.	$.47.10^{-4}$	$.18.10^{-5}$
(III)	.2	20.	.10	.05
Da : .4	.2	30.	.040	.013
β : .2	.2	40.	.014	.0033
γ : 20.0	.5	40.	.010	.0019
Overall conversion: ∿ 95%	1.0	40.	.0054	.0010

Note: (1) Reactor is adiabatic

(2) Interphase film effects are neglected

(3) Both reactions are first order

Table 4.3 - Influence of reaction order

Primary Reaction	Reaction Parameters		Concurrent Da		Consecutive Da	
	β	γ	$N_1 = 1$ $N_2 = 2$	$N_1 = 2$ $= N_2$	$N_1 = 1$ $N_2 = 2$	$N_1 = 2$ $= N_2$
Reaction II (Table 4.2)	0.5	10.0	.0213	.10	.044	.15
	0.5	20.0	.038	.020	.0019	.019
	0.5	40.0	$.37.10^{-3}$	$.31.10^{-3}$	$.3.10^{-5}$	$.16.10^{-3}$
	1.0	40.0	$.22.10^{-3}$	$.11.10^{-3}$	$.18.10^{-5}$	$.10.10^{-3}$
(IV) Da : 0.20 γ : 20.0 β : 0.20 Overall conversion $\sim$ 30%	0.2	20.0	.031	.034	1.29	1.55
	0.2	40.0	.0175	.0195	0.48	0.68
	0.5	40.0	.0095	.0113	0.34	0.50
	1.0	40.0	.0055	.0065	0.21	0.33

Note: (1) Reactor is adiabatic

(2) Interphase resistances are ignored.

in the heat transfer coefficients).

From the results in Table 4.2 it is apparent that only when the two reactions have very disparate thermal parameters is an effect caused by an initially small extent of reaction. Consecutive reactions are obviously more conversion dependent than concurrent schemes.

The initial introduction of interphase heat and mass transfer resistances (Table 4.5) slightly lowers the gas phase Damkohler number required for an effect, as the greater solid phase temperature stimulates reactant conversion. At low rates of interphase transport this effect is offset by the poorer access of reactants to the catalyst. Within the practically accessible range of H values (see above) the segregation of the phases plays little part in the onset of any phenomena.

Obviously reactor cooling makes any phenomena more difficult to introduce, although within the industrial range any variation is broadly neutral. In the presence of a film transfer resistance the disposition of the overall wall heat transfer rate between the phases may have some interesting implications (see Table 4.6). Thus, under some high conversion conditions, changing the proportions of the overall coefficient attributed to each phase, in either direction, makes the introduction of an effect easier. Changing the reactions from first order has either an inhibiting or neutral effect depending on the reaction scheme and the heterogeneous conversion.

All kinetic terms with an initial magnitude of the same order as the accuracy limit on the design, in comparison with the main reaction, would be included in the detailed kinetic scheme. Any reaction which falls outside this criteria but has a high heat of reaction and a large activation energy should also be included. Under practical reactor operating conditions segregation of the phases is not significant and the above conclusions apply to either suitable catalytic or gas phase reactions. The thermal parameters necessary are, however, more typical of a heterogeneous-homogeneous combination, than two catalytic reactions.

4.3 Model discrimination

The relationships between the different reactor models of a catalytic reaction system have been discussed in the literature. Various criteria have been proposed (Mears, 1971; Hlavacek, 1970) for selecting which phenomena are important and therefore warrant inclusion. Comparisons between the different models have normally been on a specific

Table 4.4 - Influence of reactor cooling

Primary Reaction	Cooling	Concurrent Da		
	$A_f = A_s$	A	B	C
Reaction I (Table 4.2)				
	0.0	.061	.024	.016
A : β_f: .2	1.0	.075	.046	.032
γ_f: 10.0	5.0	.084	.074	.064
B : β_f: .2	10.0	.086	.080	.075
γ_f: 30.0	20.0	.087	.084	.081
C : β_f: .5	50.0	.088	.086	.085
γ_f: 30.0	100.0	.088	.087	.087

Note: (1) Interphase film effects are neglected

(2) Both reactions are first order.

Table 4.5 - Influence of interphase transport

Primary Reaction	H = K	Consecutive Da		Concurrent Da	
		Reaction A	Reaction B	Reaction A	Reaction B
Reaction II (Table 4.2)	10^3	$.15.10^{-2}$	$.18.10^{-5}$	.012	$.43.10^{-4}$
A : β : 0.5	10^2	$.14.10^{-2}$	$.14.10^{-5}$	.012	$.42.10^{-4}$
γ : 20.0	10.0	$.11.10^{-2}$	$.11.10^{-5}$	.0098	$.30.10^{-4}$
B : β : 1.0	5.0	$.95.10^{-3}$	$.11.10^{-5}$	.0078	$.22.10^{-4}$
γ : 40.0	3.0	$.10.10^{-2}$	$.14.10^{-5}$	.0060	$.15.10^{-4}$
Reaction IV (Table 4.3)	10^3	.148	.037	.0195	.0047
A : β : 0.2	10^2	.145	.037	.0195	.0046
γ : 30.0	20.0	.141	.032	.0195	.0044
B : β : 1.0	10.0	.141	.027	.0196	.0041
γ : 40.0	5.0	.105	.020	.0198	.0036
	2.0	.041	.006	.029	.0039

Table 4.6 - Effect of differential cooling rates (i.e. $\lambda r_s/\lambda r_c$ ratio) on results

Case	A_s	A_f	Concurrent Da
Case I (Table 4.2) and β_f : 0.2 γ_f : 10.0 H : 10.0 Overall Conversion ∿ 40%	0.0	0.0	0.072
	20.0	0.0	0.085
	10.0	10.0	0.089
	0.0	20.0	0.094
Da_s : 0.4 β_s : 0.5 γ_s : 20.0 β_f : 0.5 γ_f : 30.0 H : 10.0 Overall conversion ∿ 90%	4	6	0.072
	5	5	0.080
	6	4	0.077
	8	2	0.069

Table 4.7 - Film transport effects

a) Da_s : 0.35 β_s : 0.2 γ_s : 10.0

$K = 10^6$ β_f : 0.5 γ_f : 40.0

H	Heterogeneous only		Concurrent $Da_f = 0.009$		Consecutive $Da_f = 0.03$	
	Con %	Max Change	Con %	Max Change	Con %	Max Change
1000	40.41	-	49.30	-	43.4	-
100	40.71	.75	49.75	.95	43.86	1.1
20	42.06	4.2	52.0	6.0	46.25	6.6
10	44.04	9.0	55.38	12.8	56.8	29.2
5	48.72	20.5	64.93	32.3	-	-
2	74.07	83.5	100.00	103.0	-	-

b) Da_s : 0.4 β_s : 0.2 γ_s : 20.0

$K = 10^6$ β_f : 1.0 γ_f : 40.0

H	Heterogeneous only		Concurrent $Da_f = 0.0054$		Consecutive $Da_f = 0.0005$	
	Con %	Max Change	Con %	Max Change	Con %	Max Change
1000	87.6	-	100.00	-	91.5	-
100	90.5	2.8	100.00	0.6	94.5	3.2
50	92.9	6.0	100.00	3.4	98.10	11.2

basis and conclusions therefore vary. Froment (1967) and Hlavacek (1970) suggest that the simplest model is relatively effective whereas Smith (1970, 1973) concludes the reverse.

Radial temperature gradients can clearly only be neglected, with confidence, for quasi-adiabatic systems because of the exponential dependence of rate on temperature (Carberry, 1976). The presence of a homogeneous reaction would not be expected to modify this conclusion.

The introduction of a gas phase reaction might, by lowering the film temperature difference, ameliorate the need to include a film heat transfer resistance, with a corresponding computational saving. The results presented in Table 4.7 demonstrate that this is true for concurrent reaction schemes operating under high conversion conditions. This effect is confirmed by more detailed studies (see sect. 4.4.1). If significant film resistance is present the distribution of radial heat transport between the phases becomes important (as shown in Table 4.6).

Clearly, within the industrially practical range of H values such refinements, while more realistic, may not significantly improve the predicted results. It is possible, given the difficulty of dividing the radial transport coefficients between the phases, that this refinement detracts from the predictions obtained.

4.4 Example cases

Having established, in general terms, the parameter ranges under which a homogeneous effect is exhibited, more specific examples are considered in this section. The two cases utilised by Holton (1975), nitrous oxide and methanol oxidations, are reworked to reassess the results and their relationship to heat transfer estimation methods. A further example, the oxidation of carbon monoxide, is also considered.

Comparisons are based on the externally observable system parameters, viz:

(a) Conversion and selectivity
(b) Maximum temperature (hot spot) and its location
(c) Average fluid exit temperature.

4.4.1 Thermal Decomposition of Nitrous Oxide

This is an example of a concurrent reaction scheme, nitrous oxide decomposing both catalytically and in the gas phase:

Table 4.8 - Kinetics

Reaction	Model
1	$r = K_1(g_n\rho_f)^2/(1 + K_2 g_n \rho_f)$
2	$r = K_3 (g_n\rho_f)^2$
3	$r = K_4$ Aa $g_n\rho_f$

where g_n = mass fraction of nitrous oxide

Rate constant	$\log_{10}$ A	EA Kcal/g mole
K_1	16.48	81.8
K_2	6.99	28.4
K_3	13.88	72.4
K_4	3.35	34.6

$$K = A\, e^{-EA/RT}$$

Heats of Reaction

$(-\Delta H)_1 = 1.98\ 10^6$ J Kg^{-1} (N_2O)

$(-\Delta H)_2 = 1.05\ 10^6$ J Kg^{-1} (N_2O)

$(-\Delta H)_3 = 1.98\ 10^6$ J Kg^{-1} (N_2O)

Roughness factor:

$$Rg = 1000.0\ dp$$

1. $N_2O \rightarrow N_2 + \frac{1}{2}O_2$ Homogeneous

2. $N_2O + \frac{1}{2}O_2 \rightarrow NO_2 + \frac{1}{2}N_2$ Homogeneous

3. $N_2O \rightarrow N_2 + \frac{1}{2}O_2$ Heterogeneous

The kinetics of these reactions have been studied by Halladay and Marazek (1973) in the presence of gold foil. The relative rates of the heterogeneous and homogeneous reactions were obtained by varying the surface to volume ratio of the experimental system. The kinetic model proposed by the above workers is summarized in Table 4.8. In this study the reactions will be considered to be occurring in a bed of non-porous gold coated pellets. The active surface area (Aa) is related to the geometric surface area (Ag) by: Aa = Rg.Ag where Rg is a roughness factor related to the corrugations in the gold coating.

(a) Presence of a homogeneous effect

From the results presented in Tables 4.9 and 4.10 it is clear that the 1D1P model predicts very different thermal behaviour from the other two models under all conditions. Agreement between the two 2-dimensional models is better when both reactions are occurring due to a reduction in the film temperature difference between the two phases which thus better approximate a single continuum. Unusually, in this system, one of the gas phase reactions has a lower heat of reaction than the heterogeneous one. Thus, the inclusion of the gas phase terms may, under high conversion conditions, lower the overall temperature rise.

It was assumed, in chapter two, that film mass transfer could generally be neglected. This approximation was shown to be quite satisfactory for this example, despite the absence of an intrapellet resistance.

Reference to Table 4.11 shows the extent of the homogeneous effect predicted by the different models.

(b) Effects of modifying pellet geometry

The examples in Table 4.12 serve to point out the differences between the heat transfer rates for beds of spheres and cylinders (cases 1 and 2). Similarly, pellet hollowing leads to thermal effects which

Table 4.9 - Comparison of models

Nitrous Oxide oxidation

Conditions: T:1125K Inlet mass fraction of N_2O:0.667

Spherical pellets

Note: Tpos is expressed on a fractional bed basis

Tmax is maximum temperature ┐ expressed as differences

Tout is outlet temperature ┘ from the inlet value (K)

Conditions					1D1P				2D - 1P				2D - 2P				
Gs	dp	Dt	L	Re-action	Con (%)	Sel (%)	Tmax Tpos	Tout	Con (%)	Sel (%)	Tmax Tpos	Tout	Con (%)	Sel (%)	$Tmax^s$ $Tpos^s$	$Tmax^f$ $Tpos^f$	Tout
1.70	.004	.05	1.0	Het	53.35	0	124.0 .8111	113.	66.31	0	296.6 .9198	181.0	87.91	0	495.0 .8025	473.9 .8204	226.0
				Het + Hom	71.43	8.39	176.1 .8111	143.	95.48	15.26	531.9 .6963	160.0	98.16	16.20	613.5 .5704	598.5 .5827	108.0
2.10	.004	.04	2.5	Het	55.68	0	49.7 .2667	20.3	56.47	0	75.2 .2889	20.7	57.58	0	81.77 .2821	77.94 .2864	20.0
				Het + Hom	59.09	3.75	55.2 .2667	19.6	60.23	3.93	85.7 .2889	19.4	61.30	3.85	93.10 .2833	89.10 .2877	18.7
1.10	.003	.04	1.0	Het	66.22	0	117.2 .5222	45.0	74.69	0	232.2 .5741	48.6	80.13	0	283.7 .5574	275.2 .5642	42.0
				Het + Hom	78.17	7.23	161.2 .5222	32.8	93.44	12.23	433.0 .4951	20.1	95.68	12.88	489.5 .4469	484.5 .4525	15.1

Table 4.10 - Comparison of models

Nitrous Oxide oxidation

Conditions: T:1075K Inlet mass fraction of N_2O:0.667

Spherical pellets

Conditions					1D1P				2D-1P				2D-2P					
Cs	Dt	dp	L	Re-action	Con (%)	Sel (%)	Tmax Tpos	Tout	Con (%)	Sel (%)	Tmax Tpos	Tout	Con (%)	Sel (%)	$Tmax^s_{Tpos^s}$	$Tmax^f_{Tpos^f}$	Tout	
1.70	.05	.002	1.0	Het + Hom	20.31	2.32	48.56 .9778	48.5	20.98	2.51	92.42 1.0	92.42	21.15	2.49	93.71 1.0	92.91 1.0	92.91	1
				Het	19.02	0	45.63 .9778	45.5	19.46	0	84.11 1.00	84.11	19.61	0	85.50 1.00	84.52 1.00	84.52	
1.10	.04	.003	1.0	Het + Hom	28.68	2.11	40.09 .5667	34.0	29.23	2.18	60.49 .6136	36.2	29.54	2.15	61.83 .6086	60.54 .6148	36.2	2
				Het	27.14	0	38.00 .5667	33.0	27.55	0	56.78 .6136	34.8	27.87	0	58.15 .6086	56.85 .6148	34.7	
2.10	.04	.004	2.5	Het + Hom	30.29	1.70	22.28 .300	16.3	30.44	1.72	32.15 .3173	16.6	30.78	1.69	33.55 .3136	32.20 .3185	16.5	3
				Het	29.18	0	21.44 .300	16.0	29.31	0	30.85 .3185	16.4	29.66	0	32.26 .3148	30.90 .3198	16.2	
1.80	.03	.001	2.2	Het + Hom	29.52	1.61	17.42 .2444	12.8	29.70	1.63	28.51 .2753	13.1	29.72	1.63	28.54 .2765	28.44 .2778	13.1	4
				Het	28.53	0	16.82 .2444	12.6	28.68	0	27.43 .2765	12.9	28.70	0	27.74 .2778	27.36 .2790	12.9	
0.75	.06	.005	0.31	Het + Hom	18.34	3.25	103.5 1.0	103.5	18.56	3.43	150.46 1.0	150.46	23.77	3.75	264.41 1.0	216.25 1.0	216.25	5
				Het	16.53	0	93.12 1.0	93.12	16.61	0	131.52 1.0	131.52	20.32	0	201.28 1.0	171.76 1.0	171.76	

Table 4.11 - Comparison of predicted homogeneous effects

Case	Da_s	Da_f	Max. predicted % effect		
			1D1P	2D1P	2D2P
Table 4.10 1	.126	.013	7	10	10
2	.195	.020	5	7	6.5
3	.255	.026	4	4.5	2
4	.262	.027	3.5	3.5	3.5
5	.089	.009	11	17	25
Table 4.9 1	.255	.039	42	44	26
2	.516	.079	37	87	76
3	.394	.067	11	11.5	11.5

with $\gamma_s \simeq 16.$ $\gamma_f \simeq 32.$

$\beta_s \simeq .87$ $\beta_f \simeq .47$

Table 4.12 - Effect of pellet geometry

Conditions: T: 1100 K Dt: 0.05 m
dp: 0.002 m, Gs: 0.90 kg $m^{-2}sec^{-1}$
L: 0.380 m, Mass fraction N_2O at inlet: 0.667
Thermal conductivity: 1.11 W $m^{-1}K^{-1}$

	Conditions		2D - 2P				
	Pellet Geometry	Re-action	Con-version	Selec-tivity	$Tmax^s$ $Tpos^s$	$Tmax^f$ $Tpos^f$	$Tout^f$
1a	Spheres	Het + Hom	65.03	17.38	648.9 .9531	648.1 .958	412.0
1b		Het	32.87	0	333.9 1.0	320.6 1.0	320.6
2a	Cylinders β : 2	Het + Hom	29.47	5.74	258.7 1.0	252.6 1.0	252.6
2b		Het	24.08	0	183.4 1.0	179.5 1.0	179.5
3a	Cylinders β : 2 α : 0.2	Het + Hom	87.97	19.95	798.3 .8272	798.8 .8321	291.0
3b		Het	48.66	0	786.5 1.0	786.8 1.0	786.8
4	Cylinders β : 1	Het + Hom	94.80	16.83	724.8 .6963	723.3 .7000	338.0
5	Cylinders β : 1 α : 0.2	Het + Hom	99.03	20.14	919.2 .5667	916.2 .5704	280.0
6	Cylinders β : 1.5	Het + Hom	53.69	12.13	596.0 .9778	595.2 .9827	290.0
7	Cylinders β : 1.5 α : 0.2	Het + Hom	96.45	19.83	845.1 .7160	844.4 .7198	410.0

cannot be attributed to either greater homogeneous or heterogeneous rates of heat release caused by changes in voidage ($\sim$ 4%) or surface area ($\sim$ 15%). Thus, although modifications to pellet geometry alter the kinetic rate the dominating effect is via changes in heat transfer parameters.

(c) Reactor stability

All the results presented here are either thermally stable (i.e. the axial temperature profile is concave downwards) or, in cases where the film heat transfer coefficient is low, unstable (i.e. continually increasing axial temperature profile) for both heterogeneous and combined reaction schemes. No cases of the phenomena, reported by Holton (1975), of heterogeneous stability combined with homogeneous instability have been found. However, Holton's results correlate with excessively high αw_f to αw_s ratios, as predicted by his correlations, and this may explain the phenomena. The homogeneous reaction, in fact, appears to stabilize the system by spreading the heat release between the phases and under some circumstances lowering the total heat generated.

4.4.2 Air oxidation of Methanol

The partial oxidation of methanol to formaldehyde is generally carried out over metal oxide catalysts at high air to methanol ratios. Typically 5 - 10 mole % methanol in air is reacted at between 300 and 430^{o}C over an Iron/Molybdenum catalyst (Kirk-Othmer, 1967).

Mann and co-workers (1969, 1973) have measured the kinetics for the reaction

$$CH_3OH + \tfrac{1}{2}O_2 \rightarrow HCHO + H_2O$$

over two such oxide catalysts. Using the approximation, that at low methanol to air ratios the reaction is pseudo first order (Beskov et al., 1972), Holton (1975) abstracted the following kinetic laws:

$$r = ko_s \cdot (\rho_f g_m) \text{ kg m}^{-3} \text{ sec}^{-1}$$

where g_m = mass fraction of methanol

Catalyst	ko_s (sec^{-1})
MnO_2/MoO_3 : (250 - 460°C)	$8.64 \cdot 10^7 \; e^{-17.43/RT}$
V_2O_5/MoO_3 : (300 - 470°C)	$2.69 \cdot 10^6 \; e^{-10.8/RT}$

The heat of reaction is

$$(-\Delta H)_{298} = 4.9 \cdot 10^6 \text{ J kg}^{-1}(CH_3OH)$$

Catalytic over oxidation of formaldehyde proceeds at a much lower rate than the initial oxidation (Bibin and Popov, 1969). Mann et al. (1969, 1973) failed to detect such a reaction and it has been neglected here. These kinetic expressions are coupled with an isothermal pellet effectiveness factor to yield an overall rate of reaction. Aris (1965) has shown that the infinite slab model fairly accurately predicts the effectiveness factor of both spherical and cylindrical pellet geometries, using a suitably defined Thiele modulus.

$$\eta = \frac{\tanh \phi}{\phi}$$

$$\text{where } \phi = Lp. \frac{k_{het}}{\mathcal{D}_{eff}}$$

$$\text{and } Lp = Rp/3 \quad \text{(sphere)}$$

$$= \frac{Rp(1-\alpha)\beta}{2(1-\alpha+\beta)} \quad \text{(cylinder)}$$

] Surface area to volume ratio

A lumped parameter homogeneous kinetic model for formaldehyde oxidation, developed in Appendix 2, has been used in this study and gives:

$$R_f = 2.10^8 \; e^{-22/RT}[HCHO]^2 \text{ kg m}^{-3} \text{ sec}^{-1}.$$

(a) Comparison of different catalysts and homogeneous kinetics

The result of carrying out simulations using the homogeneous kinetics proposed by Holton (1975) and those developed in Appendix 2 are presented in Table 4.13. The absence of any significant homogeneous reaction at 403 K is consistent with the results of Mann et al. (1969). Clearly, use of the low temperature catalyst avoids any homogeneous complications and would thus be preferred.

Table 4.13 - Comparison of homogeneous kinetic schemes

Conditions: Mass velocity: 1.80 kg m^{-2} s^{-1}
Tube diameter: 0.03 m
Tube length: 0.265 m
Pellets (cylinders): Diameter: 0.001 m
Aspect ratio: 2.0
Mass fraction of Methanol: 0.038

Homo-geneous Kinetics	T (K)		Con-version (%)	Selec-tivity (%)	$Tmax^s$ (K)	$Tmax^f$ (K)	Cata-lyst
Holton (1975)	403	Het. + Hom.	43.5	33.8	206.1	202.6	MnO_2/ MoO_3
	403	Het.	32.7	93.75	34.6	34.4	
Appendix 2	403	Het. + Hom.	32.7	93.75	34.6	34.4	
	673	Het.	99.48	93.75	125.4	125.0	V_2O_5/ MoO_3
	673	Het. + Hom.	99.50	92.18	127.0	126.7	

Table 4.14 - Comparison of models

Methanol partial oxidation

Conditions (T : 573K)			2D - 2P					2D - 1P				1D - 1P			
Case	Bed Length (m)	Pellet Geometry	Con (%)	Sel (%)	$Tmax^s_s$ $Tpos^s_s$	$Tmax^f_f$ $Tpos^f_f$	Tout	Con (%)	Sel (%)	Tmax Tpos	Tout	Con (%)	Sel (%)	Tmax Tpos	Tout
Gs : 1.7 dp : 0.004 Dt : 1.16 (b)	.46	Cylinder Het + Hom	94.83	82.45	350.6 1.0	347.8 1.0	347.8	92.97	85.54	320.4 1.0	320.4	92.96	84.94	314.6 1.0	314.6
		Cylinder Het	93.49	93.75	278.7 1.0	276.0 1.0	276.0	91.05	93.75	269.0 1.0	269.0	91.68	93.75	265.6 1.0	265.6
Gs : 1.80	1.06	Cylinder α = 0.2 Het + Hom	99.86	92.15	219.6 .1222	219.2 .1247	.51	99.85	92.22	214.2 .1284	.52	99.86	92.64	130.7 .1222	.41
dp : 0.001	1.01	Spheres Het + Hom	99.87	92.13	208.2 .1333	207.8 .1358	.81	99.86	92.19	204.4 .1407	.81	99.88	92.44	139.9 .1333	.60
Dt : 0.03	1.30	Cylinders Het + Hom	99.88	92.55	192.4 .100	191.8 .1012	.35	99.87	92.59	187.5 .1049	.36	99.88	92.82	175.7 .1000	.32
Gs : 1.1 dp : 0.003 Dt : 0.04	1.70	Cylinders Het + Hom	99.80	92.13	138.2 .1025	135.3 .1074	.64	99.79	92.16	133.7 .1123	.64	99.78	92.3	86.6 .100	.64
Gs : 1.7 dp : 0.004 Dt : 0.05	3.42	Cylinders Het + Hom	99.75	91.95	124.6 .1000	120.7 .1037	.70	99.73	91.98	117.9 .1086	.71	99.72	92.1	76.5 .100	.71
Gs : 2.10 dp : 0.004 Dt : 0.04	4.62	Cylinders Het + Hom	99.73	92.35	80.0 .074	76.4 .077	.45	99.72	92.36	75.7 .079	.45	99.71	92.4	51.1 .078	.45
Gs : 0.5 dp : 0.006 (a) Dt : 0.06	1.10	Cylinders Het + Hom	99.64	89.07	172.1 .1457	167.9 .1630	2.5	99.60	89.21	165.9 .1802	2.5	99.59	89.82	113.5 .1667	2.3

Table 4.15 - Effect of pellet geometry and thermal conductivity

Conditions: Temperature : 650 K

Tube diameter : 0.03 m Pellet diameter : 0.001 m

Reactor length: 0.590 m Inlet Methanol mass fraction : 0.065

Conditions			2D - 2P model				
Pellet	Reaction	Thermal Conductivity	Conversion %	Selectivity %	$Tmax^s_s$ $Tpos^s$	$Tmax^f_f$ $Tpos^f$	Tout
Cylinders	Het + Hom	1.11	99.99	87.29	248.2 .1376	248.7 .1401	3.5
Cylinders	Het + Hom	0.3	100.00	77.73	330.7 .2296	331.7 .2309	26.2
Spheres	Het + Hom	0.3	100.00	73.94	344.8 .2512	345.9 .2519	38.4
Spheres	Het	0.3	100.00	93.75	271.5 .1536	271.0 .1568	17.8
Cylinders	Het	0.3	100.00	93.75	269.1 .1500	268.6 .1531	12.7
Spheres	Het + Hom	1.11	100.00	84.70	261.8 .1494	262.6 .1525	7.5
Cylinders	Het	1.11	99.99	93.75	235.2 .1222	234.4 .1247	1.7

(b) Comparison of models

A consecutive reaction scheme exhibits an optimum reactor residence time for a maximum yield of the intermediate product, in this case formaldehyde. Due to the low rate of formaldehyde oxidation, this optimum occurs at large residence times and does not impinge on output considerations.

The three plug flow models are compared, in Table 4.14, at the optimum reactor length predicted by the simplest model. As can be seen from the high selectivity values very little homogeneous reaction is occurring. Film temperature differences are generally small and thus the two 2-dimensional models agree well. The one dimensional model predictions only agree with those of the other models when the tube diameter is large.

(c) Effect of modifying pellet parameters

A number of secondary catalyst pellet parameters may modify the degree of any homogeneous effect by changing the heat transfer characteristics of the bed and the pellet effectiveness factor. Chief among these are pellet geometry and hollowing. Although hollowing will not significantly enhance the gas phase reaction and is thus unrestricted, practical extents of hollowing do not markedly decrease the required catalyst volume.

The effects of pellet geometry and solid conductivity are given in Table 4.15. From these results it can be seen that the reactor designer could control these thermally dominated events by careful choice of catalyst support material and pellet geometry.

Axial mixing may affect the selectivity and conversion of a consecutive reaction scheme by introducing a spectrum of catalyst contact times (Denbigh and Turner, 1971). The reactor lengths used in this study preclude such phenomena. Simulations using an arbitarily enhanced homogeneous reaction rate served to demonstrate the artefact (Table 4.16). Axial dispersion raises the selectivity of formaldehyde production because mixing lowers the rate of reaction for the second order formaldehyde oxidation, while not affecting the formation reaction.

Table 4.16 - The effect of axial mixing on reaction selectivity

Conditions: Temperature: 573 K
Pellets: Cylinders ($\beta = 2$)
A_{hom}: $3.5 \cdot 10^9$

Case*	Opt Length m	Plug flow		Axial mixing	
		Con (%)	Sel (%)	Con (%)	Sel (%)
a	.17	74.33	72.72	68.62	78.54
b	.29	68.05	75.30	64.73	78.83

(* see Table 4.14)

4.4.3 Carbon monoxide oxidation

Carbon monoxide and hydrocarbon oxidation (at low reactant concentrations) has received considerable study as part of car exhaust abatement measures.

Kuo et al. (1971) measured the apparent heterogeneous oxidation kinetics of carbon monoxide and hydrocarbons over a transition metal catalyst. Olefins and aromatics were grouped as 'fast' oxidizing while paraffins were classified as 'slow'. Lord et al. (1973) reviewed the available data for carbon monoxide and hydrocarbon homogeneous oxidation and presented gross kinetic expressions. The kinetic data for hydrocarbon oxidation is confused and simulations have thus been restricted to carbon monoxide (kinetic expressions are summarized in Table 4.17).

The two dimensional-two phase model, described previously (see Chapter two) operating under adiabatic conditions was employed. The inlet conditions are broadly typical of those experienced during parts of the 'California' cycle (Wei, 1975). Reference to Table 4.18 illustrates the effect of the homogeneous reaction most clearly. Before concluding that homogeneous oxidation can play an important part in car exhaust conversion two points should be considered:

(a) Kuo et al. (1971) obtained their kinetic results from an integral reactor operating at up to 900K. As the heterogeneous and homogeneous reactions produce the same product any gas phase reaction may be implicitly included in the catalytic rate expression.

(b) The homogeneous data was obtained in reactors of low surface to volume ratio. Its application to packed bed reactors may thus overstate the reaction rate in these circumstances.

Despite these reservations, it can be expected that under high flowrate and temperature conditions (i.e. engine acceleration) homogeneous reaction can significantly increase conversion of car exhaust components.

4.5 Discussion

From the above results it is apparent that a '20% effect' is exhibited only under extreme conditions. Clearly the oxidation of methanol could be operated industrially without the homogeneous reaction being significant. Of the specific examples (see Table 4.19) only the methanol oxidation scheme contains a gas phase reaction of initially

Table 4.17 - Carbon Monoxide Oxidation - Kinetic expressions

Heterogeneous

$$r = A_{het}\, e^{-E_{het}/RT} . X_{co}$$

for $X_{O2} > .02$

$$A_{het} = \frac{6.35.10^2}{T} \quad kg/m^2/sec$$

$$E_{het} = 17.6 \text{ kcal g mol}^{-1}$$

Homogeneous

$$r = A_{hom}\, e^{-E_{hom}/RT} . X_{co}^{0.27}$$

$$A_{hom} = 1.09\ 10^5 . \quad kg/m^3/sec$$

$$E_{hom} = 28.2 \text{ kcal g mol}^{-1}$$

The heat of reaction ($-\Delta H$) for

$$CO + \tfrac{1}{2}O_2 \rightarrow CO_2$$

is $10.1 . 10^6$ J/kg CO

Table 4.18 - Car exhaust examples

Conditions: Bed diameter: 0.17 m
Bed length: 0.30 m
Feed mass fraction of CO: 0.05
Pellet diameter (spheres): 0.003 m

Mass flow ($kg\ m^{-2}s$)	Inlet Temp K		Conversion (%)	$Tmax^s$ (K)	$Tmax^f$ (K)	Tout (K)
1.0	1000.0	Het. only	29.7	169.0	164.6	164.6
1.0	1000.0	Het. + Hom.	43.2	294.6	291.2	291.2
5.0	1000.0	Het. + Hom.	7.8	42.8	40.9	40.9
1.0	900.0	Het.	12.8	67.6	65.8	65.8
1.0	900.0	Het. + Hom.	14.8	80.1	78.2	78.2

negligible extent. This reaction does not, however, affect the reactor behaviour as $\gamma_f/\gamma_s \simeq 1.0$. The generalized results obtained earlier in this chapter do, however, indicate that for γ_f/γ_s suitably large such a phenomena may occur. The predictions of the extent of a homogeneous effect differ between the various reactor models (see Table 4.11) but in no cases are these disparaties such as to undermine the general conclusions obtained using the simple one dimensional-two phase model.

The generalized studies, presented in section 4.3, indicate that a two phase model may be unnecessary unless the film heat transfer and film mass transfer groups (H and K) are significantly less than fifty. Use of the Whitaker correlation (see sect. 3.1.4) and the Chilton-Colburn analogy, relating heat and mass transfer, suggests that these two parameters will exceed fifty when Rep > 40 and (L/dp) > 150. These conditions will normally be met industrially as they ensure that the pressure drop across the bed is small (Coulson and Richardson, 1968) and that axial mixing effects can be neglected (Carberry, 1976). A two phase model would be required where either:

(a) a low feed rate, or
(b) short beds of large pellets

are used. It would thus appear that under most practical circumstances a one phase model is adequate for design purposes. In the case of a heterogeneous-homogeneous reaction scheme heat is released in both phases and a one phase model provides a better approximation to the real situation than it would for the heterogeneous reaction alone.

4.6 Conclusions

From the general and specific studies carried out here the following conclusions can be drawn:

(a) The presence of a gas phase reaction lowers the film temperature difference between the two phases, thus making a one phase continuum model an acceptable approximation.
(b) It would also appear that for most practical systems a one phase model is adequate for design purposes.
(c) A homogeneous effect, not dependent on phase segregation, will occur for systems where the activation energies of the two reactions are very disparate.
(d) The differences between the thermal transport rates of cylindrical and spherical pellets may introduce a degree of design

Table 4.19 - Summary

	Reaction		
	Methanol oxidation	Nitrous oxide oxidation	Carbon monoxide oxidation
Symbolic Representation	$A \rightarrow B \rightarrow C$	$A \nearrow B$, $A \searrow C$	$A \nearrow B$, $A \searrow C$
Typical Temperature (K)	600	1000	1000
Typical Reaction parameters			
β_s	.55	.87	.50
β_f	1.05	.47	.50
γ_s	14.0	16.3	8.9
γ_f	18.0	32.5	14.3
Da_f/Da_s	0.003	0.10	0.10
H	50.0	200.0	600.0
Cooling	Broad range	Broad range	Adiabatic
Presence of effect	No	Yes	Yes

freedom not previously considered.

(e) A concurrent gas phase reaction will tend to stabilize, not destabilize, a reaction system.

(f) The kinetic model of gas phase formaldehyde oxidation developed by Holton (1975) is in conflict with the experimental findings of Mann et al. (1969, 1973). An alternative formulation, proposed here, suggests that no significant homogeneous effect is present.

(g) The gas phase oxidation of carbon monoxide may contribute significantly to automobile exhaust clean-up in catalytic muffler systems.

CHAPTER FIVE

MODELLING OF THE BUTENE - BUTADIENE SYSTEM

5.1 Introduction

The oxidative dehydrogenation of butene to butadiene has been the subject of a continuing study since 1966.

Gabbay (1969) elucidated the kinetic scheme (see Appendix 5.1) in the range 380 - 460°C over a tin-antimony oxide catalyst, prepared at 850°C. (Supplied by B.P. Chemicals.). Corrie (1972), working with a single instrumented pellet, demonstrated that while the pellets were essentially isothermal an apparent gas phase 'light-off' was detected under some conditions. This effect was attributed to a heterogeneously induced gas phase reaction, similar to the mechanism suggested by McCain (1964) for propene oxidation.

Lam (1975) and Yeung (1976), thus, studied the gas phase reaction using catalytic and stirred tank reactors in series. These workers found that addition of acetaldehyde did not enhance or induce the homogeneous reaction, in contradiction of the batch reactor results obtained by Blundell and Skirrow (1958). Temperatures of 475°C (i.e. 50°C hotter than those encountered industrially, McCain (1976)) were required before an appreciable homogeneous reaction occurred. Yeung (1976) resolved this conflict by suggesting that free radical chains induced by aldehyde, either produced heterogeneously or injected into the gas line between the reactors, are quenched at the tube walls before reaching the jet stirred reactor.

Lozano (1973) and Corrie (1972) carried out tubular reactor and single pellet studies, respectively, under laminar flow conditions. The use of these results to either obtain kinetic data or verify Gabbay's (1969) reaction scheme is complicated by the dominating importance of heat and mass transfer resistances. Holton (1975), however, attempted a modelling study of the latter system, in the absence of any gas phase phenomena, and this study will be reassessed in Section 5.3.

The present work thus aims to complete this long term study by comparing the results of a detailed reactor model with pilot plant data. This enables the accuracy of Gabbay's (1969) kinetic scheme and the presence of a homogeneous effect to be evaluated. As the kinetic scheme involves a large number of fractional order reactions analytical effectiveness factor results cannot be utilised. A pellet model is thus developed, in the next section, to provide this information for reactor

modelling calculations.

5.2 Procedure for effectiveness factor evaluation

The catalyst pellets employed industrially are finite cylinders of height and diameter 0.0032m. The available information (Satterfield, 1970) for pressed and extruded pellets and for this catalyst in particular (Orhon et al., 1971) suggests that anisotropic diffusivities may occur. Various pellet size transformations, to enable one dimensional models to be used, have been suggested (Sorenson and Stewart, 1973; Gorliek et al., 1973) but none of these include the possibility of such anisotropy.

To accommodate this possibility a two dimensional model was proposed, for which a balance equation takes the form:

$$\mathcal{D}_z \frac{\partial^2 Ci}{\partial z^2} + \frac{\mathcal{D}_r}{r} \frac{\partial}{\partial r} \left(r \frac{\partial Ci}{\partial r}\right) = R(Cj) \quad j = 1, N \qquad - (5.1)$$

with boundary conditions

$$\text{(a)} \quad Ci = Ci_o \qquad r = Rp, \; -L \leqslant z \leqslant L$$

$$z = \pm L, \quad 0 < r < Rp$$

$$\text{(b)} \quad \left.\frac{\partial Ci}{\partial r}\right|_{r=0} = \left.\frac{\partial Ci}{\partial z}\right|_{z=0} = 0 \qquad - (5.2)$$

$$-L \leqslant z < L \qquad 0 \leqslant r < R$$

Although the reaction network is complex only five species (oxygen, the butene isomers and butadiene) are involved in the reactions and the pellets can be considered isothermal (Corrie, 1972). The five concentration balance equations (equation 5.1, above) can be recast in dimensionless form using

$$R = r/Rp; \quad Z = z/L, \quad X_i = Ci/Ci_o$$

$$\frac{\partial}{\partial R}\left(R \frac{\partial X_i}{\partial R}\right) + \left(\frac{\mathcal{D}_z}{\mathcal{D}_r}\right) \left(\frac{Rp}{L}\right)^2 \frac{\partial^2 X_i}{\partial Z^2} = \frac{Rp^2}{\mathcal{D}_r} R(X_j) \quad j = 1, N \qquad - (5.3)$$

with:

(a) $X_i = 1.0 \qquad R = 1 \qquad -1 \leqslant Z \leqslant 1$

$\qquad\qquad\quad Z = 1, \qquad 0 < R < 1$

(b) $\left.\frac{\partial X_i}{\partial R}\right|_{R=0} = \left.\frac{\partial X_i}{\partial Z}\right|_{Z=0} = 0$

$\qquad -1 < Z < 1 \qquad\qquad 0 \leqslant R < 1$

These equations have the same structure as equation 2.1, except for the absence of a bulk flow term, and the same solution procedure can thus be used (Appendix A.1). The effectiveness factor (or the average rate, which is used directly) can be rapidly obtained using the collocation quadrature formulae. Some general results of this model are presented in Section 5.4 and the model has also been used to reassess the results presented by Holton (1975) (section 5.3).

5.3 Evaluation of Holton's (1975) single pellet model and Corrie's (1972) experiments

Corrie (1972) carried out experiments, using trans-but-2-ene as feed stock, in order to measure temperature effects. The experimental system consisted of a single cylindrical sealed end pellet past which the gases flowed (see Fig. A.3.2). The flow rates were such that film diffusion of mass and heat to and from the pellet were the dominating resistances (see Appendix A.3.3).

Holton (1975) modelled this system utilising a simplified scheme for the reactions of n-butene and butadiene. The experimental results were fitted by changing the gas-pellet heat transfer coefficient (by modifying the parameter C in the equation $Nu = C.Re_e^{1/3}$) until the experimental and predicted film temperature rises agreed. This yielded values of C about six times the theoretical value for a smooth annulus (see A.3.3). Pellet roughness or disturbances in the flow pattern due to the thermocouple wires cannot explain these differences (McAdams, 1954). The results in Table 5.1 indicate the effect on C of changing the kinetics. It is thus not necessary to arbitrarily increase the film heat transfer coefficient if the correct kinetics are employed.

It would also be possible to use Corrie's (1972) published conversion and selectivity results to either obtain a kinetic model or verify the reaction scheme proposed by Gabbay (1969). Neither of these alternatives has been pursued because both would require the introduction of further arbitary parameters to account for the various uncertainties in the experimental system. These problems would have been avoided if either

the pellet had been suspended in a jet stirred reactor or a recycle configuration had been used.

Table 5.1 - Effect of kinetic scheme on the predicted heat transfer parameter (C)

Feed: O_2 : 1.15
C_4H_8 : 0.67
C_4H_6 : 0.091
} Kmol m^{-3} (x 10^3)

Temperature: 715.5 K

Feed	C	ΔT(K)
Experimental (trans-but-2-ene)		7.5
butene - 1	5.0	30.9
butene - 1	15.7	8.7
cis - but - 2 - ene	3.2	5.6
trans - but - 2 - ene	5.0	4.2

5.4 Single pellet results

(a) Different isomer kinetics:

It is clear that the kinetic schemes for the isomers are significantly different. For example, under similar conditions to section 5.3, but with a pellet of diameter and length 0.0032m, the heat release rates for n-butene, cis-2-butene and trans-2-butene are respectively 117.0, 69.8 and 69.8 kW m^{-3} of catalyst. Relatively more over oxidation occurs with n-butene than with the other two isomers and the reaction is more strongly diffusion controlled (effectiveness factor about 0.77 compared to 0.90).

(b) Consideration of pellet characteristics:

Variation of the ratio of axial to radial pellet diffusivities in

the range 0.5 to 2.0 has a less than 10% effect on the butadiene yield for the industrial size of pellet. It is thus clear that anisotropic diffusion effects are unimportant. In this study pellet hollowing effects have not been considered as the effectiveness factor was generally high (greater than 0.65) and the catalyst material is prone to crumble (Gabbay 1969).

(c) Consideration of the homogeneous reaction:

Lam's (1975) results for the homogeneous reaction of butene - 1 were utilized (see Appendix A.3.2). These were applied to all three butene species as it was not expected that major differences between the isomers would be seen in the gas phase reactions. Using a simple stirred tank analogy to a section of an industrial reactor the conversion and selectivity of the combined heterogeneous - homogeneous scheme was compared to that of the heterogeneous reaction. The feed conditions of Table 5.2.b are typical of the industrial reactor. It is only with artificially oxygen rich conditions and a less heterogeneously active isomer that any effect is apparent (Table 5.2.a).

Table 5.2 - Comparison of heterogeneous and homogeneous rates

Simple cell model, cell volume = 0.01 of industrial reactor

(a) Cell Feed (Wt %)

Oxygen : 15.0
c-but-2-ene : 5.3
butadiene : 16.8

T (K)	Conversion (%)		Selectivity (%)		CO Selectivity (%)	
	Het	Het + Hom	Het	Het + Hom	Het	Het + Hom
700	3.68	3.68	20.71	20.71	16.19	16.19
800	12.6	12.6	5.29	5.18	15.74	15.80

(b) Cell Feed (Wt %)

Oxygen : 10.0
n-butene : 10.0
butadene : 6.0

T (K)	Conversion (%)		Selectivity (%)		CO Selectivity (%)	
	Het	Het + Hom	Het	Het + Hom	Het	Het + Hom
700	8.98	8.98	88.71	88.71	1.27	1.27
800	27.10	27.10	85.33	85.31	1.43	1.43

5.5 Pilot scale reactor modelling

The data, kindly provided by B.P. Chemicals International (McCain, 1976), is presented in Appendix A.3.4 and the conditions summarized in Table 5.3a.

A one dimensional-one phase plug flow model of this reactor was employed. The heterogeneous reaction rate was evaluated using the pellet model introduced in Section 5.2. Model parameters were obtained, a priori, using the methods discussed in Chapter 3. The results of this exercise are presented in Tables 5.3 - 5.6 and Figs. 5.1 to 5.3. Typical central processor times were about 200 C.D.C. seconds per run.

The model results overestimate butadiene and carbon monoxide yields in all cases. Predictions of peak temperature rise are poor for runs one to three but are relatively good for the second set of results (runs four to seven) where the catalyst used was prepared in the same way as that over which the kinetic scheme was obtained (Gabbay, 1969).

Obviously, the comparison between the experimental and simulation results could be improved by modifying reaction or heat transfer parameters. This would, however, be an unsound approach because of deficiencies in the experimental information which may be more significant. For example, despite the very different reactivities of the three isomers (see section 5.4) the mixed butene feed was reported as only approximately equimolar. Despite these reservations, the correspondence between the simulation and experimental results for runs four to seven is sufficiently close to suggest that the main cause of the poor fitting of the other results is changes in catalyst activity with changes in preparation temperature.

Tables 5.4 - 5.6 contain some supplementary results,

(a) The negligible effect of the homogeneous reaction on the predicted results.

(b) The need to utilise the complete kinetic model to obtain reasonable correspondence with experimental results.

(c) The effect of changing the orthogonal polynomials (computer times are about 30% greater when $w = 1 - x^2$). This provides an estimate of the numerical reliability of the computed results.

Table 5.3.a - Summary of experimental conditions

Run No.	Catalyst Preparation Temp (K)	Initial bed Temp (K)	Temperature Measurement
1	1073	683	Single thermo-couple withdrawn along well
2		688	
3		708	
4	1123	659	Array of thermo-couples in single well. Less complete results.
5		684	
6		695	
7		695	

Table 5.3b - Pilot scale data (Tables A.5.1/2) compared to simulations

(Note: w = 1 in collocation equations)

Run No.	Max Temp* (°C)		Outlet Temp* (°C)		Hotspot position (m)		C_4H_6 out (w% w)		C_4H_8 out (w% w)		CO out (w% w)	
	Expt	Theory	Expt	Theory	Expt	Theory	Expt	Theory	Expt	Theory	Expt	Theory
1	15.0	29.43	8.0	6.6	.247	.234	11.0	14.08	6.26	3.86	.1	.359
2	19.0	32.26	10.0	6.68	.247	.234	11.7	14.36	6.44	3.42	.13	.380
3	33.0	42.6	10.0	6.68	.247	.234	12.30	15.13	4.40	2.63	.21	.433
4	-	20.7	-	6.27	-	.300	11.6	12.95	7.20	7.30	.08	.205
5	29.0	33.5	-	7.06	.35	.234	12.15	14.60	5.3	5.45	.125	.285
6	36.0	40.6	-	6.65	.410	.268	12.6	15.16	4.30	4.74	.187	.316
7	36.0	30.59	-	8.05	.494	.300	11.5	13.53	6.5	6.56	.135	.240

* Difference from inlet temperature

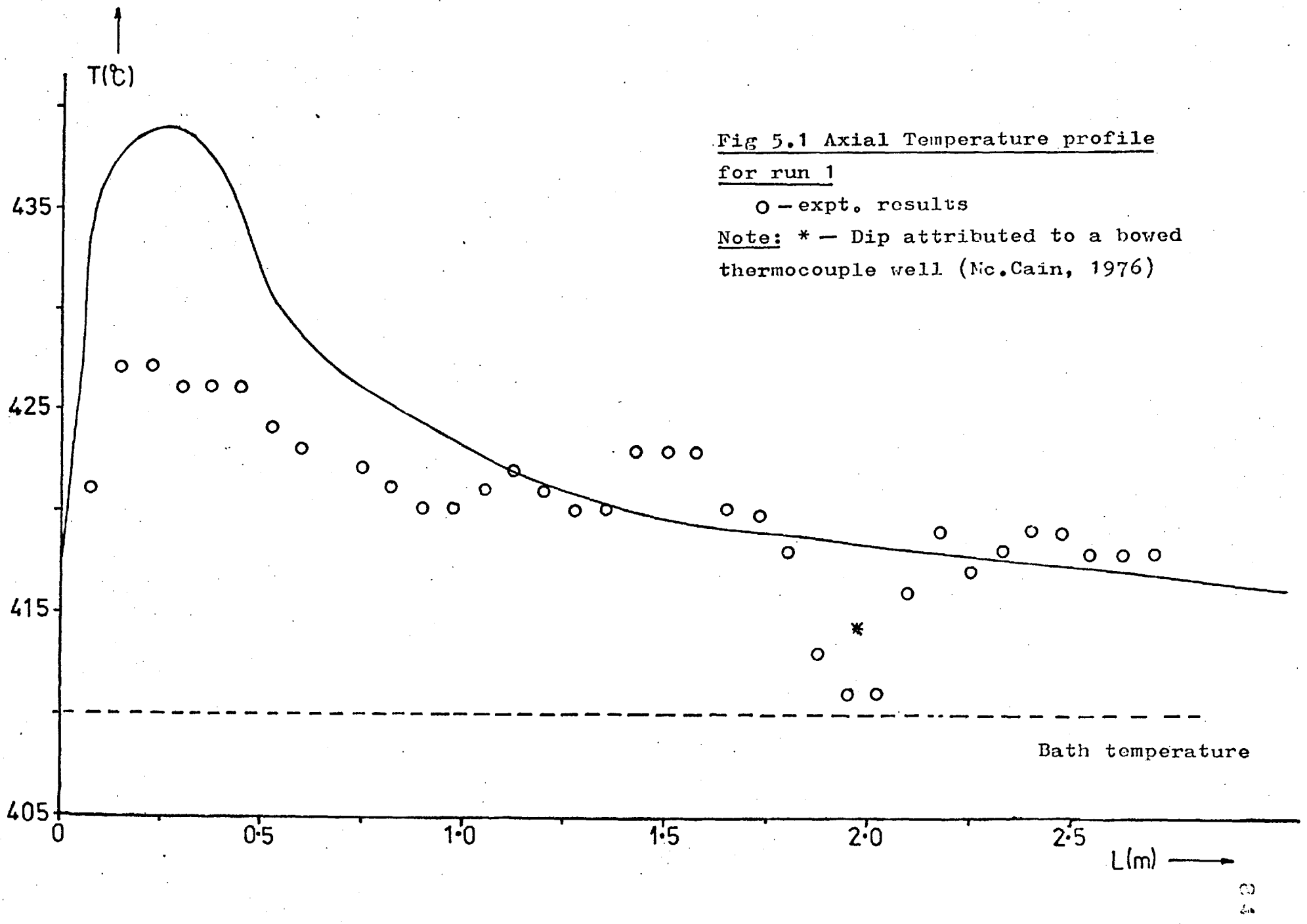

Fig 5.1 Axial Temperature profile for run 1

o – expt. results

Note: * — Dip attributed to a bowed thermocouple well (Mc.Cain, 1976)

Fig 5.2 Axial Temperature profile for run 2

O – expt. results

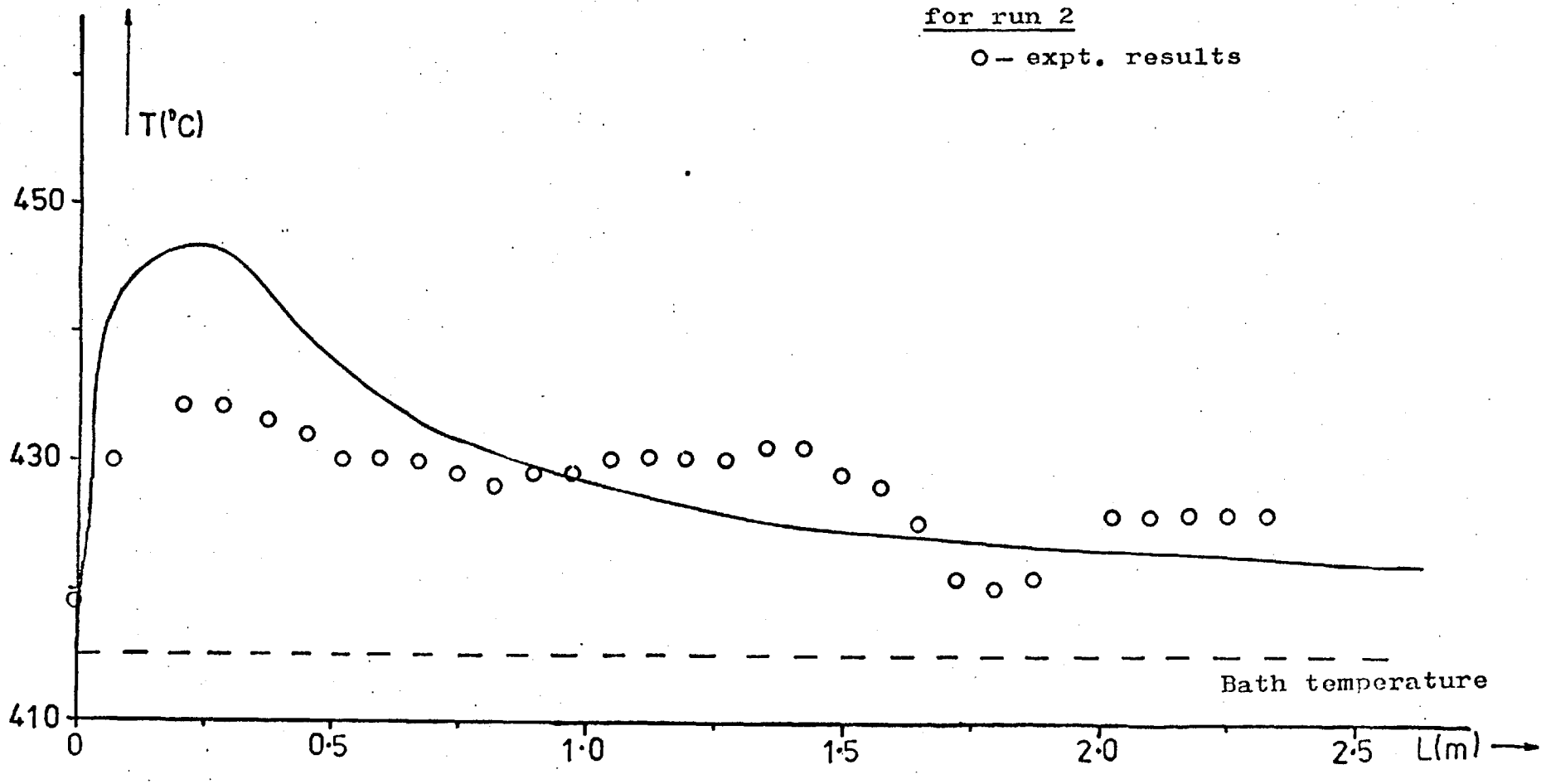

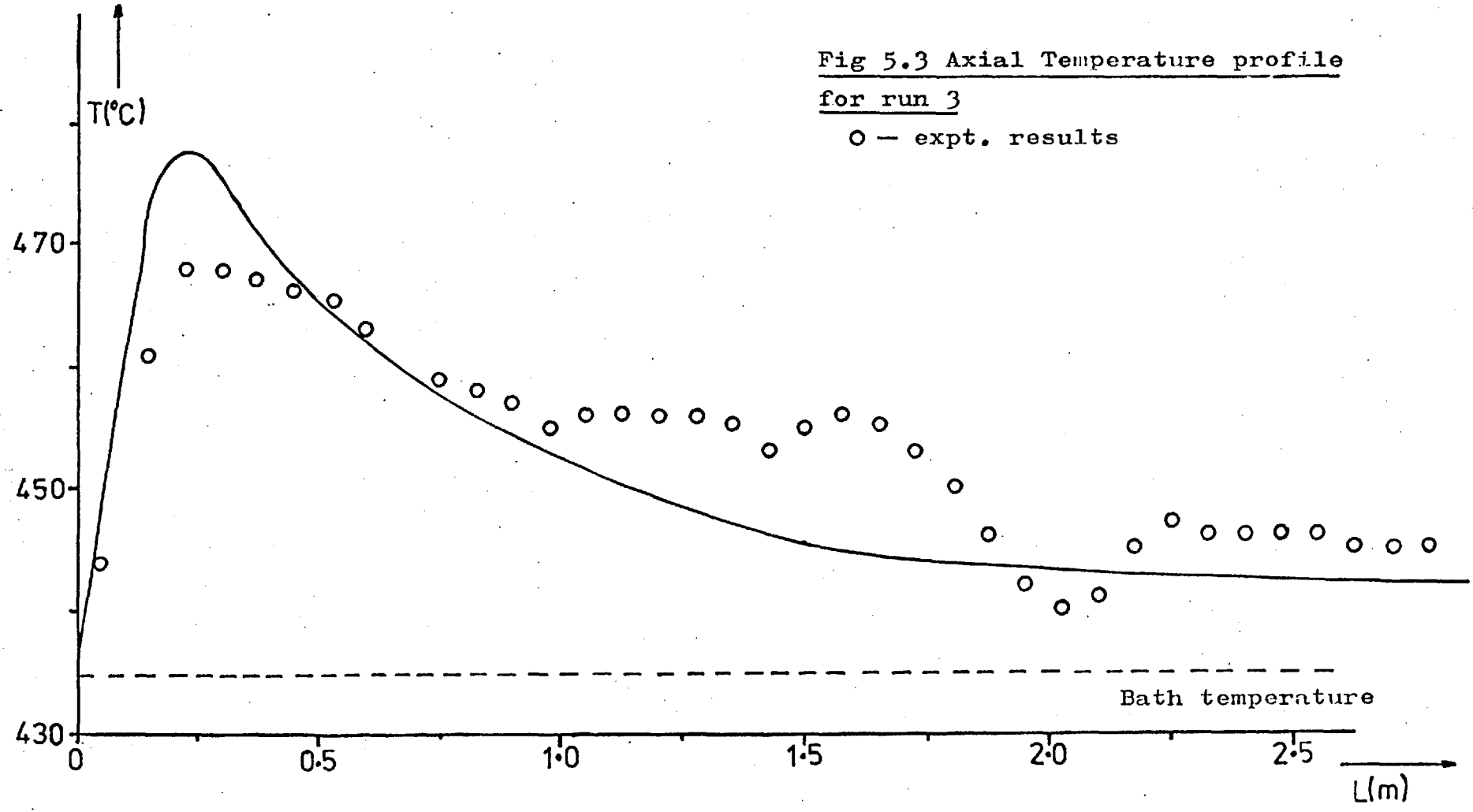

Fig 5.3 Axial Temperature profile for run 3

o — expt. results

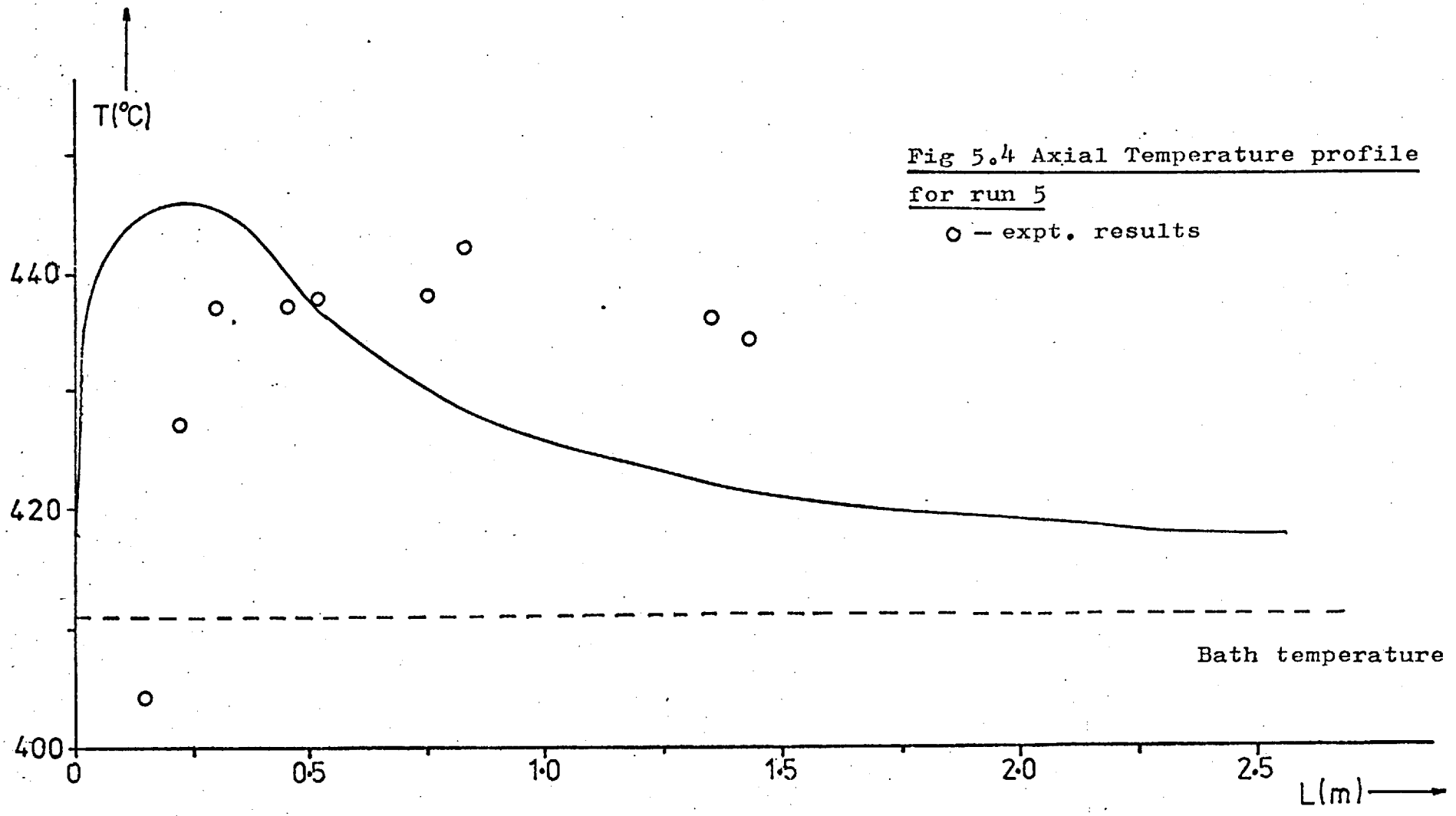

Fig 5.4 Axial Temperature profile for run 5

o — expt. results

Table 5.4 - Effect of homogeneous reaction and subcooled feed

(Conditions as run 1, Table 5.3a)

	ΔTpos (m)	ΔTmax (°C)	ΔTout (°C)	C_4H_6 out (w% w)	C_4H_8 out (w% w)	CO out (w% w)
Base case (Table 5.1)	0.234	29.427	6.6	14.082	3.857	0.3593
Homogeneous reaction included	0.234	29.429	6.65	14.076	3.857	0.3596
Feed subcooled to 677 K	0.267	28.993	6.6	14.082	3.868	0.3585

Inclusion of the homogeneous term reduces the n-butene outlet mass fraction from $0.61.10^{-4}$ to $0.30.10^{-4}$ but this is not reflected in the total butenes value.
ΔTpos, ΔTmax, ΔTout are differences from the inlet value.

Table 5.5 - Comparison of different isomer kinetics

(Conditions of run 3, Table 5.3a)

Butene Species	Δ Tmax (°C)	Reactant Exhausted at (% of bed)
cis - but - 2 - ene	247.7	23.3
n - butene	314.52	5.6
cis - but - 2 - ene (but concentration reduced by factor of 3)	38.95	58.0

Table 5.6 - Comparison of results for different approximating polynomials

Run No.	w = 1						w = 1 - x^2					
	ΔTmax (°C)	ΔTout (°C)	ΔTpos (m)	C_4H_6 out (%)	C_4H_8 out (%)	CO out (%)	ΔTmax (°C)	ΔTout (°C)	ΔTpos (m)	C_4H_6 out (%)	C_4H_8 out (%)	CO out (%)
1	29.43	6.6	0.234	14.08	3.86	.359	31.6	6.84	0.238	14.11	3.70	.360
4	20.7	6.27	0.300	12.95	7.30	.205	21.34	6.42	0.305	13.15	7.19	.205

5.6 Discussion and Conclusions

It is clear, from the reactor simulation results, the the homogeneous oxidation of butene and butadiene does not have an appreciable effect on the reactor outlet conditions. The effects seen by Lam (1975) are consistent with the homogeneous combustion of butene and butadiene, without catalytic initiation.

The simulation results presented above have been obtained without recourse to parameter fitting. Some of the deficiencies in the experimental information have already been considered and these could contribute to the poorness of the comparison between the simulations and experiments. The results for runs four to seven are sufficiently close to the experimental values, except in over estimating butadiene yield, to suggest that a more significant error lies in the kinetic modelling of the butadiene degradation reactions. The differences between the accuracy of the predictions for the two different groups of runs can probably be attributed to alterations in catalyst activity caused by changes in catalyst preparation technique (i.e. different calcining temperatures). (Gabbay, 1969) and the amounts of diluent steam used in the feed.

The heterogeneous and homogeneous kinetic schemes presented by Gabbay (1969) and Lam (1975) have been found to be consistent with the pilot plant results obtained by B.P. Chemicals. It has also been established that no significant gas phase effect occurs. The 'light-off' observations reported by Corrie (1972) imply the presence of some form of heterogeneous - homogeneous coupling; which may have been able to develop in the low surface to volume ratio experimental apparatus employed, but will not occur in a packed bed environment or the reactors in series configuration used by Lam (1975) and Yeung (1976).

CHAPTER SIX

MULTIPLICITY PHENOMENA

6. MULTIPLICITY PHENOMENA

6.1 Introduction

In this chapter a detailed model of a single catalyst pellet and its surrounding fluid is proposed from which multiplicity information can be derived. Use is made of a number of limiting cases of this model to relate the present work to that reported in the literature. These limiting results also apply to other reaction systems of possible interest (viz. slurry reactors, catalyst gauzes).

Multiple solutions of the equations describing the rate of production of some species (heat or mass) and its rate of removal is best illustrated by the diagrammatic treatment of a one phase system. The essential requirement for multiplicity is that the generation function (G) should have the sigmodial shape shown.

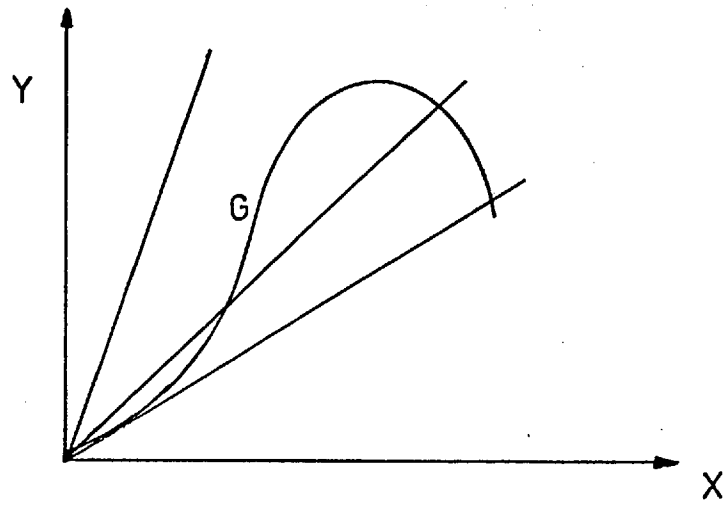

In thermal systems this is caused by a combination of activation energy (G increases with rising temperature) and reactant depletion (G decreases) effects. Similar behaviour can be caused by concentration variations, in isothermal systems, where the kinetics are sufficiently reactant or product inhibited (Matsuura and Kato, 1967).

Multiplicity and stability studies of chemical reactor systems have recently been reviewed by Schmitz (1975). Uppal et al. (1974) have presented a thorough consolidation of the previous work concerning a single exothermic reaction occurring in a continuous stirred tank. The more directly relevant contributions dealing with complex reaction schemes consists of the following studies:

(a) A two phase system and concurrent reaction scheme (Schmitz and Amundson, 1963).

(b) A one phase consecutive reaction scheme (Hlavacek et al., 1972).

(c) A one phase concurrent reaction scheme (Luss and Chen, 1975).

Interparameter plots are more difficult to obtain for two phase systems because of the greater parametric complexity and thus Schmitz and Aris (1963) considered only a few specific reaction conditions. Luss and Chen (1975) demonstrate the presence of five steady states for $Da_f/Da_s \sim 10^{-7}$ with very disparate activation energies. It should be noted that these parameters are not characteristic of two competing catalytic reactions. For the examples listed by the authors, of two desired reactions, the practically more important phenomena is the extinguishing of multiplicity at higher Da_f to Da_s ratios. Hlavacek et al. (1972) considering a consecutive mechanism discuss the case $\gamma_s, \gamma_f \to \infty$, for algebraic simplicity, although the phenomena demonstrated are not unique to these conditions.

For these multi-parameter systems a number of different presentations have been used. The use of Damkohler number plots, in this study, was governed by

(a) The principal aim of showing that an extra reaction could make the parameters necessary for non-uniqueness less extreme.

(b) The ability of these types of plots to demonstrate areas not detected by other workers.

Liu and Amundson (1962) have shown that the conditions for overall reactor multiplicity can be determined by studying the conditions under which a single pellet has multiple solutions. This approach has been utilised by McGreavy and Thornton (1970) to establish graphical bounds on the uniqueness zone for catalytic reactions. In the same spirit, in the presence of a homogeneous reaction, a reactor will exhibit multiple solutions if somewhere in the reactor a pellet and its immediate environment has non-unique solutions.

The experimental support for the very large body of theoretical knowledge in this area is extremely meagre. The correspondence between theory and experiment is qualitative rather than quantitative because of the difficulty in accurately determining kinetic data. Stirred tank experiments have been restricted to studies of the reactions between

(a) Sodium thiosulphate and sulphuric acid (Schmitz and Vejtasa, 1970).

(b) N-decane and gaseous chlorine (Luss et al., 1974).

Schmitz (1975) summarizes the single pellet studies, most of which have been poorly characterized. No systems exhibiting more than three steady states have been reported.

This study seeks to demonstrate that a homogeneous reaction can significantly expand the parameter range under which non-unique solutions are obtained. Reactor design and optimization may thus be restricted, as such areas of non-uniqueness must be avoided in order to obtain stable operation. This effect may also make experimental verification easier by making the phenomena less sensitive to parameter variation.

6.2 Model development

The conceptual model consists of a catalyst pellet bathed in a perfectly mixed reactant fluid. A chemical reaction is considered to be occurring in each phase. The pellet behaviour can be described by a distributed pellet model.

First order mass action kinetics and adiabatic conditions have been assumed to simplify the development.

6.2.1 Mathematical treatment

Both consecutive and concurrent reaction schemes will be considered in this chapter. For the consecutive kinetic scheme, $A \underset{solid}{\rightarrow} B \underset{gas}{\rightarrow} C$, the following describing equations are obtained:

(1) Pellet mass balance for species A, where ko_s is defined on a total volume basis (i.e. gas and pellet):

$$\nabla^2 Ca_s - \frac{ko_s e^{-E_s/RT_s} Ca_s}{\mathcal{D}_{eff}(1-\varepsilon)} = 0$$

with the boundary condition

$$\bar{n} \cdot \nabla Ca_s \Big|_b = \frac{kg}{\mathcal{D}_{eff}} (Ca_f - Ca_s)$$

where $\Big|_b$ indicates evalutation at the pellet surface.

(2) Pellet heat balance:

$$\nabla^2 T_s + \frac{(-\Delta H)_s \, ko_s \, e^{-E_s/RT_s} Ca_s}{K_{eff}(1-\varepsilon)} = 0$$

with boundary condition

$$\bar{n} \cdot \nabla T_s \Big|_b = \frac{h}{K_{eff}} (T_f - T_s)$$

(3) Pellet mass balance for species B:

$$Ca_f - Ca_s \Big|_b = Cb_s \Big|_b - Cb_f$$

(4) Fluid phase mass balance for species A:

$$v\,(Ca_f^o - Ca_f) - kg.S.V(Ca_f - Ca_s \Big|_b) = 0$$

(5) Fluid phase heat balance:

$$vCp.\rho_f(T_f^o - T_f) - h.S.V(T_f - T_s \Big|_b)$$

$$+ (-\Delta H)_f . ko_f e^{-E_f/RT_f} . Cb_f = 0$$

(6) Fluid phase mass balance for species B:

$$v(Cb_f^o - Cb_f) - kg.V.S(Cb_f - Cb_s \Big|_b)$$

$$- ko_f . e^{-E_f/RT_f} . Cb_f = 0$$

These equations constitute a non-linear coupled set, in temperature and composition, the solution of which would be complex indeed. Fortunately, under normal conditions a catalyst pellet can be considered isothermal and subject to this assumption equation (2) can be replaced with an overall

Table 6.1 - Dimensionless variables

$Y_s : T_s/T_f^o$ $\quad X_s : Ca_s/Ca_f^o$

$Y_f : T_f/T_f^o$ $\quad X_f : Ca_f/Ca_f^o$

$Z_s : Cb_s/Ca_f^o$ $\quad Y_o : T_o/T_f^o$

$Z_f : Cb_f/Ca_f^o$

Table 6.2 - Dimensionless parameters

$$H : \frac{h\ S\ V}{\rho Cp\ v}$$

$$K : \frac{kg\ S\ V}{v}$$

$$\alpha_s : ko_s \frac{Ca_o^{n-1} V}{v}$$

$$\alpha_f : ko_f \frac{Ca_o^{m-1} V}{v}$$

$$\lambda_s : \frac{\mathcal{D}_{eff}(1-\varepsilon)V}{Rp^2 v}$$

$$L_s : \frac{\rho_s Cp_s}{\rho_f Cp_f}$$

$$A : \frac{U\ So}{\rho_f Cp_f} \frac{V}{v}$$

Note: All parameters are defined on a total reactor volume basis

heat balance, viz.

$$(2') \quad h\ S\ V(T_f - T_s) = (-\Delta H)_s\ kg\ S\ V(Ca_f - Ca_s\big|_b)$$

Introducing the dimensionless parameters and variables defined in Tables 6.1 and 6.2 gives:

$$(1) \quad \nabla^2 X_s - \frac{\alpha_s X_s}{\lambda_s} = 0$$

with boundary condition

$$\bar{n}.\nabla X_s\big|_b = \frac{K}{m\,\lambda_s}(X_f - X_s\big|_b)$$

where m depends on pellet geometry (m = 3 for spheres, m = 2 for infinite cylinders)

$$(2) \quad H(Y_f - Y_s) = \beta_s K\,(X_f - X_s\big|_b)$$

$$(3) \quad X_f - X_s\big|_b = Z_s - Z_f$$

$$(4) \quad 1 - X_f - K(X_f - X_s\big|_b) = 0$$

$$(5) \quad 1 - Y_f - H(Y_f - Y_s) + \alpha_f \beta_f e^{-\gamma_f/Y_f} Z_f = 0$$

$$(6) \quad Z_f^o - Z_f - K(Z_f - Z_s\big|_b) - \alpha_f e^{-\gamma_f/Y_f} Z_f = 0$$

For spherical pellet geometry equation (1) can be solved analytically to yield:

$$X_s(r) = f(Y_s, X_s, \alpha_s, \lambda_s, K, m)$$

A pellet effectiveness factor could be calculated from this expression (as was done in Chapter 4) but it is more convenient to work in terms of the surface concentration:

$$(7) \quad X_s\big|_b = X_f\,F(Y_s)$$

$$\text{where} \quad F(Y_s) = \frac{\frac{K}{3\lambda s} \tanh\left(\frac{q}{\lambda s}\right)}{\left(\frac{q}{\lambda s} + \tanh \frac{q}{\lambda s} \cdot \left(\frac{K}{3\lambda s} - 1\right)\right)}$$

with $q = \alpha_s e^{-\gamma_s/Y_s}$. The use of spherical geometry is not a severe restriction on the generality of the method as Sorenson et al. (1973) have shown that using a suitably defined pellet size parameter the behaviour of other geometries can be approximated. The set of equations for the concurrent scheme are somewhat simpler and consist of equations (1) and (2), above, plus a pair of expressions similar to equations (5) and (6) but in terms of X_f.

The limiting cases of the model are:

(a) $\lambda_s \to \infty$: 'perfectly mixed' solid
(b) H and $K \to \infty$: one phase model
(c) $\alpha_f = 0$: solid phase reaction only

These limiting cases enable the model to be related to the previously published results. Applying all three of the above limits reduces the equations to the set:

$$(8) \quad 1 - X - \alpha_s e^{-\gamma_s/Y} \cdot X = 0$$

$$(9) \quad 1 - Y + \alpha_s \beta_s e^{-\gamma_s/Y} X = 0$$

the behaviour of which has been studied by numerous workers (see Uppal et al., 1974). Similarly, invoking limits (a) and (b) generates the systems of equations studied by Hlavacek et al. (1972) (Consecutive reaction) and Luss and Chen (1975) (Concurrent reaction).

6.2.2 Numerical method

A sufficient condition for uniqueness is that α_f (say) is monotonically increasing or decreasing in the permissible interval of Y_s, for given values of the remaining parameters. Those cases for which analytical criteria can be obtained are discussed in the next section but generally a simple grid search procedure for obtaining all the stationary points in the curve of α_f versus Y_s was employed (see appendix A.5.2).

For each model a subroutine was written which provided α_f and derivative values for any given Y_s. After approximately locating the turning points, their location was refined, using a finer grid, and the number of steady states interpreted.

6.2.3 Analytical results

The general model can be manipulated analytically when $\lambda s \to \infty$ and only one reaction is occurring. Two cases are considered:

(a) Solid phase reaction under adiabatic conditions:

This outlines the procedure carried out numerically for the more complex models and relates the work to the results of Liu and Amundson (1962). Under these conditions the describing equations can be manipulated to yield:

$$\frac{(Y_s - 1)K}{(1 + K)\alpha_s} = e^{-\gamma_s/Y_s}\left(1 - Y_s + \beta_s \frac{K(1 + H)}{H(1 + K)}\right) = G$$

A necessary condition for non-uniqueness of solutions is that $\frac{dG}{dY_s} < 0$ somewhere in the range $1 < Y_s < 1 + \frac{\beta_s K}{H}\frac{(1 + H)}{(1 + K)}$. This is analogous to the more conventional treatment, which renders the pellet equations dimensionless in terms of the fluid conditions. Both approaches yield a necessary condition for multiplicity of the form:

$$\beta' (\gamma_s - 4) > 4$$

for $\alpha_1 < \alpha' < \alpha_2$

but where the symbols have the meanings:

(1) Liu and Amundson (1962):

$$\beta' = K\beta_s/H$$

$$\alpha' = \alpha_s/K$$

(2) This study:

$$\beta' = \frac{K(1 + H)\beta_s}{H(1 + K)}$$

$$\alpha' = \alpha_s (1 + K)/K.$$

Clearly, when K = H both models predict the same results, but when K < H the model developed here predicts that under practical conditions (i.e. H < 1.0) non-uniqueness phenomena would be easier to induce.

(b) Single reaction, non-adiabatic conditions:

In Table 6.3 results for a non-adiabatic model for either the fluid or solid reaction alone are given. This enables the combined reaction studies to be classified as initially unique or non-unique.

6.3 Results and discussion

For numerical convenience the effects of the various reaction and transport parameters have been investigated using the 'well mixed pellet' limiting case (i.e. $\lambda s \to \infty$).

6.3.1 Simple model

(a) Steady state results

With equal mass and heat transfer parameters variation of the activation energies and heats of reaction leads to four distinct cases (Table 6.3).

(1) Both reactions unique separately.
(2) Both reactions non-unique separately.
(3) Gas phase reaction unique.
(4) Solid phase reaction unique.

Generally, within these groups, increases in activation energies and heats of reaction yield multiplicity phenomena at lower Damkohler numbers.

(1) Under these conditions the concurrent scheme is trivially unique. However, the consecutive reaction scheme can show multiplicity phenomena when interphase transport is sufficiently fast (i.e. H and K > 0.1) (See Fig. 6.1). For Da_s and Da_f large enough the reactions then behave as A → C with some effective overall β value.

Table 6.3 - Multiplicity criteria

Generally: $\beta'(\gamma' - 4A') > 4A'^2$

(a) Solid phase reaction only

$$\beta' = \frac{\beta_s K (1 + H + A)}{(1 + K) H}$$

$$\gamma' = (1 + A) \gamma_s$$

$$A' = (1 + A Y_o)$$

(b) Fluid phase reaction only

$$\beta' = \beta_f$$

$$\gamma' = (1 + A) \gamma_f$$

$$A' = (1 + A Y_o)$$

(For the gas phase reaction in the consecutive scheme this analysis applies for $Z_f^o = 1.0$)

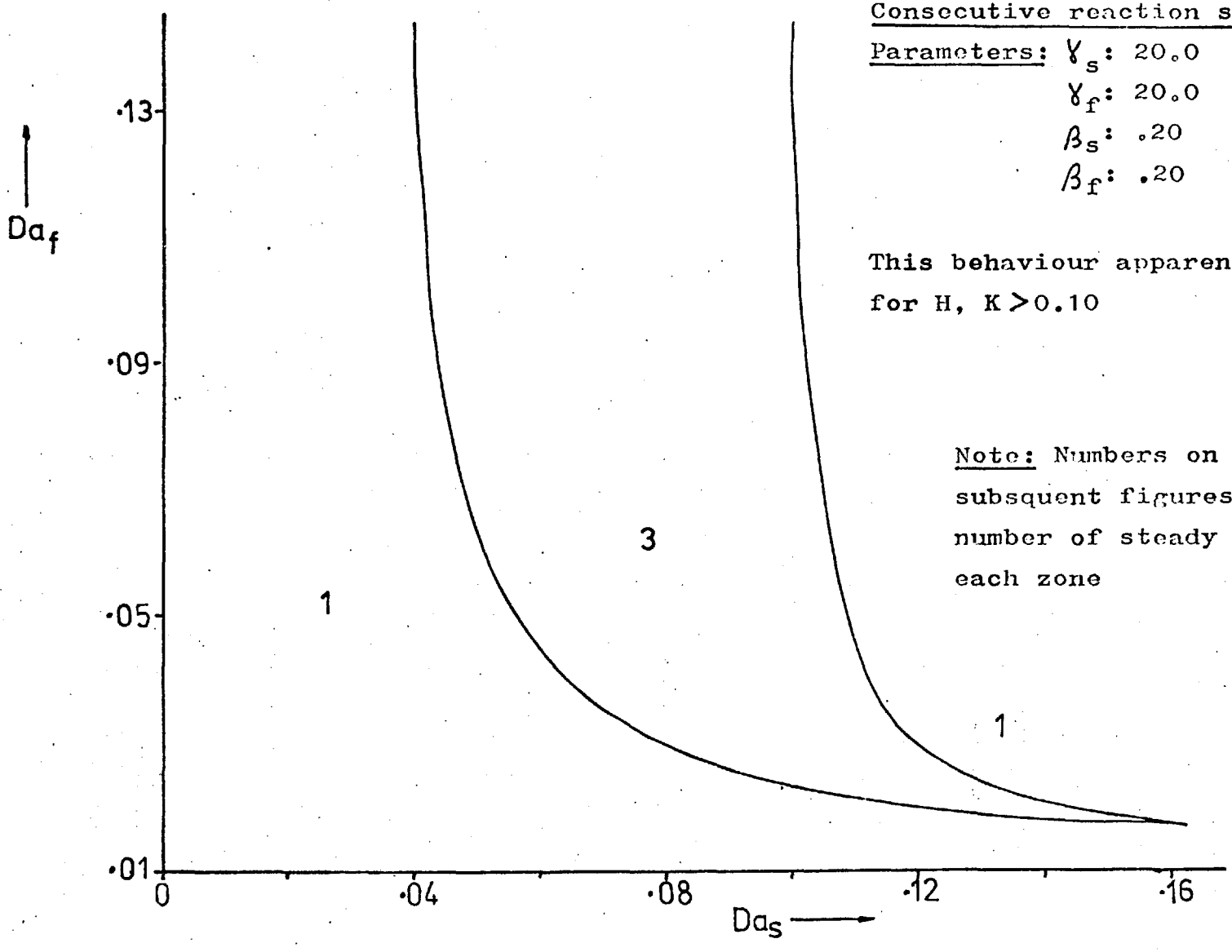

Fig 6.1 Both reactions unique separately

Consecutive reaction scheme

Parameters: γ_s: 20.0 H: 10.0

γ_f: 20.0 K: 10.0

β_s: .20

β_f: .20

This behaviour apparently persists for H, K $>$ 0.10

Note: Numbers on plot (and on subsquent figures) refer to number of steady states in each zone

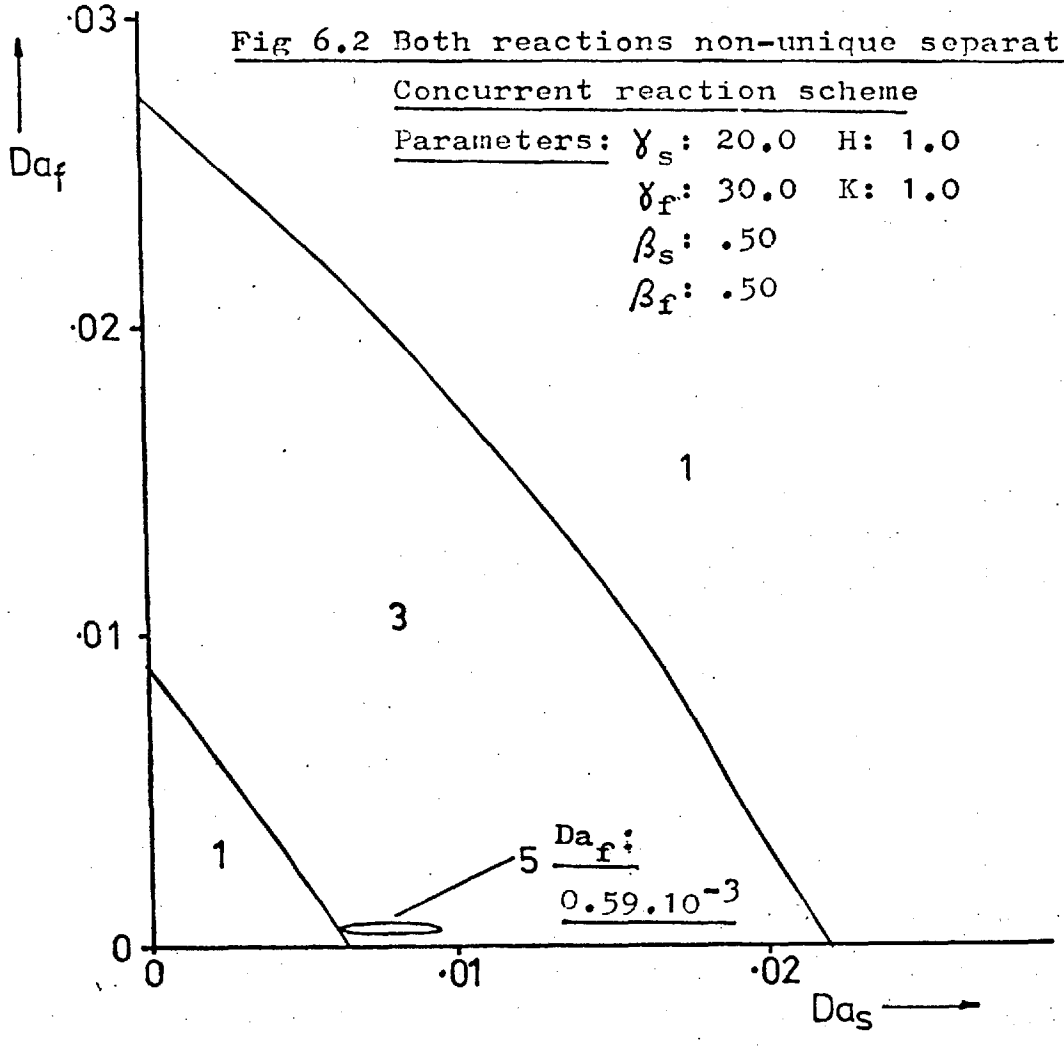

Fig 6.2 Both reactions non-unique separately

Concurrent reaction scheme

Parameters: γ_s: 20.0 H: 1.0

γ_f: 30.0 K: 1.0

β_s: .50

β_f: .50

Fig 6.3 Both reactions non-unique separately

Consecutive reaction scheme

Parameters: γ_s: 20.0 H: 1.0

γ_f: 30.0 K: 1.0

β_s: .50

β_f: .50

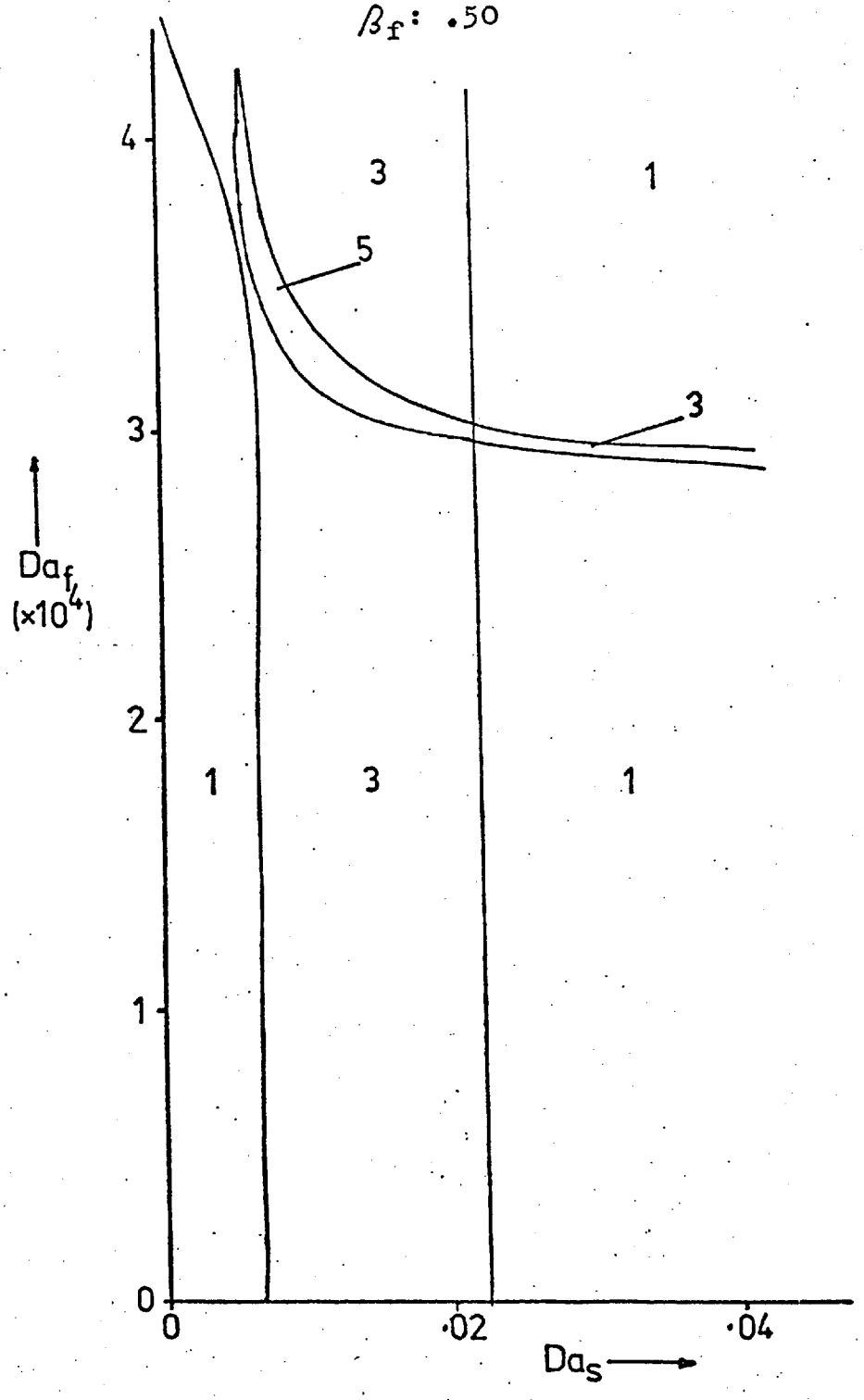

(2) The characteristic plots for concurrent and consecutive reaction schemes are shown in Figs. 6.2 and 6.3 respectively.

For the concurrent scheme purely gas phase multiplicity is independent of changes in the transport parameters. With H and K $\rightarrow \infty$ the system behaves as one reaction with an augmented Damkohler number but as H and K decrease multiplicity is induced for values of the combined Damkohler number less than for the single reaction. The example in the figure exhibits an area of five steady states. Luss and Chen (1975) have demonstrated a similar phenomena for a one phase system but only under more severe reaction conditions, which are uncharacteristic of two catalytic reactions.

Turning to the consecutive reaction scheme variation of transport parameters has little effect on the shape of the multiplicity diagram apart from moving it to lower Damkohler numbers as they decrease. The areas of multiplicity to note are (Fig. 6.4):

(a) The area of three steady states at low solid Damkohler numbers.
(b) The cusp of 5 steady states outside the solid phase multiplicity zone.
(c) The area of 3 steady states at high Damkohler numbers.

These areas extend multiplicity across the solid phase Damkohler number range. When the gas phase reaction parameters are less extreme the behaviour shown in Fig. 6.5 is obtained, where the gas phase effect is more modest but still extends the range of multiplicity.

(3) For the concurrent scheme the plots are similar to those for case (2) but the area of multiplicity does not extend to $Da_s = 0$. Similarly the consecutive reaction scheme exhibits behaviour analogous to Fig. 6.5 except that the shift to lower Da_s values is less pronounced.

(4) Fig. 6.6 demonstrates the phenomena under these circumstances for the concurrent scheme. The area of five steady states persists for H values in the range 7.0 to 15.0 and is thus a two phase artefact. The behaviour of the consecutive reaction is shown in Fig. 6.7 and 6.8. In the latter case the solid phase reaction is made unique by the effect of cooling.

In all these cases multiplicity phenomena are being induced or extended by the presence of very small extents of gas phase reaction.

A further group of reactions, which can be included with those of type (4), is the combination of an endothermic solid phase reaction

Fig 6.4 Both reactions non-unique separately

Consecutive reaction scheme

Parameters: γ_s: 20.0 H: 10.0 β_s: .50

γ_f: 30.0 K: 10.0 β_f: .50

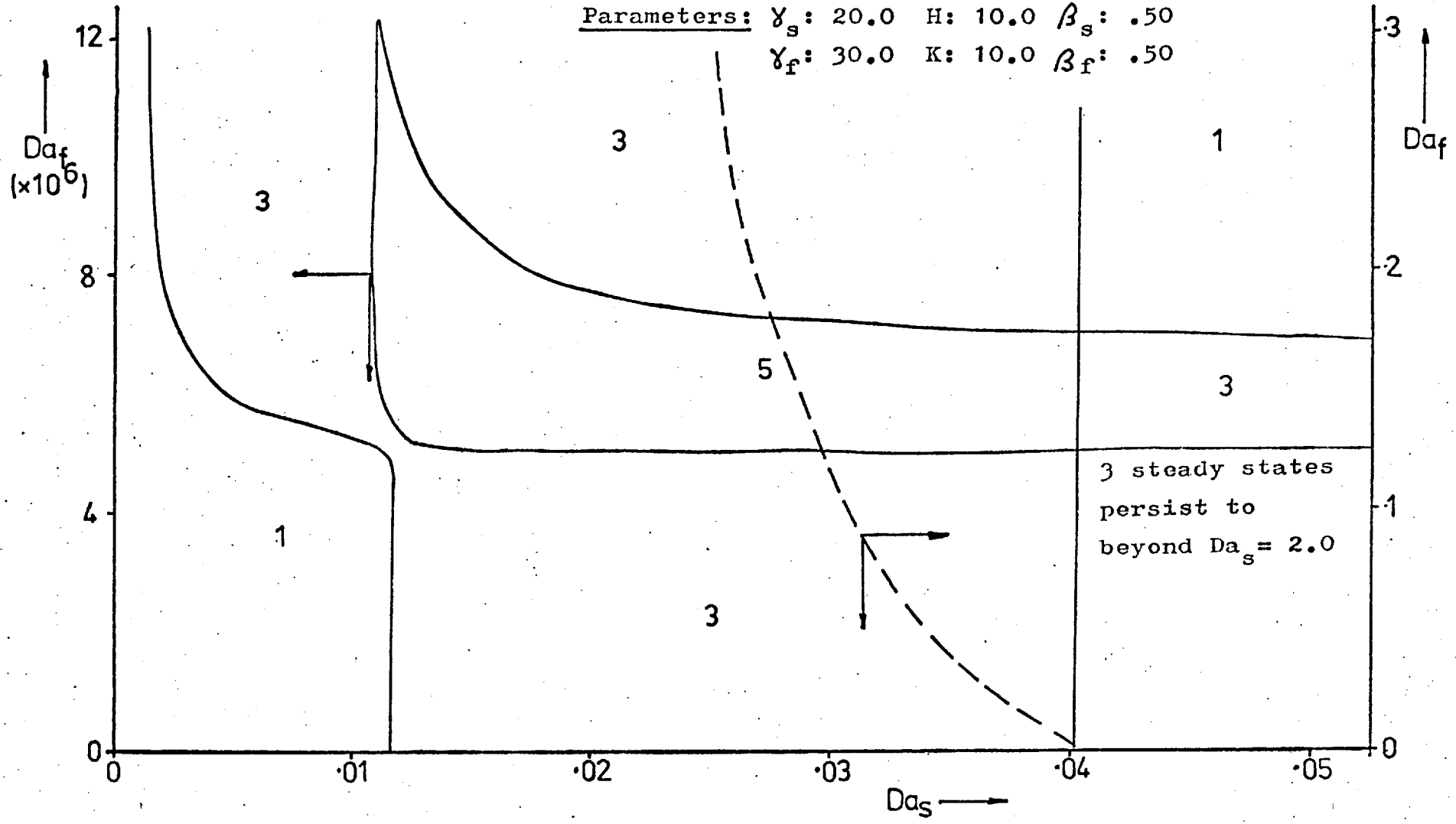

Fig 6.5 Both reactions non-unique separately

Consecutive reaction scheme

Parameters: γ_s: 20.0 H: 1.0

γ_f: 20.0 K: 1.0

β_s: .50

β_f: .50

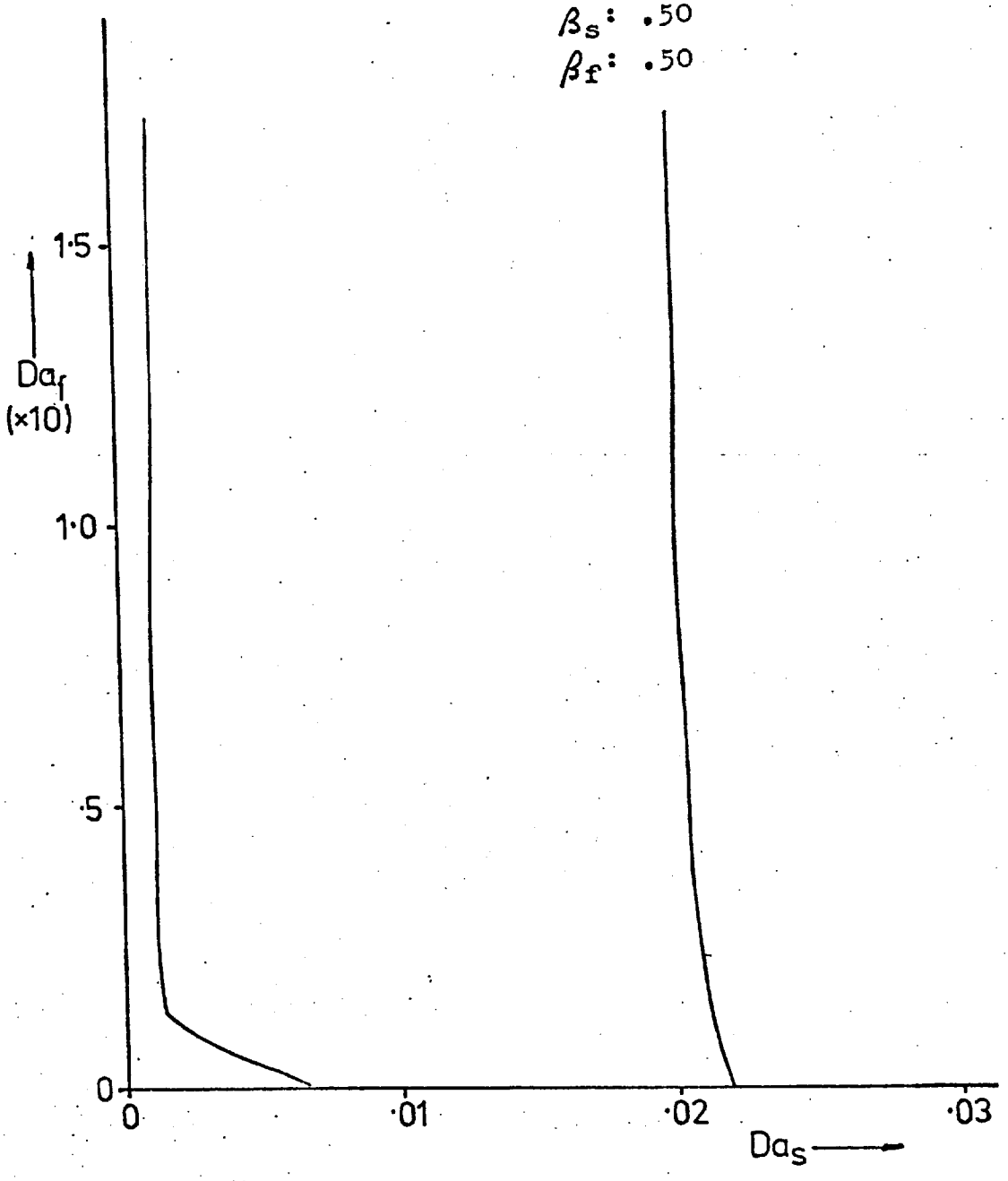

Fig 6.6 Solid phase reaction unique

Concurrent reaction scheme

Parameters: γ_s: 20.0 H: 10.0

γ_f: 30.0 K: 10.0

β_s: .20

β_f: .50

This behaviour persists in the range of H and K from 7.0 to 15.0

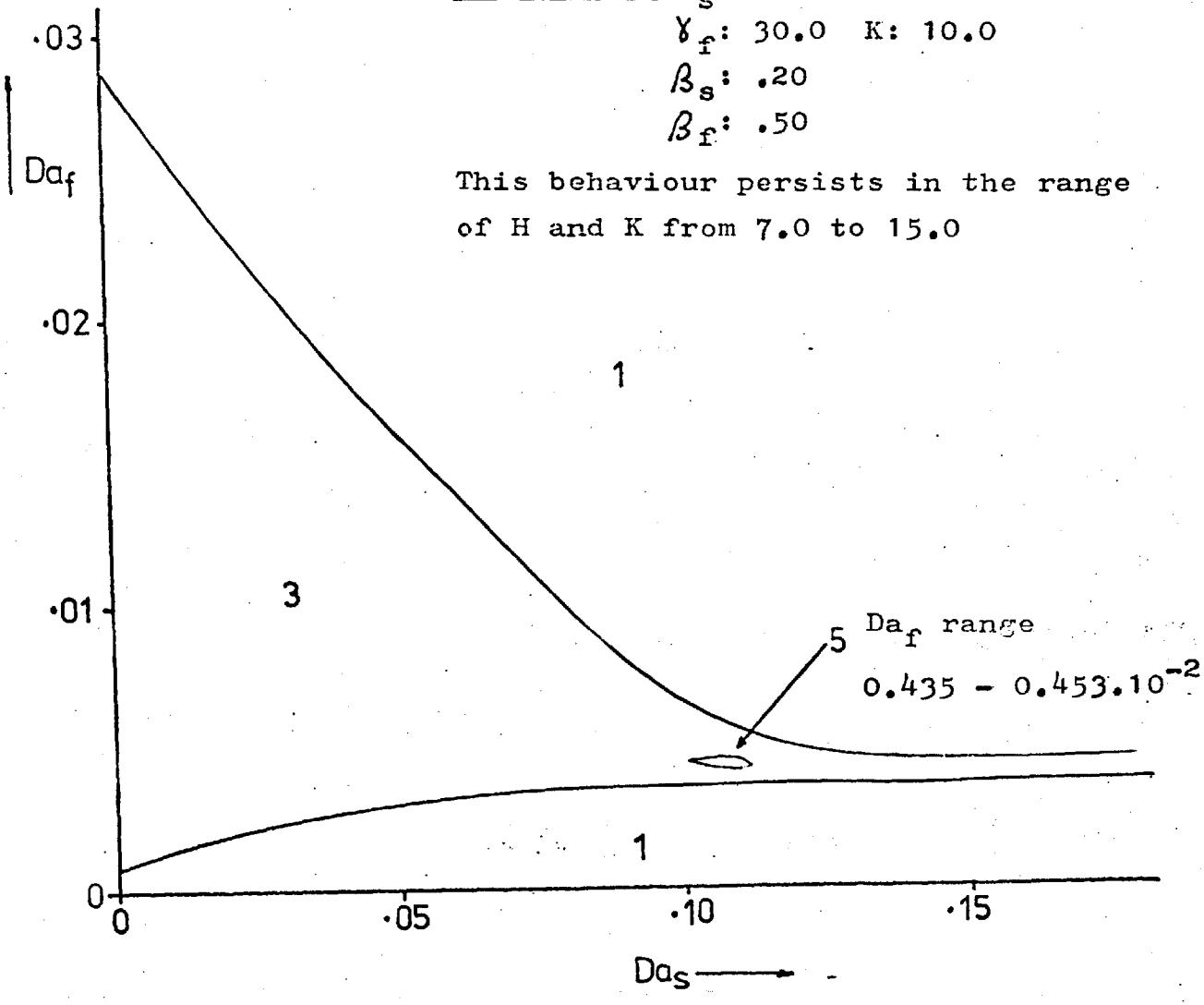

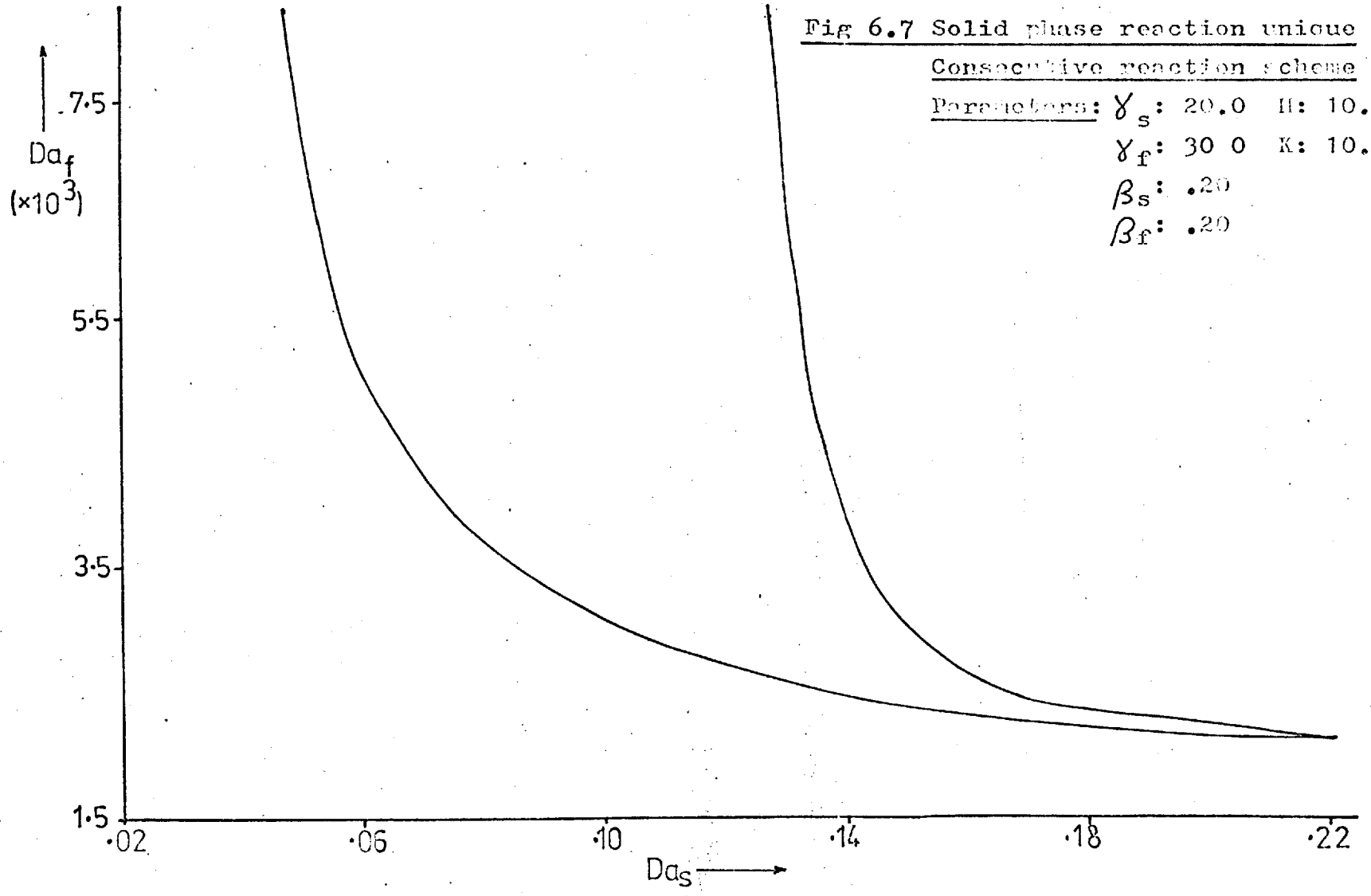

Fig 6.7 Solid phase reaction unique

Consecutive reaction scheme

Parameters: γ_s: 20.0 H: 10.0

γ_f: 30 0 K: 10.0

β_s: .20

β_f: .20

Fig 6.8 Solid phase reaction unique
(Unique due to reactor cooling)
Consecutive reaction scheme
Parameters: γ_s: 20.0 H: 10.0
γ_f: 30.0 K: 10.0
β_s: .50
β_f: .50
A : 2.0 Y_o: 1.0

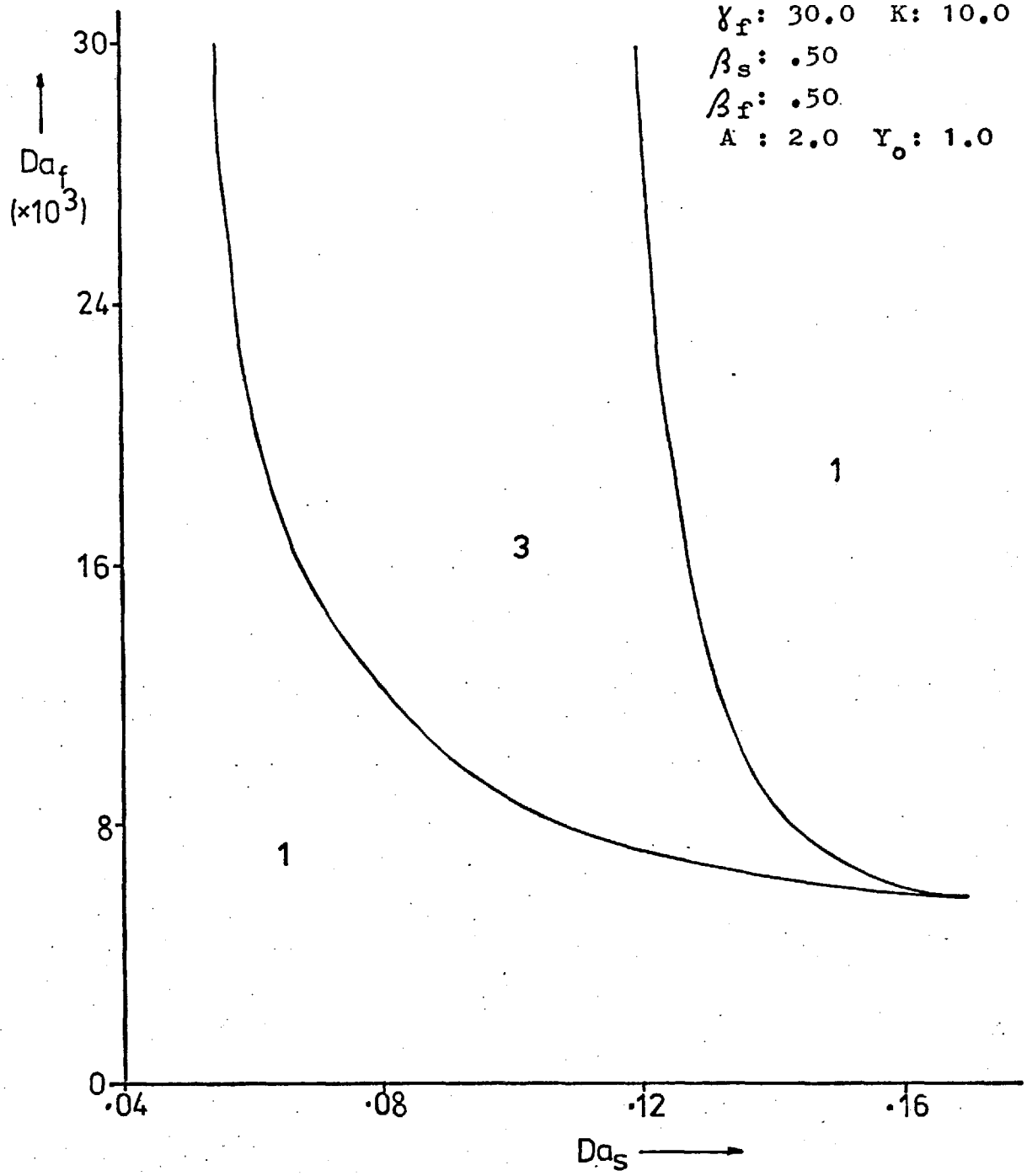

with an exothermic gas phase one. Fig. 6.9 shows the typical behaviour for a concurrent reaction scheme. For the consecutive scheme the fluid phase Damkohler numbers needed to cause an effect are similarly increased by the presence of the catalytic reaction.

When the two transport parameters differ the conditions under which the above results occur are modified but no new phenomena are introduced.

(b) Dynamic behaviour

For a gas-solid system the parameter Ls $(\frac{\rho_s Cp_s}{\rho_f Cp_f})$, which represents the ratio of the temperature time constants, has a value of about one thousand and the transient equations are thus 'stiff'. This problem can be by-passed by considering that the transient response of all the variables, except solid temperature, is so rapid that these variables are in a pseudo-steady state.

The stability of the steady states can be established by applying the Hurwitz criteria to the characteristic matrix $\underline{\underline{A}}$ of the linearized perturbation equation (Friedly, 1972)

$$\frac{d\underline{\eta}}{d\tau} = \underline{\underline{A}} \cdot \underline{\eta}$$

where $\underline{\eta} = \begin{pmatrix} (Y_s - Y_s^*) \\ (Y_f - Y_f^*) \end{pmatrix}$

This analysis yields:

(a) Det A < 0, tr A > 0 : unstable saddle point

(b) Det A > 0, tr A = 0 : centre : (limit cycle behaviour)

(c) Det A > 0, tr A < 0 : locally asymptotically stable solution.

It is apparent that for large values of Ls limit cycle or periodic phenomena cannot occur as all the system eigenvalues cannot simultaneously have zero real parts (Ray et al., 1974). The characteristic transient plots (Fig. 6.10) thus contain only nodes and saddle points.

(c) Comparison to other work

Some of the results obtained by Luss and Chen (1975) have been mentioned above. Schmitz and Amundson (1963) similarly detected five steady states under rather contrived conditions (Fig. 6.11). The present formulation exhibits these phenomena over a wider range of less severe conditions.

Fig 6.9 Endothermic solid phase reaction, exothermic gas phase reaction
Concurrent reaction scheme
Parameters: γ_s: 20.0 H: 10.0
γ_f: 30.0 K: 10.0
β_s: -.10
β_f: .50

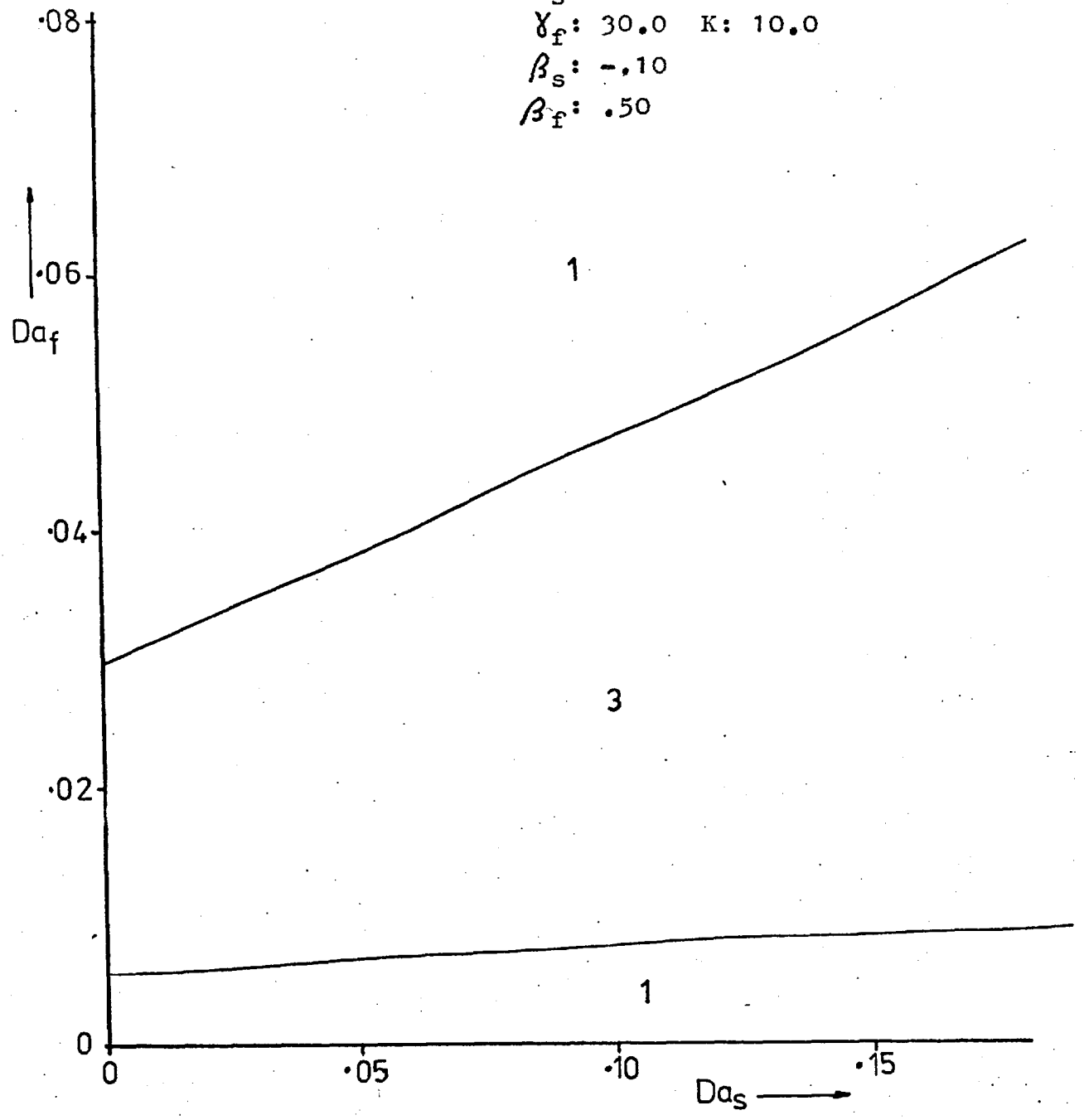

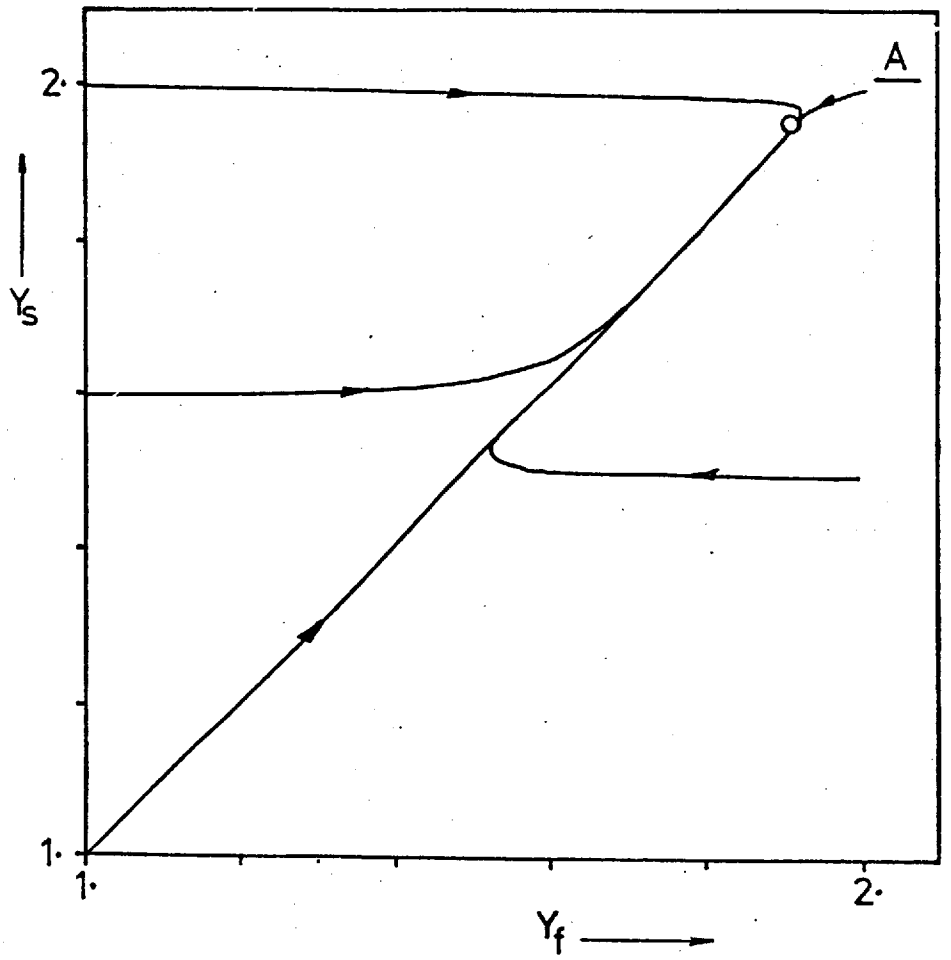

Fig 6.10 Transient behaviour - phase plane plots

Consecutive reaction scheme

Parameters: γ_s: 20.0 H: 10.0
γ_f: 30.0 K: 10.0
β_s: .50
β_f: .50

a) Da_s=0.03 Da_f=0.15 - Unique solution
b) Da_s=0.03 Da_f=$2.0.10^{-6}$ - Three solutions
c) Da_s=0.03 Da_f=$6.0\ 10^{-6}$ - Five solutions

o - node

+ - saddle point

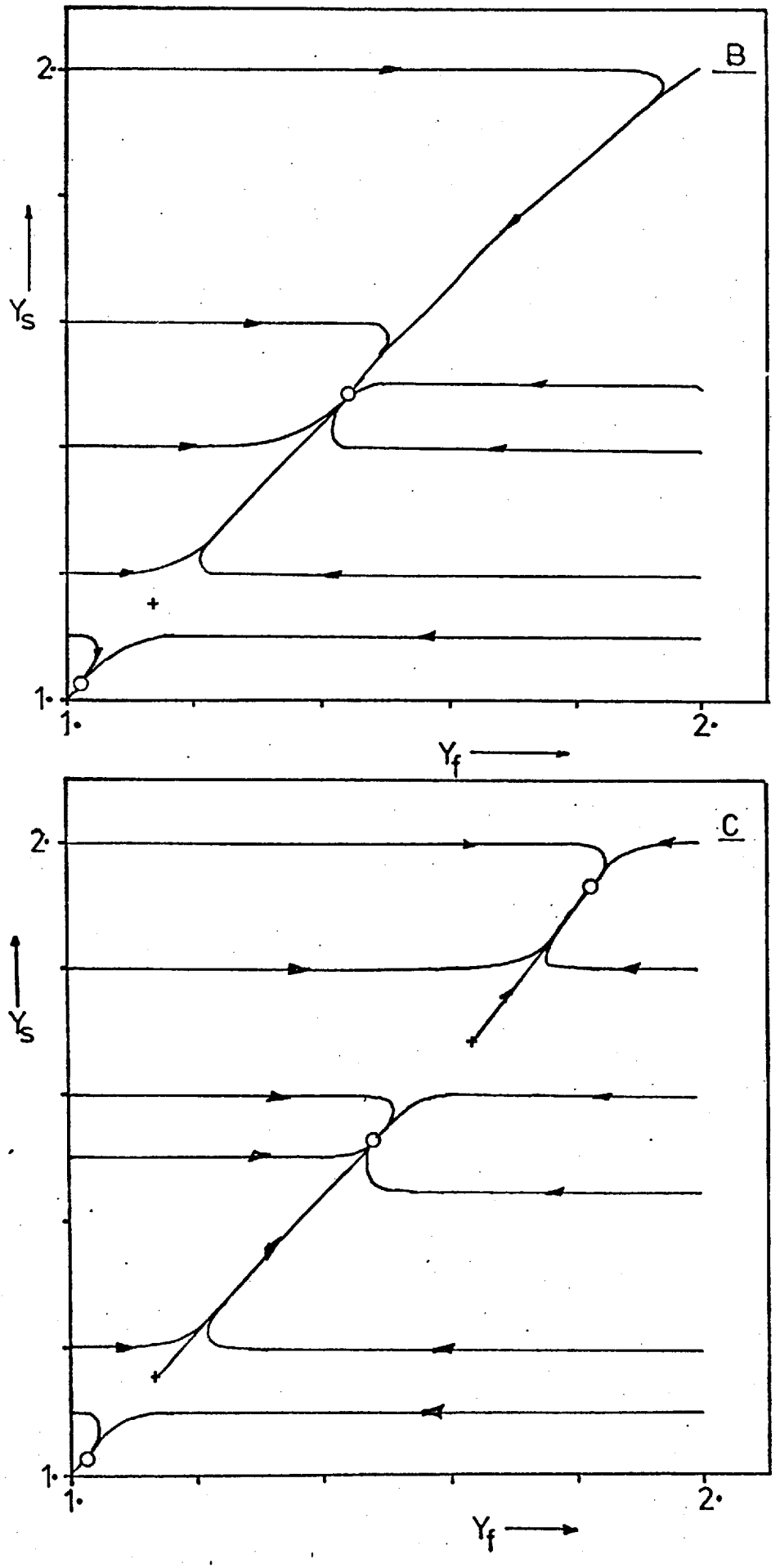

Fig 6.10 Transient behaviour(continued)

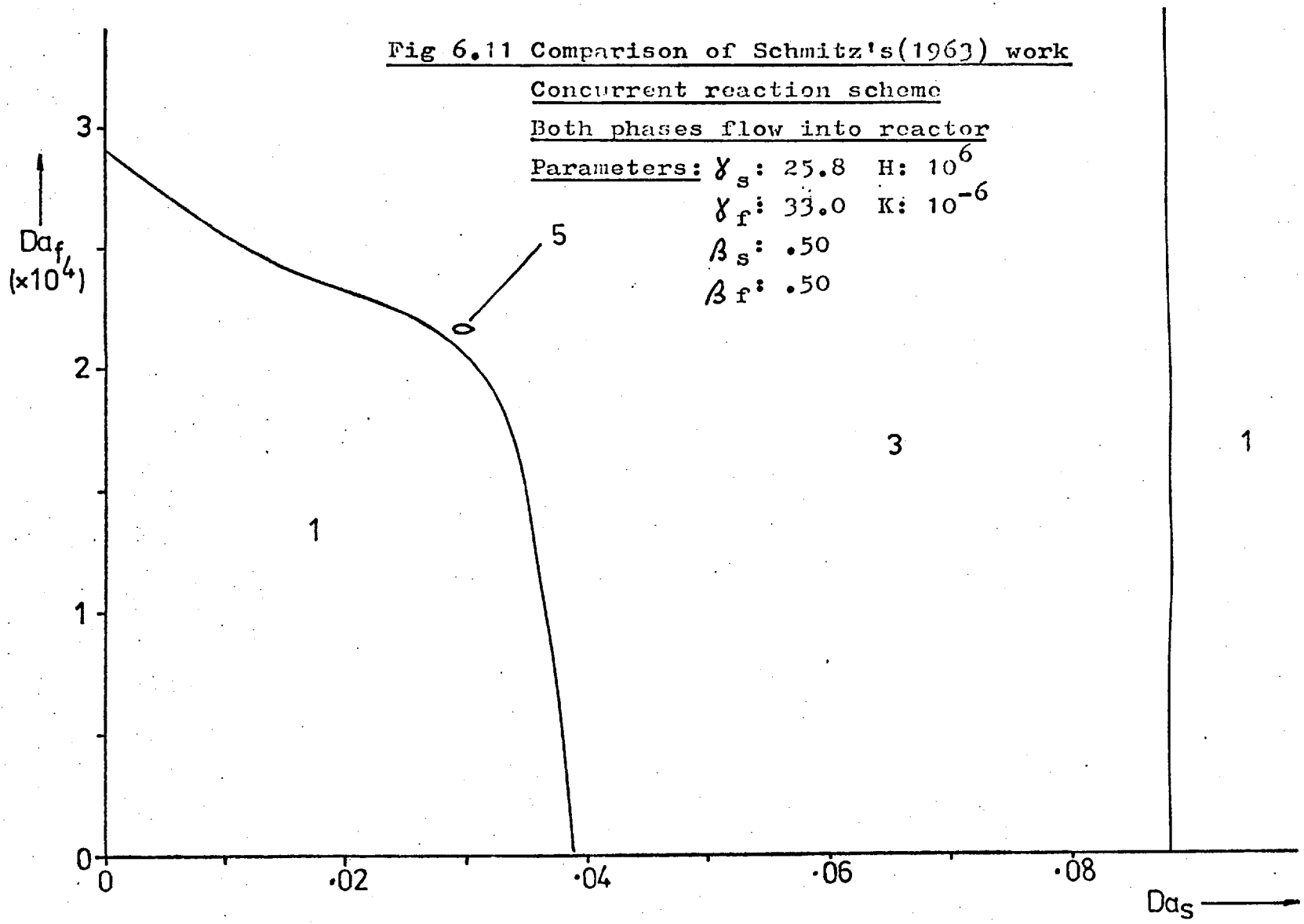

Fig 6.11 Comparison of Schmitz's(1963) work

Concurrent reaction scheme

Both phases flow into reactor

Parameters: γ_s: 25.8 H: 10^6

γ_f: 33.0 K: 10^{-6}

β_s: .50

β_f: .50

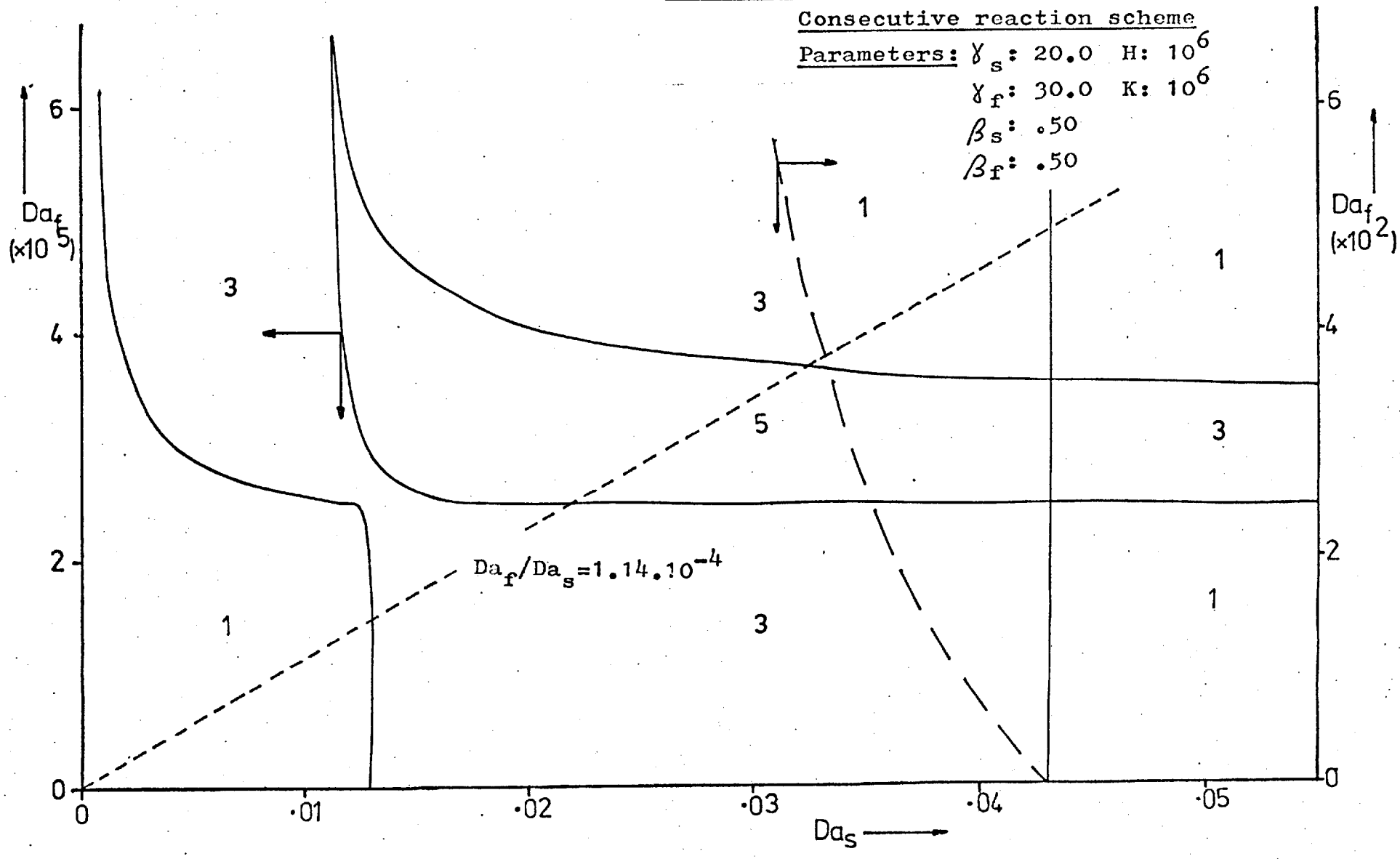

Fig 6.12 Comparison with Hlavacek's(1972) plots

Fig 6.13 Hlavacek(1972) type plot

Consecutive reaction scheme

Parameters: γ_s: 20.0 H: 10^6

γ_f: 30.0 K: 10^6

$\beta_s = \beta_f$

$Da_f/Da_s = 1.14.10^{-4}$

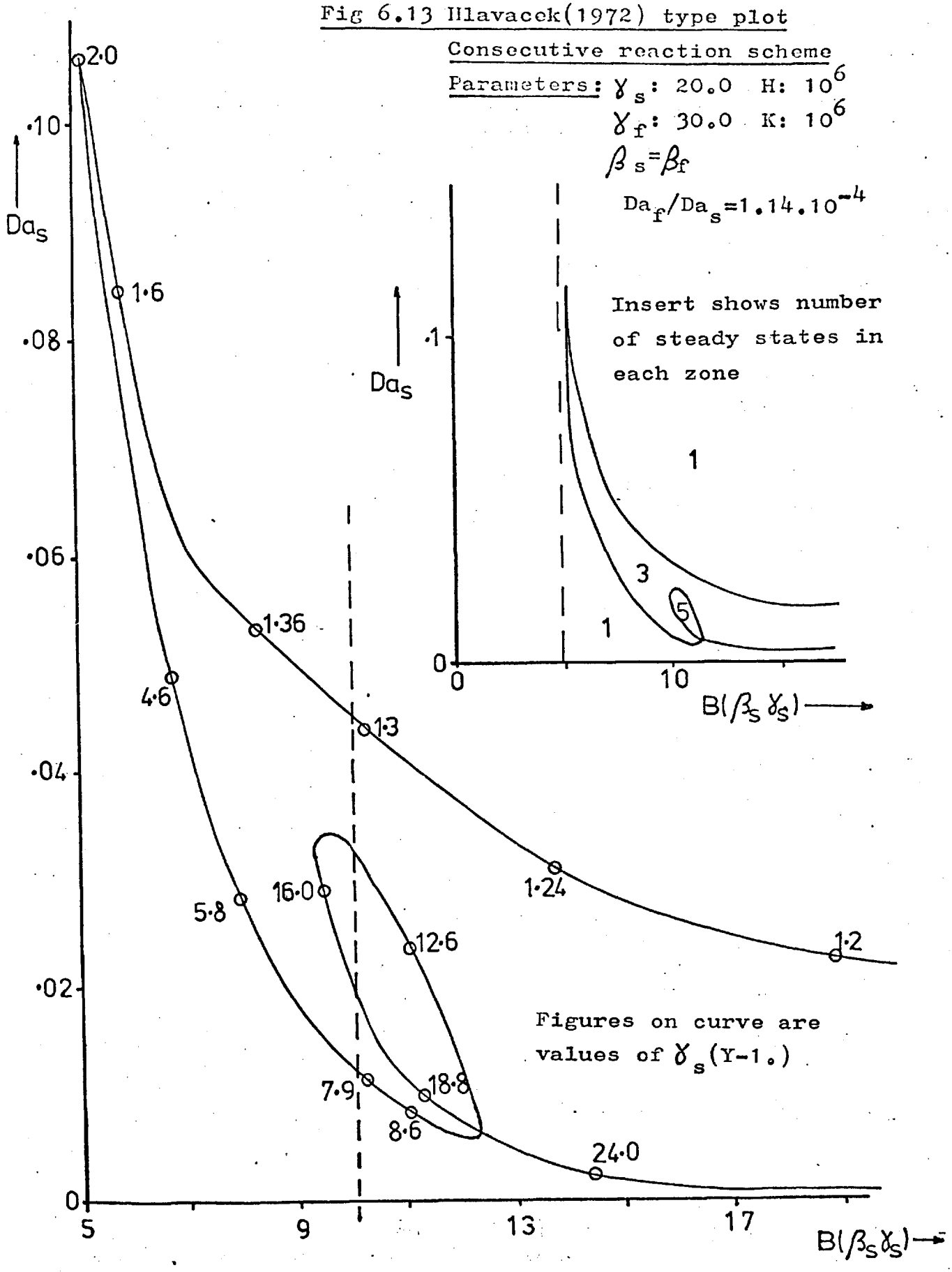

The presentation of results adopted by Hlavacek et al. (1972), which only applies to one phase systems, is compared with the diagram employed here in Figs.6.12 and 6.13. For cases where the activation energies of the two reactions do not tend to infinity diagrams of the former type are difficult to construct and a large number would be needed to encompass the range of behaviour exhibited on Fig. 6.12.

6.3.2 Extension of simple model

(a) Distributed pellet

The parameter λs describes the extent of diffusional resistance to reaction. Fig. 6.14 demonstrates the effect decreasing this parameter has on the multiplicity phenomena of the concurrent reaction scheme. (For clarity the 5 steady state zone is omitted but this is extinguished below $\lambda s = 0.1$). This diagram illustrates that although solid phase multiplicity is rapidly extinguished by decreasing λs very small extents of gas phase reaction can reintroduce multiplicity. For the consecutive scheme the results are similar, in that multiplicity is retained at low Da_f values.

(b) Imperfectly mixed fluid phase

It is to be expected that the fluid phase phenomena would be extinguished if that phase was in plug flow past the pellet. Whilst the fluid around each pellet in a packed reactor is not ideally mixed the mixing is quite intense. Matching variances of a pulse input disturbance (Levenspiel, 1962) yields that Pe = 2 is equivalent to 1.75 stirred tanks in series. Thus, although no exact treatment of the actual system is possible, the phenomena described in previous sections would be expected to persist.

(c) Other applications

The simple lumped parameter models used in the bulk of this work apply rigorously to non-porous catalyst pellets or catalytic wires. Ray et al. (1974) have demonstrated that flickering phenomena observed with catalytic wires (Edwards et al., 1973) cannot be attributed to non-uniqueness of the solid phase steady state solutions. Similarly, the characteristic transfer resistances for this system (Shah and Roberts, 1974) and the low residence time preclude any gas phase phenomena.

The steady state results developed in previous sections apply equally well to liquid-solid systems such as trickle bed and slurry reactors. As the thermal response of the two phases is more nearly equal in these

Fig 6.14 Effect of pellet diffusion

Concurrent reaction scheme

Parameters: γ_s: 20.0 H: 10.0

γ_f: 30.0 K: 10.0

β_s: .50

β_f: .50

λ_s values: a) λ_s = 1000. (stirred tank) ————

b) λ_s = 0.1 —·— ——

c) λ_s = 0.01 - - - - - - - -

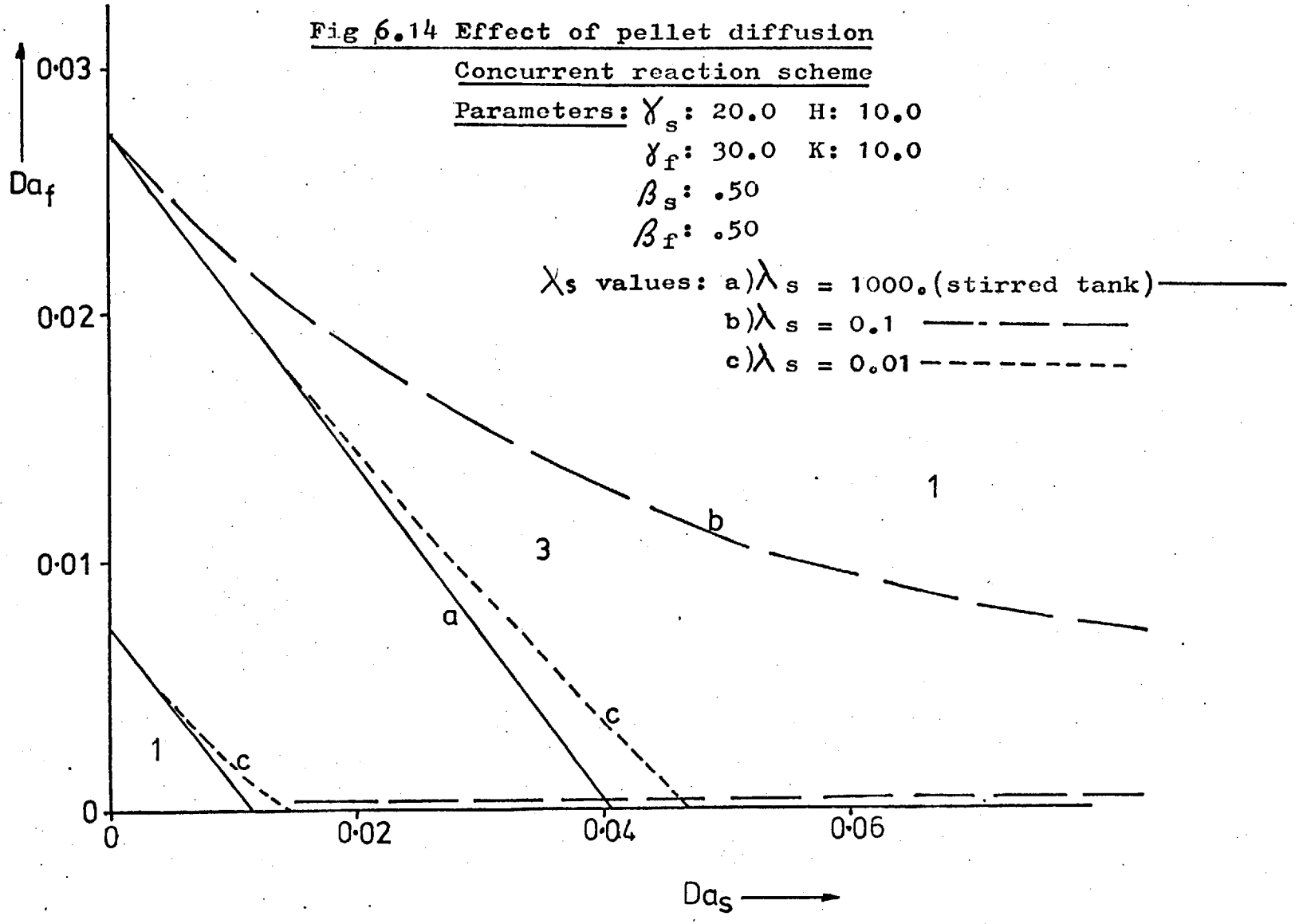

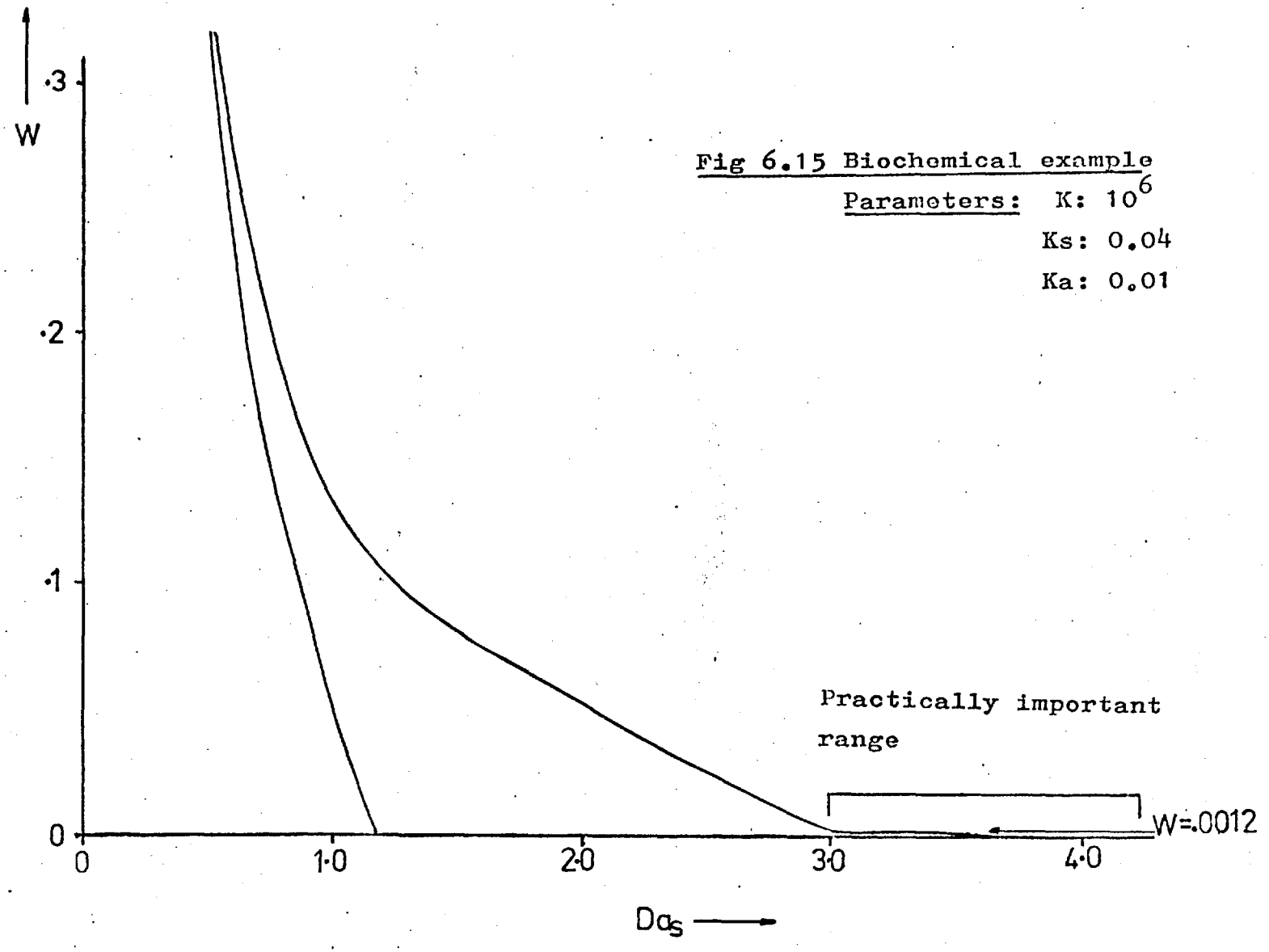

Fig 6.15 Biochemical example

Parameters: K: 10^6

Ks: 0.04

Ka: 0.01

Fig 6.16 Biochemical example

Parameters: K: 10
Ks: 0.04
Ka: 0.01

Insert shows detail at low wash-out rate

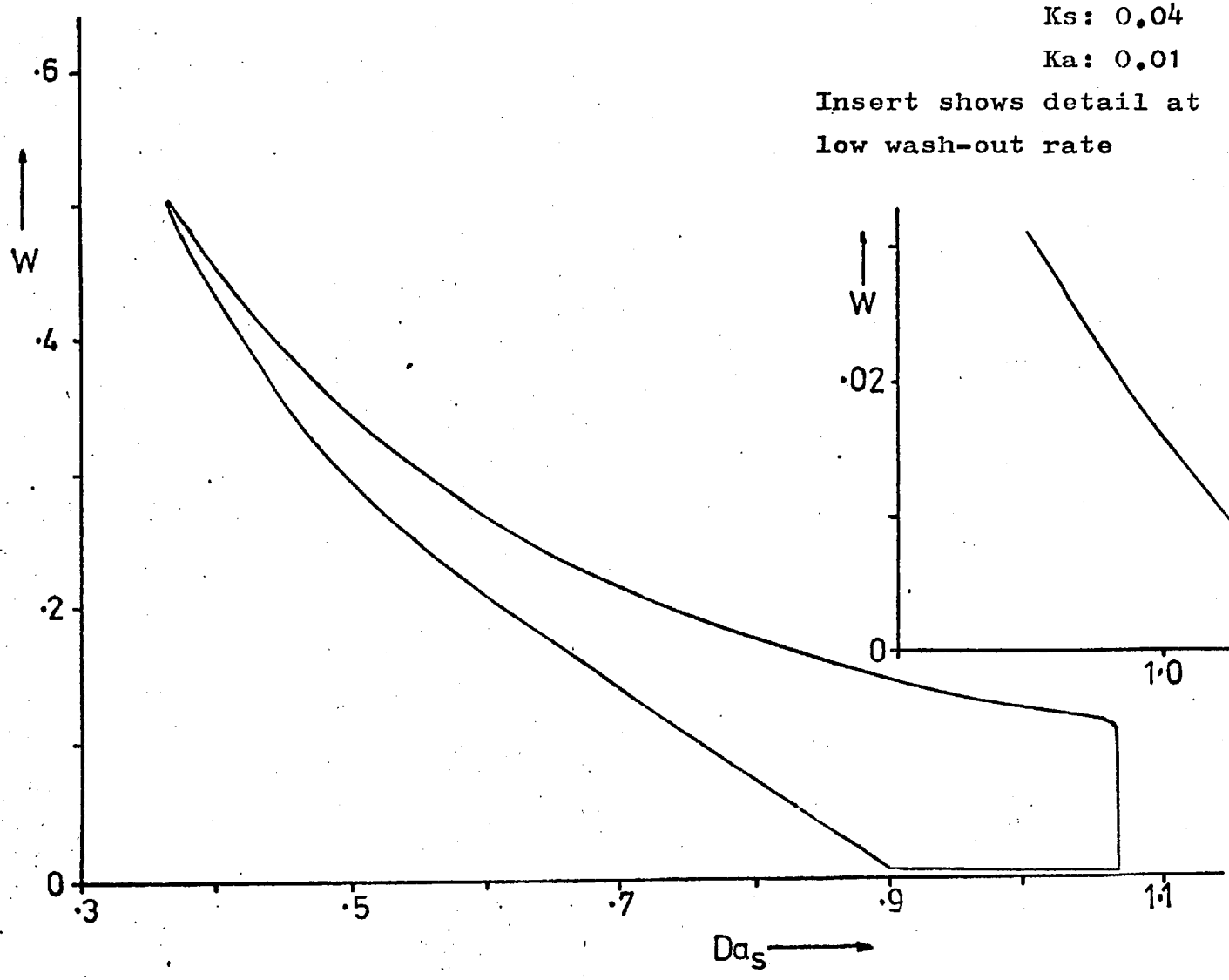

Note: Bound enzyme is unique alone

cases more complex dynamic behaviour could be anticipated.

(d) Biochemical systems

As was mentioned in the introduction product or reactant inhibited rate laws can lead to concentration multiplicity under isothermal conditions.

O'Neil et al. (1971) demonstrated this phenomena for a bound enzyme system in a backmix reactor. In general the specific activity of the enzyme drops with time as enzyme is washed out of the reactor (Aiba et al., 1973). The model of O'Neil et al. (1971) is extended to include eluted enzyme, which remains active, and a mass transfer resistance between the solid and fluid phases (see Appendix A.4).

Typical results, presented as plots of washout rate (W) versus Damkohler number, are given in Figs. 6.15 and 6.16. For an enzyme reaction system to be of practical importance the wash out rate must be low so that high specific activity is retained. The results indicate that under realistic wash-out conditions (say $W < 0.01$) the range of multiplicity phenomena is extended or non-uniqueness is introduced. These types of system are also novel in that the Damkohler number decreases with time. Thus, design is restricted to initial Damkohler numbers smaller than the lower multiplicity limit.

6.4 Conclusions

This study has shown that the introduction of a gas phase reaction into a fixed bed reactor system can introduce effects which are not present in the absence of either the extra reaction or phase segregation. Apart from, in some cases, increasing the number of possible steady states the region of solid phase parameters over which mulitplicity phenomena occur is greatly extended. This has important implications in the design and optimization of chemical reactors as it broadens the area of multiplicity and thus restricts the operational range. Experimental verification of non-uniqueness phenomena may be made easier as the phenomena are less sensitive to variations in experimental parameters.

DISCUSSION AND CONCLUSIONS

DISCUSSION AND CONCLUSIONS

This study was initiated with the primary aim of elucidating when and if any important heterogeneous-homogeneous effects occur in packed bed chemical reactors. A digression from this main theme has shown the inadequacy, for design purposes, of the available heat transfer estimation techniques. Fortunately, the practical values of film heat transfer resistance generally makes a two phase model unnecessary, thus circumventing the unsatisfactory allocation of continuum parameters between the separate phases.

A generalised study of heterogeneous-homogeneous reaction schemes indicates that the changes in reactor performance are not facilitated by the introduction of an interphase resistance. However, for an initially neglectable reaction to significantly modify the observable reactor behvaiour the activation energies of this and the main reaction must be very disparate. This behaviour is not typical of two catalytic reactions, but would be more readily exhibited by a two phase reaction scheme. Case studies support these findings in that initially neglectable reactions, with similar activation energies to the main reaction, have a negligible effect on performance. It can be anticipated that the necessary parameters would be exhibited by the oxidation of alcohols and hydrocarbons with higher molecular weights than those considered here. The results obtained differ from those reported by Holton (1975) in predicting different kinetics for the gas phase oxidation of formaldehyde and in not detecting instabilities due to gas phase reactions. The presence of a concurrent gas phase reaction leads to more even heat release thus lowering the film temperature difference and improving stability.

The comparison of reactor simulation results for the butene-butadiene system with pilot plant data indicates that gas phase oxidation occurs to a negligible extent. Catalyst preparation temperature was, however, found to be an important and largely unexplored variable.

Multiplicity studies using an idealized model of a single catalyst pellet and its fluid environment have shown that the presence of a gas phase reaction can significantly increase the range of parameters over which non-uniqueness of solutions occurs. Phenomena dependent on the presence of interphase resistance and the division of the reactions between the phases have also been established. As an aside, the conditions under which multiplicity of solutions occurs for

supported enzyme systems have been extended by considering the possibility of active eluted enzyme.

Three areas have been identified as requiring further experimental work:

(a) Clarification of heat transfer correlations.

(b) Investigation of the effect of catalyst preparation temperature on the activity of tin-antimony oxide catalyst for butene oxidative dehydrogenation.

(c) Practical demonstration of theoretical non-uniqueness phenomena. A contribution has been made to this largely neglected area by showing that these effects could be more relevant to actual systems and are less sensitive to parameter uncertainty than was known hitherto.

In summary the following conclusions can be drawn:

(1) As two phase models are generally unnecessary, for design purposes, the inclusion of a gas phase reaction adds only to the kinetic complexity of the models.

(2) For a small extent of an additional reaction to significantly modify reactor performance its thermal parameters must be much larger than those of the main reaction. A condition more characteristic of a gas rather than a solid phase reaction.

(3) Of the case studies considered, the methanol and butene systems did not exhibit any change in performance when the gas phase reaction was introduced. The two concurrent schemes, nitrous oxide and carbon monoxide oxidations, did, however, demonstrate that gas phase reactions can significantly modify reactor behaviour.

(4) The presence of fluid phase reactions can increase the parameter ranges over which non-uniqueness of steady state solutions are predicted by models of a single catalytic pellet together with its surrounding fluid and a biochemical slurry reactor.

APPENDIX A.1 - NUMERICAL METHOD

Holton (1975) employed finite difference methods for the solution of the two dimensional reactor models; whilst being generally satisfactory these methods required about 100 secs of central processor time (CDC 6400) per simulation. In this study the more rapid method of orthogonal collocation has been applied.

A.1.1 Collocation procedures

Orthogonal collocation is one of the family of weighted residual methods in which an approximate solution is sought by requiring that the 'residual', obtained by substituting an approximating polynomial into the original differential equation, is zero at some specified points. In orthogonal collocation the collocation points are taken as the roots of the approximating polynomial. The choice of the latter is, however, largely a matter of numerical experience. For boundary value problems, this has been overcome by employing trial functions which satisfy the boundary conditions (Villadsen and Stewart, 1967).

Orthogonal collocation can either be applied directly across the whole integration field, as in this study, or the integration range can be broken into a series of finite elements over which the method is applied separately (Carey and Finlayson, 1975). This latter approach has been applied to effectiveness factor calculations for cases where most of the reaction occurs in a small effective reaction zone of the pellet (Paterson and Cresswell, 1971).

The approximation can be expressed in terms of the values of the variable at the collocation points, rather than as functions of the polynomial coefficients, making a simple matrix solution possible. Accurate quadrature formula are also available to enable the abstraction of properties requiring integration. Orthogonal polynomials are defined by:

$$\int_0^1 w.Pj(u) \; . \; Pi(u).x^{a-1} \, dx = Di.\delta ij \qquad (A.1.1)$$

where $j = 1, i$

Pi is the polynomial

w(x) is the weighting function

u is a function of x

$\delta ij = 1, \quad i = j$

$= 0, \quad i \neq j$

and Di is some constant.

Table A.1.1 - Polynomial types

Name	Definition	Comment
Jacobi	$w = 1 - x^2$ $u = x^2$ Application: $y(1) = y(x) + (1 - x^2)$. (A) $\sum a_i P_{i-1}(x^2)$	Symmetrical about origin. Applied to effectiveness factor calculations etc.
Legendre	$w = 1$ $u = x^2$ Application: as Jacobi	As Jacobi, but often more rapid
Shifted Legendre	$w = 1$ $u = x$ Application: $y(x) = b + cx + x(1 - x) \sum a_i P_{i-1}(x)$	No special symmetry properties. Applied to axial dispersion problem.

Equation (A) (Table A.1.1) is a polynomial of degree N in x^2 and can be expressed as:

$$y(x) = \sum_{i=1}^{N+1} p_i \, x^{2i-2}$$

where p_i are constants.
Differentiating this and evaluating the expressions at each collocation point (i.e. j = 1, N + 1) gives:

$$y(x_j) = \sum_{i=1}^{N+1} x_j^{2i-2} \, p_i$$

$$\frac{\partial y}{\partial x}\bigg|_{x_j} = \sum_{i=1}^{N+1} \frac{\partial x^{2i-2}}{\partial x}\bigg|_{x_j} p_i$$

Expressing this in matrix form, with $\underline{P}$ and $\underline{Y}$ the vector of p_i and $y(x_j)$ respectively, yields:

$$\underline{Y} = \underline{\underline{Q}} \cdot \underline{P} \quad \text{and} \quad \frac{\partial \underline{Y}}{\partial x} = \underline{\underline{S}} \cdot \underline{P}$$

where $q_{ij} = x_j^{2i-2}$ (an element of matrix $\underline{\underline{Q}}$)

and $s_{ij} = \dfrac{\partial x^{2i-2}}{\partial x}\bigg|_{x_j}$ (an element of matrix $\underline{\underline{S}}$)

Eliminating $\underline{P}$ gives:

$$\frac{\partial \underline{Y}}{\partial x} = \underline{\underline{S}} \cdot \underline{\underline{Q}}^{-1} \cdot \underline{Y}$$

$$= \underline{\underline{A}} \cdot \underline{Y}$$

Matrix $\underline{\underline{A}}$ thus replaces the differential operator $\frac{\partial}{\partial x}$. A similar treatment is followed for the second derivative. Finlayson (1974) has reviewed the method and presents tables of polynomial zeros. In the absence of published values polynomial roots were obtained by successive application of Graeffe's root squaring (Carnham et al., 1969) and Newton's methods.

In reactor simulation problems orthogonal collocation lowers computer time by drastically reducing the number of 'grid' points required for a given accuracy, compared to finite difference techniques (Ferguson and Finlayson, 1972). The time involved in solving the resulting matrix

equations may exceed that needed for a finite difference scheme but much less kinetic information has to be calculated and herein lies the computational saving.

A.1.2 Application to present models

All the equations used in the steady state simulations have the general form:

$$A\frac{\partial^2 y}{\partial z^2} + B\frac{\partial y}{\partial z} + C\frac{1}{R}\frac{\partial}{\partial R}\left(R\frac{\partial y}{\partial R}\right) + R_s = 0$$

where R_s is the kinetic term, and A, B, C are constants.

(a) For initial value problems in z (i.e. A = 0), e.g. fluid phase equations for the two dimensional reactor, the remaining second derivative can be removed by collocation and the resulting set of ordinary differential equations (one for each radial grid point) can be solved by some simple integration method (e.g. trapezium rule).

(b) For boundary value problems, such as the pellet model in Chapter 5, application of orthogonal collocation, to replace all the derivatives, yields an equation like (A.1.2).

$$(A.1.2) \quad A\sum_{j=1}^{nz} bz_{jz,j} \cdot y_{j,kr} + B\sum_{j=1}^{nz} az_{jz,j} \cdot y_{j,kr} + C\sum_{k=1}^{nr} br_{kr,k} \cdot y_{jz,k} + R_s = 0$$

for $kr = 2, nr - 1$

$jz = 2, nz - 1$

$i = 1, m$

where nr = number of radial collocation points

nz = number of axial collocation points

m = number of species

$az_{jz,j}$ etc. are elements of the collocation matrices $\underline{\underline{A}}$ etc.

and $y_{j,k}$ denotes the value of y at grid point j,k.

Boundary conditions of the form

$$\left.\frac{\partial y}{\partial R}\right|_{R=1} = F(y)$$

where F is some function of y, are expressed as:

$$\sum_{k=1}^{nr} ar_{nr,k} \cdot y_{jz,k} = F(y_{jz,nr}) \qquad jz = 1, nz \qquad (A.1.3)$$

This set of non-linear algebraic equations can be solved by a Newton-Iterative Scheme (Young and Finlayson, 1973) but the Jacobian matrix can become quite large for modest polynomial orders if a number of reacting species are involved. Inspection of equations A.1.2 and A.1.3 shows that coupling between the different species only occurs via the reaction expression. The resulting Jacobian structure was exploited by removing the reaction rate derivatives and thus obtaining a smaller constant Jacobian for each species

$$\underline{\underline{J}} = \begin{bmatrix} \underline{\underline{j}} & & 0 \\ & \underline{\underline{j}} & \\ 0 & & \underline{\underline{j}} \end{bmatrix} + \begin{bmatrix} \diagdown\!\diagdown & & \\ & \diagdown\!\diagdown & \\ & & \diagdown\!\diagdown \end{bmatrix}$$

The sparse diagonal matrix, $\underline{\underline{D}}$, can be more compactly stored as the set of vectors $\underline{d}_{ij}$, where $\underline{d}_{ij}$ is the vector of rate expression derivatives for species i with respect to species j at each grid point.

A full Newton alogorithm would consist of

$$\underline{Y}^{\ell+1} = \underline{Y}^{\ell} - \underline{\delta}$$

where $\underline{\delta} = \underline{\underline{J}}^{-1} \cdot \underline{F}$

and ℓ is an iteration parameter.

Using the Jacobian structure described above a sequential solution procedure for each species in turn can be obtained:

$$\underline{\delta}_i^{\ell+1} = \underline{\underline{j}}_i^{-1} \cdot (\underline{f}_i - \sum_{j=1}^{m} d_{ij} \underline{\delta}_j^{\ell})$$

(for i = 1, m)

where $\underline{F}$ and $\underline{\delta}$ have each been broken into m fragments ($\underline{f}_i$, $\underline{\delta}_i$), one for each species. As $\underline{\underline{j}}_i$ is constant, throughout the iterations, only one inversion is required per solution. The procedure increases the number of iterations required but was found to be up to five times faster than the Newton technique. Unlike a Newton scheme, convergence from some neighbourhood of the solution cannot be proved but no problems were

encountered during the study reported here.

A.1.3 Convergence of solutions

The numerical method outlined above was tested for convergence using Jacobi polynomials with weighting functions $w = 1$ and $w = 1 - x^2$. Finlayson (1974) has suggested that the first type of polynomial is more rapid in chemical engineering applications as the zeros are nearer the boundary $r = 1$, where gradients are steepest. The alternative polynomial normally gives more accurate results.

The convergence of the reactor models was tested using an extreme Nitrous oxide reactor example (see Table A.1.2). The results of radial and axial convergence tests are summarized in Tables A.1.2 and A.1.3 respectively. The two phase model was also compared to the results of DeWasch and Froments (1971) simulation for hydrocarbon oxidation. Within the limits of the data and results presented by the authors the two fomulations agree in their predictions. Convergence results for the single pellet model from Chapter 5 are summarized in Table A.1.4.

The numerical methods can be seen to be converging to a definite solution, independent of the polynomial used. Reactor results have generally been obtained with NR = 5 and w = 1. The single pellet model has been utilized in reactor simulations with NR = NZ = 2 which is accurate enough ($\pm$ 10%) for this purpose.

Table A.1.2 - Radial convergence of 2D2P model

Conditions: Gs: 1.10 Dt: 0.04 m AL: 1.0 m

Dp: 0.03 m T: 1125 K

X: 0.667 NZ: 810

	NR	w = 1	$w = 1 - x^2$
$Tmax_s$	3	470.42	476.31
Conv		97.20	94.10
$Tmax_s$	4	488.77	490.42
Conv		95.72	96.00
$Tmax_s$	5	489.52	490.15
Conv		95.68	95.70
$Tmax_s$	7	489.69	490.15
Conv		95.68	95.72

Table A.1.3 - Axial convergence of 2D2P model

Conditions : As above with NR = 5, w = 1

NZ	450	630	810	1260
$Tmax_s$	490.31	489.72	489.52	489.54
Conv	95.85	95.70	95.68	95.66

Table A.1.4 - Convergence of single pellet model solutions

Species	NR = NZ	Effectiveness factor	
		w = 1	$w = 1 - x^2$
1	2	.7565	.8198
3		.6540	.7456
Cp time (secs)		1.71	2.1
1	3	.7936	.7950
3		.7073	.7100
Cp time (secs)		3.71	3.91
1	4	.7972	.7966
3		.7124	.7118
Cp time (secs)		7.36	6.84

Note: Species 1 = Oxygen
Species 3 = Butadiene

APPENDIX A.2 - THE KINETICS OF GAS PHASE FORMALDEHYDE OXIDATION

Formaldehyde oxidizes in the gas phase via a free radical chain reaction. The reaction has received considerable study because of its importance in more complex chain reactions and the reactants and products simplicity. In this appendix the steps necessary to obtain the overall kinetic expression used in section 4.4.2 are described.

A.2.1 Reaction scheme

Hessam (1971) carried out a mass-spectroscopic study of this reaction and postulated the following kinetic scheme:

(1) $HCHO + O_2 \rightarrow HCO + HO_2$

(2) $HCO + O_2 \rightarrow HCO_3$

(3) $HCO_3 + HCHO \rightarrow HCO_3H + HCO$

(4) $HCO_3H \rightarrow OH + \text{products}$

(5) $HCO + O_2 \rightarrow HO_2 + CO$

(6) $OH + HCHO \rightarrow HCO + H_2O$

(7) $HO_2 + HCHO \rightarrow OH + \text{products}$

(8) $HO_2 + HCHO \rightarrow H_2O_2 + HCO$

(9) $2HO_2 \rightarrow \text{termination.}$

This scheme involves only gas phase terminations, although gas-solid terminations have been proposed (Vardanyan et al., 1974). Applying the usual steady state approximation to the intermediate radicals gives:

$$\frac{\partial}{\partial t}[HCHO] = [HCHO]^2 \cdot \left\{ \frac{(k_7 + k_8)^2}{(k_5 - k_2)^2} \frac{k_2^2}{k_9} + \frac{k_2 k_7}{k_9} \frac{(k_7 + k_8)}{(k_5 - k_2)} + \frac{(k_7 + k_8)^2 \, k_2}{k_9 \, (k_5 - k_2)} \right\}$$

For k_2^2 small and $k_7 = k_8$ this reduces to

Table A.2.1 - Kinetic data for formaldehyde oxidation

Reaction	$Log_{10}A$	E (kcal/mol/k)	Source
2	3.9 - 4.2	0	(see analysis which follows)
5	7.78	0	Vardanyan et al. (1974)
7	10.06	11.0	Vardanyan et al. (1974) and Hessam (1971)
8	10.06	11.0	
9	8.78	0.0	

$$-\frac{\partial [HCHO]}{\partial t} = \frac{6\, k_2 k_8^2\, [HCHO]^2}{k_9\,(k_5 - k_2)}$$

Hessam suggests that reaction (2) competes unfavourably with reaction (5) and hence $k_2 << k_5$. No data for the value of k_2 is available in the literature; Holton associates reaction (2) with the analogous reaction for the acetyl radical

(2') - $CH_3CO + O_2 \rightarrow CH_3CO_3$

(5') - $\rightarrow CO + CH_3CO_2$

However, the ratio $k_2'/k_5 \simeq 3$ in contradiction of Hessam's results. A more correct approach would be to associate the ratio (k_2/k_5) with (k_2'/k_5') for the acetyl scheme, rather than using an odd pair of reactions.

As no published data is available (Hochstim, 1969; Ratajack, 1967 and 1969; Kerr, 1972) a method of estimating either k_2 or k_5' was sought. As, however, k_5' pertains to an exchange reaction no estimate is possible. An estimation method is, however, available for the association reaction (Benson, 1968)

(2) - $HCO + O_2 \underset{y}{\overset{x}{\rightleftharpoons}} HCO_3$

This consists of:

(a) Obtaining the standard entropy change for the reaction.

(b) Hence obtaining the equilibrium constant for the reaction ($Keq = e^{\Delta S/R}$).

(c) Considering the decomposition (reaction y) postulate an intermediate which forms slowly, but decomposes rapidly and its rate of formation is thus the limiting step.

($k_y = \frac{e\,k\,T}{h}\, e^{\Delta S+/R}$, where $\Delta S+$ is the entropy change in moving to the complex, k is Boltzmans constant and h is Plancks constant).

(d) Finally evaluating k_x, the required result.

Benson (1968) contains extensive tables of group and bond entropy contributions, necessary for the estimation.

Working through this analysis gives k_2 in the range $\underline{(0.85 - 1.57)\ 10^4\ m^3\ kmol^{-1} sec^{-1}}$ and thus (k_5/k_2) lies between 3.81 and 7.12×10^3 in line with Hessam's (1971) experimental findings. Introducing this data into the overall kinetic scheme gives

$$-\frac{\partial[HCHO]}{\partial t} = (0.61 - 1.14)\ 10^8 . e^{-22/RT}[HCHO]^2$$

Hessam (1971) obtained the following results for this decomposition in a glass sphere with an initial formaldehyde pressure of 30 mm mercury.

Temperature (K)	Max rate ($\times 10^7$) (kmole/m^3sec)
623	23.8
643	36.62
658	49.37
673	54.55
693	99.40

Fitting these results using the model

$$-\frac{\partial[HCHO]}{\partial t} = ko\ e^{-22/RT}[HCHO]^2$$

gives ko = $\underline{1.96 . 10^8}$. The agreement between this result and the theoretical prediction is quite good considering the approximations involved in the latter. This result should be contrasted with a value for ko of $3.9 . 10^{14}$ obtained by Holton (1975), using the incorrect (k_2/k_5) ratio. Holton (1975) obtained an overall value for the heat of reaction, using Hessam's (1971) product spectrum, of $(-\Delta H)_{298}$ = $9.3 . 10^6$ J kg^{-1} HCHO. This value has also been used in this study.

A.2.2 Effect of surface area to volume ratio and nature of surfaces

The scheme discussed above involves only a gas phase termination reaction and thus the surface to volume ratio of the reactor or the nature of the surface are not parameters. Various surface terminations have been proposed (Vardanyan et al., 1971), involving H_2O_2 and HO_2 radicals, where doping of the reactor walls had a profound effect on

the rate. Lewis and Von Elbe (1961) reviewing earlier results for this reaction conclude that:

(a) The rate is independent of vessel size and hence chain termination and initiation must be either gas phase or surface effects.

(b) Inert gas inhibition of the rate precludes surface terminations (and thus surface initiation).

(c) The activation energy is 21 kcal/mole at 325 - 370°C rising to 39 kcal/mole at 450 - 470°C due to an increase in radical chain length.

Most experimenters use total pressure rise as a measure of extent of reaction but many intermediate steps are isobaric. Most experimental results in the field of free radical kinetics have been obtained at low reactant pressures in vessels with a small surface to volume ratio (Mulchahy, 1973). The applicability of these results to a reactor environment, where the surface area to volume ratio is much larger, is open to doubt.

APPENDIX A.3 - BUTENE - BUTADIENE KINETIC MODELLING

A.3.1 Heterogeneous kinetics

Gabbay (1969) obtained the following kinetic information for the oxidative dehydrogenation of butene to butadiene over a tin-antimony oxide catalyst (Sn : Sb = 1 : 4), supplied by B.P. Chemicals (International). The reaction scheme is summarized in Figure A.3.1. Table A.3.1 contains the stoichiometric equations and Table A.3.2 summarizes the kinetic parameters.

Table A.3.1 - Details of Butene - Butadiene catalytic reaction scheme

Reaction	
1	$C_4H_8 + {}^1\!/_2O_2 \rightarrow C_4H_6 + H_2O$
2	$C_4H_8 + 6O_2 \rightarrow 4CO_2 + 4H_2O$
3	$C_4H_8 + 4O_2 \rightarrow 4CO + 4H_2O$
4	$C_4H_8 + {}^3\!/_2O_2 \rightarrow C_4H_4O + 2H_2O$
5	$C_4H_8 + {}^5\!/_2O_2 \rightarrow C_3H_4O + CO_2 + 2H_2O$
6	$C_4H_8 + {}^1\!/_2O_2 \rightarrow C_3H_7CHO$
7	$C_4H_8 + O_2 \rightarrow 2CH_3CHO$
8	$C_4H_6 + {}^{11}\!/_2O_2 \rightarrow 4CO_2 + 3H_2O$
9	$C_4H_6 + {}^7\!/_2O_2 \rightarrow 4CO + 3H_2O$
10	$C_4H_6 + O_2 \rightarrow C_4H_4O + H_2O$
11	$C_4H_6 + 2O_2 \rightarrow C_3H_4O + H_2O + CO_2$
12	$C_4H_6 + H_2O \rightarrow C_3H_7CHO$
13	$C_4H_6 + 3O_2 \rightarrow CH_3CHO + 2CO_2 + 2H_2O$

Reactions 14 - 19 are isomerizations between the various butene species.

Fig A.3.1 - Schematic of Butene - Butadiene heterogeneous kinetics

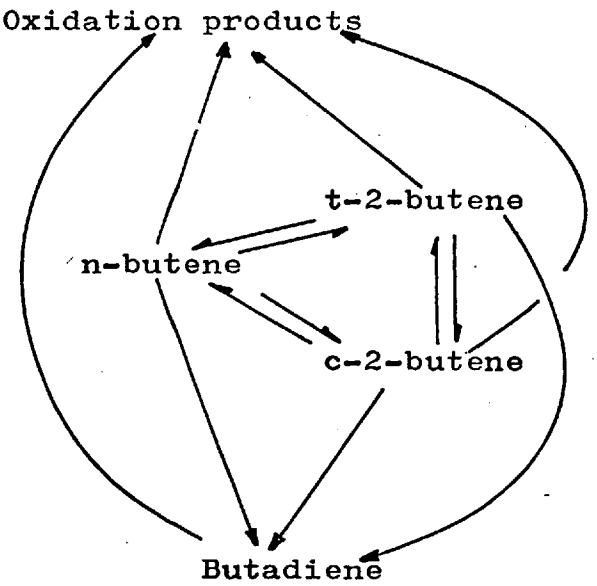

Table A.3.2 - Kinetic parameters for butene - butadiene catalytic scheme

Rates are expressed as: $Ae^{-E/RT}[O_2]^a[C_4H_8]^b[C_4H_6]^c$

$kmol(kg\ cat)^{-1}sec^{-1}$

Source : n - butene

	Product (Principal)	a	b	c	$\log_{10}A$	E
1	C_4H_6	0.44	0.44	-	1.813	17.4
2	CO_2	1.15	0.80	-	5.352	23.8
3	CO	1.6	0.90	-	6.801	26.3
4	C_4H_4O	0.85	0.33	-	3.884	27.5
5	C_3H_4O	1.2	0.75	-	5.000	25.0
6	C_3H_7CHO	1.0	1.0	-	1.265	15.0
7	C_3CHO	1.0	1.0	-	2.550	17.5
14	c - 2 - butene	0.74	1.1	-	- 2.5229	0
16	t - 2 - butene	0.74	1.1	-	- 2.6271	0

Source : c - 2 - butene

	Product	a	b	c	$\log_{10}A$	E
1	C_4H_6	0.50	0.63	-	1.6628	16.8
2	CO_2	1.15	0.8	-	6.65	29.0
3	CO	1.45	0.8	-	7.31	30.5
4	C_4H_4O	0.85	0.33	-	3.27	26.5
5	C_3H_4O	0.83	0.50	-	3.83	27.0
6	C_3H_7CHO	1.0	1.0	-	0.72	15.0
7	CH_3CHO	1.0	1.0	-	3.23	21.0
15	n - butene	0.25	1.27	-	- 3.5528	0.0
18	t - 2 - butene	0	1.0	-	- 2.1938	7.4

Table A.3.2 continued

Source : t-2-butene

	Product	a	b	c	$\log_{10}A$	E
1	C_4H_6	0.45	0.59	-	1.7404	17.5
2	CO_2	1.15	0.80	-	6.8325	29.5
3	CO	1.45	0.80	-	7.28	30.5
4	C_4H_4O	0.85	0.33	-	3.29	26.5
5	C_3H_4O	0.83	0.50	-	3.83	27.0
6	C_3H_7CHO	1.0	1.0	-	0.72	15.0
7	CH_3CHO	1.0	1.0	-	3.23	21.0
17	n-butene	0.25	1.27	-	- 3.5528	0.0
19	c-2-butene	0	1.0	-	- 3.1221	4.0

Source : Butadiene

	Product	a	b	c	$\log_{10}A$	E
8	CO_2	0.57	-	1.0	2.602	17.0
9	CO	0.75	-	1.0	2.021	15.7
10	C_4H_4O	1.7	-	0.1	4.539	25.0
11	C_3H_4O	1.5	-	0.55	3.973	21.0
12	C_3H_7CHO	1.0	-	1.5	1.342	10.0
13	CH_3CHO	1.0	-	1.0	2.954	21.0

A.3.2 Homogeneous Kinetics

Lam (1975) postulated the following network of reactions involving the principal products he identified.

$$C_4H_8 + O_2 \rightarrow C_3H_6 + CO + H_2O \quad - 1$$

$$C_4H_6 + \tfrac{1}{2}O_2 \rightarrow C_3H_6 + CO \quad - 2$$

$$C_3H_6 + O_2 \rightarrow C_2H_4 + CO + H_2O \quad - 3$$

$$C_2H_4 + 2O_2 \rightarrow 2CO + 2H_2O \quad - 4$$

$$CO + \tfrac{1}{2}O_2 \rightarrow CO_2 \quad - 5$$

The following kinetic constants were obtained by linear regression, the rate being expressed as

$$r_i = A\, e^{-E/RT} C_i^{n_i} C_{O2}^{n_{O2}} \quad \text{g mol/m}\ell\text{/sec}$$

where n_i and n_{O2} are the stoichiometric coefficents in the above equations.

Table A.3.3 - Butene - Butadiene homogeneous kinetics

Reaction	A	E kcal gmol^{-1}	n_i	n_{O2}
1	$6.3 \cdot 10^{4}$	9.78	1	1.0
2	$3.94 \cdot 10^{17}$	62.3	1	0.5
3	$1.37 \cdot 10^{27}$	9.13	1	1.0
4	$5.68 \cdot 10^{51}$	167.0	1	2.0
5	$3.76 \cdot 10^{11}$	38.3	1	0.5

This is a complex reaction scheme and in a reactor model would require that two extra species, ethene and propene, were accounted for. The amounts of these materials produced during Lam's experiments were always several orders of magnitude smaller than carbon monoxide production, and considerable uncertainty must be associated with these results. As the available industrial data takes no account of alkenes production a simplification of the scheme was used which:

(a) overstates the actual degradation rate

(b) provides an estimate of the extent of the homogeneous reaction in terms of an industrially detected by-product (carbon monoxide).

The relative reaction rates at 700 K are:

Reaction	Relative Rate
1	57.0
2	0.40
3	0.34
4	0.01
5	10.0

Assuming reactions (3) and (4) are rapid compared to the initial oxidations clearly overstates the actual rate of carbon monoxide formation and reduces the reaction network to:

1. $C_4H_8 + 4O_2 \rightarrow 4CO + 4H_2O$
2. $C_4H_6 + 3\frac{1}{2}O_2 \rightarrow 4CO + 3H_2O$
3. $CO + \frac{1}{2}O_2 \rightarrow CO_2$

A.3.3 Physical parameters

(1) Heats of formation at 298 K

	$(-\Delta Hf)_{298}$ (KJ/Kmol)	Source
C_4H_6	$1.016 \cdot 10^5$	b
$n-C_4H_8$	$1.172 \cdot 10^3$	b
$c-2-C_4H_8$	$-5.699 \cdot 10^3$	b
$t-2-C_4H_8$	$-10.06 \cdot 10^3$	b
CO	$-1.106 \cdot 10^5$	b
CO_2	$-3.938 \cdot 10^5$	b
H_2O (g)	$-2.412 \cdot 10^5$	b
O_2		
C_4H_4O	$-6.195 \cdot 10^4$	a+
C_3H_4O	$-8.568 \cdot 10^4$	b
C_3H_7CHO	$-2.196 \cdot 10^5$	b
CH_3CHO	$-1.6632 \cdot 10^5$	b

a - Kirk-Othmer (1967) b - Perry (1963) + - Furan, boils at 304 K and this value is for the 'theoretical' gas at 298 K.

(2) Specific Heats

For most materials these were available as polynomials of the absolute temperature (Hougen et al., 1954). A polynomial for furan was estimated using the method of Bennewitz, Rosiner and Dobratz, while functions for acrolein and n-butylaldehyde were obtained using Rihani and Doraiswamys group contribution method (Reid and Sherwood, 1966).

$$Cp = a + bT + cT^2 \quad \text{cal/g mole K}$$

	a	b	c
furan	5.13	$5.262 \cdot 10^{-2}$	$-1.914 \cdot 10^{-5}$
acrolein	3.80	$4.402 \cdot 10^{-2}$	$-1.304 \cdot 10^{-5}$
n-butylaldehyde	4.92	$7.36 \cdot 10^{-2}$	$-2.60 \cdot 10^{-5}$

(3) Catalyst pellet properties

(a) Catalyst bulk density : 4881 kg/m^3

(b) Effective thermal conductivity :

$$K_{eff} = 0.0952. + 0.44.10^{-3} T_s \quad W\ m^{-2} \qquad \text{(Corrie, 1972)}$$

(c) Effective gas diffusivities : Corrie (1972) measured the temperature dependence of the diffusivity of oxygen and butadiene. This data is adequately fitted over the industrially important range (380 - 430°C) by an equation of the form (Knudsen flow):

$$\mathcal{D}_{eff} = C_D \sqrt{T_f/Mw} \quad m^2/sec$$

where $C_D(O_2) = 3.3 \cdot 10^{-7}$

$C_D(C_4H_6) = 4.2 \cdot 10^{-7}$

and Mw = molecular weight.

In this study the value of C_D pertaining to oxygen was used for carbon monoxide and carbon dioxide while that pertaining to butadiene was used for butene.

(4) Film transfer coefficients

The procedure for the estimation of the gas film transfer coefficients follows Holton (1975). The mass and heat transfer coefficients

are related by the Chilton - Colburn analogy:

$$\frac{h}{Cp.\rho_f} \; Pr^{2/3} = kg \,.\, Sc^{2/3}$$

and the heat transfer coefficient was estimated using the correlation given by Kern (1950) for pipe flow.

(5) Corrie's (1972) experimental arrangement

Figure A.3.2 - Corrie's (1972) apparatus

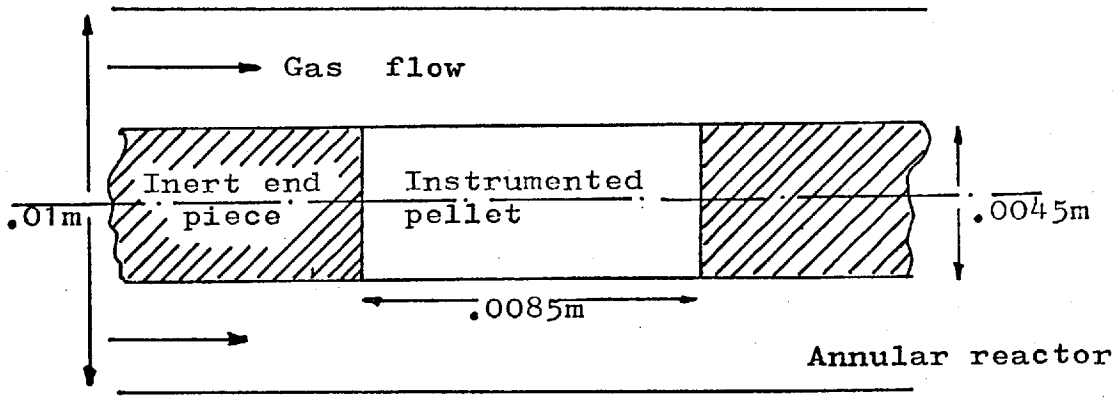

Kern (1950) gives for tube flow:

$$\frac{h\ De}{kf} = Nu = 1.86\ Re_e^{1/3} \left(\frac{\ell'}{De}\right)^{-1/3} Pr^{1/3}$$

where De is the equivalent diameter of the annulus and ℓ' is a mixing length. The ratio (ℓ'/De) has a relatively small effect on h and Holton (1975) associated ℓ' with the pellet length. Holton also included a parameter to allow for the effect of surface roughness (C'), recasting the equation as,

$$Nu = C\ Re_e^{1/3}$$

where $C = 1.86\ Pr^{1/3}\ C' \,.\, (\ell'/De)^{1/3}$ and used as a starting value

$C' = 2.33$, giving $C = 3.12$

A.3.4 Pilot scale data

These results were obtained, by B.P. Chemicals (McCain 1976), in a single tube pilot plant reactor operating under normal industrial conditions. The tube was cooled by an air-stirred bath of molten salt and the wall temperature can be considered axially constant. As discussed in Chapter 5 the description of the experimental apparatus and procedure is not comprehensive. The data is summarized in the accompanying tables. The axial temperature profiles for the runs in Table A.3.4 are much more complete than those for Table A.3.5. In both sets of runs the feed contained approximately equimolar amounts of the three butene isomers, n-butene, cis-2-butene and trans-2-butene.

Table A.3.4 - Pilot plant results

Catalyst: Sb/Sn : 4/1 treated at 800°C for 16 hrs.

Feed: 10% butenes, 30% steam, 60% air, by volume.

Reactor: 10' x 1" i.d. mild steel tube with 0.3" O.D. thermocouple pocket down the centre.

Wt% Inlet: C_4H_8 : 20.1 H_2O : 19.4 Air : 60.5 (of which 12.7% is O_2)

Run No.	Bath Temp (K)	Inlet Pressure (atm)	Gs $kg/m^2/sec$	Wt % outlet				C Balance %
				C_4H_8	C_4H_6	CO_2	CO	
1	683	1.26	0.76	6.26	11.0	1.5	.1	95.0
2	688	1.26	0.76	6.44	11.7	1.65	.13	100.6
3	708	1.25	0.795	4.40	12.30	2.5	.21	99.2

Table A.3.5 - Pilot plant data

Catalyst: Sb/Sn : 4/1 heat treated at 850°C for 16 hours

Feed: 10% butenes, 40% steam, 50% air

Reactor: 10' x 1.136" i.d. stainless steel tube.
A 0.3" o.d. thermocouple pocket extended down the centre of the tube.

Wt% inlet: C_4H_8 : 22.0 H_2O : 26.4 Air : 51.6 (of which 10.85% is O_2)

Run No.	Bath Temp (K)	Inlet Pressure (atm)	Gs $kg/m^2/sec$	Wt % outlet				C Balance %
				C_4H_8	C_4H_6	CO_2	CO	
4	659	1.22	0.795	7.2	11.6	.795	.083	102
5	684	1.22	0.815	5.3	12.15	1.02	.125	97.8
6	695	1.22	0.812	4.3	12.6	1.49	.187	98.4
7	695	1.22	1.171	6.5	11.5	1.19	.135	100.4

APPENDIX A.4 - BIOCHEMICAL REACTOR MODEL

The rate of the bound enzyme reaction is given by:

$$r = \frac{k\,E_s}{V} \cdot \frac{1}{(1 + Ka/C_s + C_s/Ks)}$$

where Ka and Ks are constants (mol/ℓ), while the fluid enzyme reaction rate is:

$$r' = \frac{k\,E'_f}{v} \left(\frac{1}{1 + Ka/C_f}\right)$$

where E'_f = the amount of enzyme in the effluent (Aiba et al., 1973). Clearly $E'_f = Ke.E_s$, where Ke is some elution rate. Using the nomenclature of Chapter 6 the following describing equations for a stirred tank biochemical reactor can be developed; where Ca_o is the inlet concentration (mol/ℓ)

Fluid phase mass balance:

$$1 - X_f - Da_s\, W \left(\frac{X_f}{Ca_o X_f + Ka}\right) - K(X_f - X_s) = 0$$

Solid phase mass balance:

$$K(X_f - X_s) - \frac{Da_s\, X_s}{(Ca_o X_s + Ka + Ca_o^2 X_s^2/Ks)} = 0$$

with

$$Da_s = \left(\frac{k\,E_s}{V}\right)$$

$$W = \text{'washout rate'} = \left(\frac{V}{v}\,Ke\right)$$

The values of Ka, Ks and Ca_o (= 0.1 mol/ℓ) utilised in this study are drawn from O'Neil et al. (1971).

APPENDIX A.5 - COMPUTER PROGRAMS

The computer programs written in the course of this study can be divided into two groups concerned with steady state modelling and multiplicity analysis.

A.5.1 Coding for steady state modelling

This group can be further subdivided into programs solving the reactor models themselves and service routines providing kinetic and other input information or outputing results. Of the five reactor models developed only the coding of the two dimensional - two phase example is included, the other cases use similar techniques and can be considered generic. A list of computer symbols and their equivalent in the text is given in Table A.5.1. The names and functions of the various service routines are given in Table A.5.2.

The logic of the reactor (subroutine RE2DP) and pellet model (subroutine PELL3) should be clear from the flow diagrams (Figs. A.5.1 and A.5.2) and associated listing.

Table A.5.1 - List of variables for reactor and pellet models

Computer Variable	Common Block	Definition	Equivalent in text
DP	SYSTEM	pellet diameter	dp
DT	SYSTEM	tube diameter	Dt
AL	SYSTEM	reactor length	L
GS	SYSTEM	mass velocity	Gs
THI	TDIM2	voidage	ε
T	TDIM2	temperature	T
P	TDIM2	pressure	P
X( )	TDIM2	Gas composition vector	-
PF	TDIM2	fluid density	ρ_f
ALS	PHASE 2	Effective radial conductives for solid, fluid and continuum	λr_s
ALF	PHASE 2		λr_f
ALC	PHASE 2		λr_c
PMR2	PHASE 2	Radial heat peclet no.	-
ALPHAS	PHASE 2	Wall heat transfer coefficients for solid, fluid and continuum	αw_s
ALPHAF	PHASE 2		αw_f
ALPHAC	PHASE 2		αw_c
HV	PHASE 2	film heat transfer coefficient	h
CP	PROPS	specific heat	Cp
AMU	PROPS	dynamic viscosity	μ

Table A.5.1 - Continued

Computer Variable	Common Block	Definition	Equivalent in text
AKF	PELL 2	Fluid thermal conductivity	kf
SET	PELL 2	D_z/D_r	-
BETA	PELL 2	Pellet length to radius ratio	β
ALPHAP	PELL 2	hollowing	α
AKS	PELL 2	Solid thermal conductivity	ks
PB	PELL 2	pellet density	ρ_s
ARS,BRS, AZS		- collocation matrices	ar etc.
BZS,XRS, WS			
QP,DER			
PR( )		Peclet numbers	Pe_r
R		solid phase rate groups	R_s and R_{ts}
RG		fluid phase rate groups	R_f and R_{tf}
XC		Dimensionless continuum concentration	X_c
XG		Dimensionless gas concentration	X_f
XGA			-
XS		Dimensionless solid concentration	X_s
F,FS		Function vector (solution procedure)	-
TS		Solid phase centreline temperature	-
DRT		Derivative vector (solution procedure)	-

Table A.5.1 - Continued

Computer Variable	Definition	Equivalent in text
NSPH	Pellet shape parameter	-
NDEC( )	Sequential bed packing vector	-
TB	Wall and inlet temperature	T_o/T_w
NGMAX,NSMAX	Location of hotspot (grid number)	-
TGMAX,TSMAX	Hotspot value	-
TGPOS,TSPOS	Location of hotspot	-
TAV	Radial average temperature	-
XAV	Radial average concentration	-
TC	Centreline temperature	-
DHET,DHOM	Heats of reaction	$(-\Delta H)_s, (-\Delta H)_f$
SAV	Surface area/volume ratio for pellets	-
B	Effective conductivity parameter	β_v
AV	Specific surface area	a_v
NSTART	Matrix controlling pellet solution	-
DIR	Effective diffusivity	$\mathcal{D}_{eff}$
XB	Bulk or inlet dimensionless concentration	X_o

Table A.5.2 - Service Routines

(a) General

PRINT1, PRINT2, PRINT3, PRINT4 — Various Tabular output options

DRAW1, DRAW2, DRAW3, DRAW4 — Various Graphical output options

HEAD2 - Output of inlet conditions and heat transfer parameters

PROPS* - Calculation of fluid properties

HTMT* - Calculation of heat transfer coefficients

(b) Chapter 4

OCL2 - Calculates collocation matrices using a small library of subroutines

Three sets of subroutines were written to provide kinetic information, only those for nitrous oxide oxidation are tabulated below:

RAE1* — Heterogeneous rate calculation

DERAE1* — Calculates derivative of heterogeneous rate

RAGAS1* — Homogeneous rate calculation

RAT1 — Combines output from RAE1 and RAGAS1 for one phase models

Table A.5.2 - Continued

(c) Chapter 5

OCLPEL - As OCL2

RAE7* - As RAE1

PELL3* - Isothermal pellet solution (called by RAE7)

AIMPNEW*, F2ISO* - Subroutines used by PELL3 in Newton solution scheme.

Thirteen further subroutines (occupying 2500 words of store) were also used to manipulate and evaluate the kinetic information.

Note: * - Documented coding of program is included.

Fig A.5.1 - Logic diagram for 2D2P reactor model coding

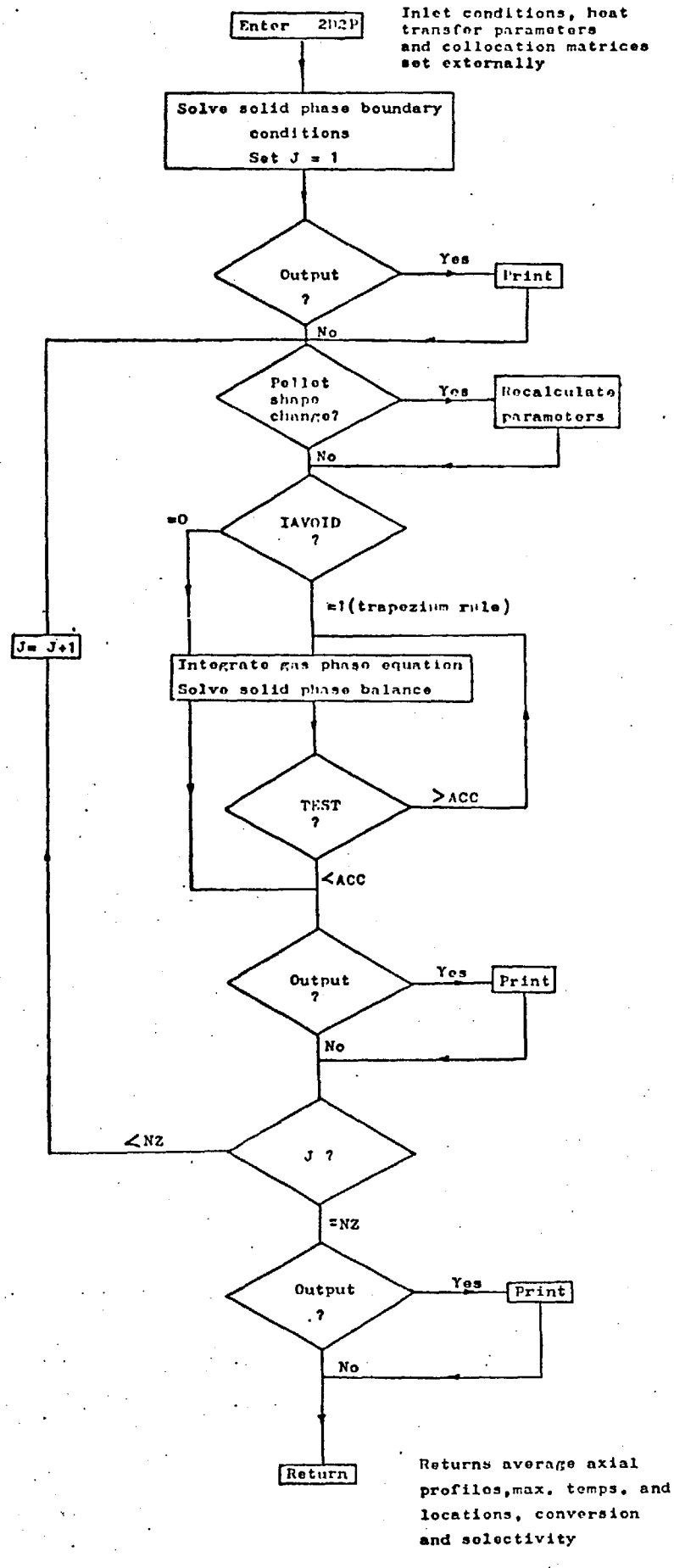

Fig A.5.2 - Logic diagram for butene pellet coding

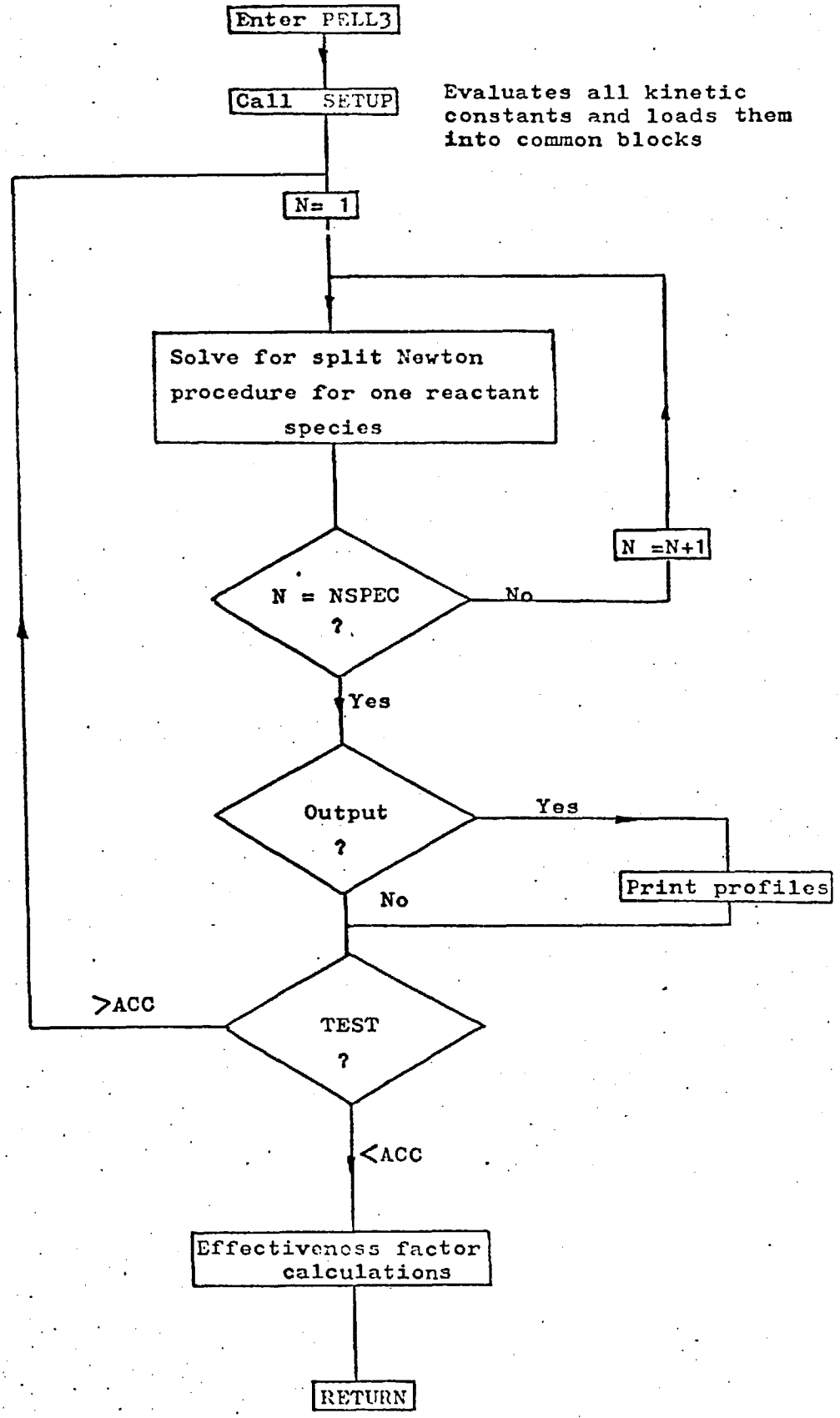

```
      SUBROUTINE HF2D2P(   PR,XB,ARS,BRS,XRS,WS,NR,NZ,NSPEC,RAE,RATGAS,
     1 DRAW1,DRAW2,TC,R,RG,XG,XGA,F,XAV,US,FS,XS,TAV,TS,DER,DERAE,DRT,NR
     22)
C
C      SOLVES  2D/2P RED MODEL FOR HETEROGENEOUS - HOMOGENEOUS REACTION
C
      DIMENSION DRT(NR)
      DIMENSION ARS(NR,NR),BRS(NR,NR),XRS(NR),WS(NR)
       DIMENSION XG(NR,1,NSPEC),F(NR,1,NSPEC),XAV(NSPEC,NS)
       DIMENSION XGA(NR,1,NSPEC)
      DIMENSION R(NR,1,NSPEC),RG(NR,1,NSPEC),PR(NSPEC)
      DIMENSION SH(5)
      DIMENSION XB(NSPEC)
      DIMENSION              TS(1,NS),FS(NR,1),XS(NR,1,NSPEC)
      DIMENSION TAV(1,NS)
      DIMENSION TC(1,NS),X(10)
      DIMENSION DER(NR2,NR2)
       DIMENSION STORE(20),COR(20)
      DIMENSION IPRINT(2),IDRAW(2)
      COMMON/SHAPE/NSPH
       COMMON/QUAD/GP(20)
       COMMON/FILM/ICONT,GK
      COMMON/TDIM2/T,P,X,DSP,PEI
      COMMON/PELL2/ PS,SH,AKS,SET,PETA,ALPHA
      COMMON/SYSTEM/DP,DT,AL,GS,THI
      COMMON/ALL/UCO,TB
      COMMON/HET/IHET
      COMMON/PROPS/CP,AMU,AKF
      COMMON/CONTR/IAVOID,IPRINT,IDRAW,IDIAG
      COMMON/PHASE2/ALS,ALF,HV,PR2,ALPHAS,ALPHAF
      COMMON/TYPE/NDEC(10)
      COMMON/D2P2/TSMAX,TGMAX,TSPOS,TGPOS
      EXTERNAL DERAE
      EXTERNAL RAE,RATGAS,DRAW1,DRAW2
C      CONTROL VARIABLES
C     IAVOID=0-EULER METHOD
C           =1 -TRAPEZIUM RULE
C     IPRINT=0 - PRINT OUT
C     IDRAW=0 - GRAPHS
C      IHET=0- HET+HOM
C           =1- HET ONLY
C
      US= ALPHAS
      UF= ALPHAF
      NOST= NDEC(1)
      JS= 1
      NT= 3
      IF(NSPEC.EQ.5) NT= 4
      JNEW=0
      E= THI
      ACC= 0.005
      NEREW= NZ/(NS-1)
      ALD= 2.0*AL/DT
      DPD= 2.0*DP/DT
      ALT= ALD*DPD
      XX= GS*CP*DT/AL/2.0
      DO 19 J= 1,NR
       STORE(J)= 0.0
      DO 19 N= 1,NSPEC
      XS(J,1,N)= XB(N)
   19 XG(J,1,N)= XB(N)
      NCOUNT= 0
      JT= 1
      DZ= 1.0/FLOAT(NZ)
      TC(1,1)= XB(NT)
       DO 27 N= 1,NSPEC
   27 XAV(N,1)= XB(N)
C
C      OBTAIN SOLID PHASE TEMP. PROFILE AT INLET
C
C      SOLVE SOLID PHASE EQNS BY NEWTONS METHOD
   50 CONTINUE
      CALL DERAE(XS,R,DRT,NSPEC,NR,1,NT)
       DO 51 JR= 1,NR-1
      FS(JR,1)= (1.0-F)*R(JR,1,NT)-HV*(XS(JR,1,NT)-XG(JR,1,NT))
      DO 51 J= 1,NR
       FS(JR,1)= FS(JR,1)+4.0*ALS/(DT**2)*BRS(JR,J)*XS(J,1,NT)
   51 CONTINUE
      TEST= 0.0
      DO 53 J= 1,NR-1
      COR(J)= 0.0
       DO 54 K= 1,NR-1
   54 COR(J)= COR(J)+ DER(J,K)*(FS(K,1)-DRT(K)*STORE(K)*(1.-E))
      XS(J,1,NT)= XS(J,1,NT)-COR(J)
       DEL= ABS(COR(J)/XS(J,1,NT))
      IF(DEL.GT.TEST)TEST= DEL
   53 CONTINUE
      DO 55 J= 1,NR-1
      STORE(J)= COR(J)
   55 CONTINUE
C      BOUNDARY CONDITION
      FS(NR,1)= 0.0
      DO 52 J= 1,NR
      FS(NR,1)= FS(NR,1) + ARS(NR,J)*XS(J,1,NT)*2.0*ALS/DT
   52 CONTINUE
      FS(NR,1)= FS(NR,1)-ARS(NR,NR)*XS(NR,1,NT)*2.0*ALS/DT - US*TB
      AA=-US-ARS(NR,NR)*2.0*ALS/DT
```

```
      XNEW= FS(NR,1)/AA
       IF(XS(JR,1,NT).EQ.0.0) GO TO 110
      DEL= ABS((XNEW-XS(JR,1,NT))/XS(JR,1,NT))
       IF(DEL.GT.TEST) TEST= DEL
  110 CONTINUE
       XS(JR,1,NT)= XNEW
      IF(TEST.GT.ACC) GO TO 50
C     END OF SOLID PHASE SOLUTION
       TS(1,1)= 0.0
      TAV(1,1)= 0.0
      DO 60 J= 1,NR
       TS(1,1)= TS(1,1)+ DP(J)*XS(J,1,NT)
      TAV(1,1)= TAV(1,1)+ XS(J,1,NT)*WS(J)
   60 CONTINUE
C
C      INITIALIZATION COMPLETE
C
C
C      INTERMEDIATE OUTPUT
C
      JZ= 1
      IF(IPRINT(1).NE.0) GO TO 93
      CALL PRINIT(XG,RG,NSPEC,JZ)
      CALLPRINT(XS,NR,NSPEC,JZ,NT)
   93 CONTINUE
C
C      COMMENCE INTEGRATION ALONG REACTOR
C
      DO 15 JZ= 2,NZ+1
      NCOUNT= NCOUNT+1
      IF(NCOUNT.NE.NFREQ) GO TO 91
      JS= JS + 1
C
C     FACILITY FOR SEQUENTIAL BED PACKING
C
      IF(NDEC(JS).EQ.NOST) GO TO 92
      IF(NDEC(JS).EQ.0) CALL SUBRA(NSPH)
      IF(NDEC(JS).EQ.1) CALL SUBRB(NSPH)
      CALL HTMT(NSPH)
      NOST= NDEC(JS)
   92 CONTINUE
   91 CONTINUE
      ITRAP=0
   14 CONTINUE
C
C      HETEROGENEOUS KINETICS
      CALLRAE(XS,R,NSPEC,NR,1)
      IF(IMET.NE.0) GO TO 28
C     HOMOGENEOUS KINETICS
      CALL RATGAS(XG,RG,NSPEC,NR,1)
      GO TO31
   28 CONTINUE
      DO 30 N= 1,NSPEC
      DO 30 JR= 1,NR
      RG(JR,1,N)= 0.0
   30 CONTINUE
   31 CONTINUE
C     SOLUTION OF GAS PHASE EQUATIONS
C
C     METHOD USED CONTROLLED BY IAVOID
       DO 3 JR= 1,NR-1
      DO 33 N= 1,NSPEC
      F(JR+1,N)=(E*RG(JR,1,N)+(1.0-E)*R(JR,1,N))*AL/GS
   33 CONTINUE
       F(JR+1,NT)= (F(JR,1,NT)-(1.-E)*R(JR,1,NT)*AL/GS)/CP
      F(JR+1,NT)= F(JR,1,NT)+HV*AL*(XS(JR,1,NT)-XG(JR,1,NT))/GS/CP
      DO 3 J=1,NR
      DO 34 N= 1,NSPEC
       F(JR+1,N)= F(JR,1,N)+ARS(JR,J)*XG(J,1,N)/PR(N)*ALT
   34 CONTINUE
    3 CONTINUE
      IF(ITRAP.NE.0)GO TO 9
       DO 38 JR= 1,NR-1
      DO 8 N=1,NSPEC
      XGA(JR,1,N)= XG(JR,1,N) + DZ*F(JR,1,N)/2.0
      XG(JR+1,N)=XG(JR,1,N)+DZ*F(JR,1,N)
    8 CONTINUE
   38 CONTINUE
      DO 1 N=1,NSPEC
      F(NR,1,N)= 0.0
      DO 4 J=1,NR
    4 F(NR,1,N)=F(NR,1,N)+ARS(NR,J)*XG(J,1,N)/PR(N) *ALT
    1 CONTINUE
      F(NR,1,NT)= F(NR,1,NT)-UF*TR/XX
      DO 32 N= 1,NSPEC
      F(NR,1,N)= F(NR,1,N)-ARS(NR,NR)*XG(NR,1,N)/PR(N)*ALT
      AA= -ARS(NR,NR)*ALT/PR(N)
      IF(N.EQ.NT) AA= AA-UF/XX
      XG(NR+1,N)=  F(NR,1,N)/AA
   32 CONTINUE
C
C
    9 CONTINUE
      IF(ITRAP.EQ.0) GO TO 10
      TEST=0.0
       DO 39 JR= 1,NR-1
      DO 11 N=1,NSPEC
      XNEW= XGA(JR,1,N) + DZ*F(JR,1,N)/2.0
      IF(XG(JR,1,N).EQ.0.0) GO TO 63
      DEL= ABS((XNEW-XG(JR,1,N))/XG(JR,1,N))
```

```
      IF(DEL.GT.TEST) TEST=DEL
   63 CONTINUE
      XG(JR,1,N)= XNEW
   11 CONTINUE
C     BOUNDARY CONDITION
   39 CONTINUE
      DO 45 N= 1,NSPEC
      F(NR,1,N)= 0.0
      DO 45 J= 1,NR
      F(NR,1,N)=F(NR,1,N)+ARS(NR,J)*XG(J,1,N)/PR(N) *ALT
   45 CONTINUE
      F(NR,1,NT)= F(NR,1,NT)-UF*TB/XX
      DO 44 N= 1,NSPEC
      F(NR,1,N)= F(NR,1,N)-ARS(NR,NR)*XG(NR,1,N)/PR(N)*ALT
      AA=-ARS(NR,NR)*ALT/PR(N)
      IF(N.EQ.NT) AA= AA-UF/XX
       XNEW= F(NR,1,N)/AA
       IF(XG(NR,1,N).EQ.0.0) GO TO 130
       DEL= ABS((XNEW-XG(NR,1,N))/XG(NR,1,N))
      IF(DEL.GT.TEST) TEST= DEL
  130 CONTINUE
       XG(NR,1,N)= XNEW
   44 CONTINUE
   10 CONTINUE
C
C      SOLVE SOLID PHASE EQNS BY NEWTONS METHOD
C
      CALL DERAF(XS,R,ORT,NSPEC,NR,1,NT)
       DO 40 JR= 1,NR-1
      FS(JR,1)= (1.0-E)*R(JR,1,NT)-HV*(XS(JR,1,NT)-XG(JR,1,NT))
      DO 40 J= 1,NR
      FS(JR,1)= FS(JR,1)+4.0*ALS/(DT**2)*ARS(JR,J)*XS(J,1,NT)
   40 CONTINUE
      DO 61 J= 1,NR
       STORE(J)= 0.0
   61 CONTINUE
       TEST2=0.0
       DO 42 J= 1,NR-1
      COR(J)= 0.0
       DO 43 K= 1,NR-1
   43 COR(J)= COR(J)+ DER(J,K)*(FS(K,1)-ORT(K)*STORE(K)*(1.-E))
      XS(J,1,NT)= XS(J,1,NT)-COR(J)
      DEL= ABS(COR(J)/XS(J,1,NT))
       IF(DEL.GT.TEST2) TEST2=DEL
   42 CONTINUE
       DO 62 J= 1,NR-1
       STORE(J)= COR(J)
   62 CONTINUE
      FS(NR,1)= 0.0
      DO 41 J= 1,NR
      FS(NR,1)= FS(NR,1) + ARS(NR,J)*XS(J,1,NT)*2.0*ALS/DT
   41 CONTINUE
      FS(NR,1)= FS(NR,1)-ARS(NR,NR)*XS(NR,1,NT)*2.0*ALS/DT - US*TR
      AA=-US-ARS(NR,NR)*2.0*ALS/DT
       IF(XS(NR,1,NT).EQ.0.0) GO TO 120
       XNEW= FS(NR,1)/AA
      DEL= ABS((XNEW-XS(NR,1,NT))/XS(NR,1,NT))
       IF(DEL.GT.TEST2) TEST2= DEL
  120 CONTINUE
       XS(NR,1,NT)= XNEW
       IF(TEST2.GT.ACC) GO TO 10
C     END OF SOLID PHASE SOLUTION
C
C      CONVERGENCE TEST
C
      IF(ITRAP.EQ.0) GO TO 12
      IF(TEST.LT.ACC) GO TO 13
   12 CONTINUE
      IF(IAVOID.EQ.0)GO TO 13
      ITRAP=1
      GO TO 14
   13 CONTINUE
      DO 37 JR= 1,NR
      TST=  XS(JR,1,NT)
      DO 36 N= 1,NSPEC
   36 XS(JR,1,N)= XG(JR,1,N)  *
   37 XS(JR,1,NT)= TST
C
C      CHECK FOR NEGATIVE CONC
C
      DO 22 N= 1,NSPEC
      IF(N.EQ.NT) GO TO 22
      DO 22 J= 1,NR
      IF(XG(J,1,N).LT.0.0) GO TO 23
      IF(XS(J,1,N).LT.0.0) GO TO 23
   22 CONTINUE
      GO TO 25
   23 CONTINUE
      DO 81 N= 1,NSPEC
      IF(N.EQ.NT) GO TO 81
      DO 81 J= 1,NR
      IF(XG(J,1,N).LT.0.0) XG(J,1,N)= 0.0
      IF(XS(J,1,N).LT.0.0) XS(J,1,N)= 0.0
   81 CONTINUE
      IF(JREC.NE.0) GO TO 80
      WRITE(6,1000)
      WRITE(6,10011) J7
      WRITE(6,1000)
```

```
      JNEQ= 1
   80 CONTINUE
C
C       EVALUATE AND STORE CENTRE LINE TEMPERATURES
C
   25 CONTINUE
       GX= 0.0
       SX= 0.0
       DO 500 J= 1,NR
       GX= GX+OP(J)*XG(J,1,NT)
  500  SX= SX+ OP(J)*XS(J,1,NT)
       IF(SX.GT.TSMAX) NSMAX= JZ
       IF(SX.GT.TSMAX) TSMAX= SX
       IF(GX.GT.TGMAX) NGMAX= JZ
       IF(GX.GT.TGMAX) TGMAX= GX
      DO 100 J= 1,NR
      IF(XG(J,1,NT).GT.TGMAX) NGMAX= JZ
      IF(XS(J,1,NT).GT.TSMAX) NSMAX= JZ
      IF(XG(J,1,NT).GT.TGMAX) TGMAX= XG(J,1,NT)
      IF(XS(J,1,NT).GT.TSMAX) TSMAX= XS(J,1,NT)
  100 CONTINUE
      IF(NCOUNT.NE.NFREQ) GO TO 24
      JT= JT+1
      NCOUNT= 0
C
C       STORE AND EVALUATE AVERAGE VALUES
C
       TC(1,JT)= 0.0
       TS(1,JT)= 0.0
      TAV(1,JT)= 0.0
      DO 82 J = 1,NR
        TC(1,JT)= TC(1,JT)+OP(J)*XG(J,1,NT)
       TS(1,JT)= TS(1,JT)+ OP(J)*XS(J,1,NT)
       TAV(1,JT)= TAV(1,JT) + WS(J)*XS(J,1,NT)
   82 CONTINUE
      DO 16 N=1,NSPEC
      XAV(N,JT)= 0.0
      DO 16 J=1,NR
      XAV(N,JT)= XAV(N,JT) + WS(J)*XG(J,1,N)
   16 CONTINUE
   24 CONTINUE
C
C       INTERMEDIATE OUTPUT OPTIONS
C
      IF(NCOUNT.NE.0) GO TO 17
      IF(IPRINT(1).NE.0) GO TO 17
      CALL PRINT1(XG,NR,NSPEC,JZ)
      CALL PRINT3(XS,NR,NSPEC,JZ,NT)
   17 CONTINUE
      IF(NCOUNT.NE.0) GO TO 21
      IF(IDRAW(1).NE.0) GO TO 21
      CALL DRAW1(XG,XRS,NR,NSPEC)
   21 CONTINUE
      IF(IDIAG.EQ.0) GO TO 15
      CALL PRINT1(XG,NR,NSPEC,JZ)
      CALLPRINT3(XS,NR,NSPEC,JZ,NT)
   15 CONTINUE
C
C       COMPLETION OF INTEGRATION
C
       DO 46 N= 1,NSPEC
      XB(N)= XAV(N,NS)
   46 CONTINUE
C
C       FINAL OUTPUT OPTIONS
C
      IF(IPRINT(2).NE.0) GO TO 18
      CALL PRINT2(XAV,TC,NS,NSPEC)
      CALL PRINT4(TAV,TS,NS)
   18 CONTINUE
      IF(IDRAW(2).NE.0) GO TO 20
      CALL DRAW2(TC,XAV,NS,NSPEC)
   20 CONTINUE
   26 CONTINUE
      TGPOS= FLOAT(NGMAX-1)*DZ
      TSPOS= FLOAT(NSMAX-1)*DZ
 1000 FORMAT(21X,50H--------------------------------------------------,/
     1)
 1001 FORMAT(21X,26HREACTANT EXHAUSTED AT JZ =,I3,10X,17HCONC. SET TO ZE
     1RO,/)
      RETURN
      END
```

```
      SUBROUTINE RAE1(XC,R,NSPEC,NR,N)
C
C     NITROUS OXIDE  OXIDATION
C
C     HETEROGENEOUS  TERMS
C
C     SPECIES.....
C
C     1 = NITROUS OXIDE(N2O)
C
C     2 = NITROGEN DIOXIDE(NO2)
C
C     3 = TEMPERATURE
C
C     RATE  EVALUATED ON KG/M3/SEC / MASS FRACTION BASIS
C
      DIMENSION  R(NR,N,NSPEC),XC(NR,N,NSPEC)
      COMMON/PELL2/PR,SH,AKS,SET,BETA,ALPHA
       COMMON/FIL2/NCONT,GK
      COMMON/SHAPE/NSPH
      COMMON/SYSTEM/DP,DT,AL,GS,THI
      COMMON/PROPS/CP,AMU,AKF
      COMMON/TEMP2/T,P,X,NSP,PFI
      DIMENSION X(10),SH(5)
      DATA AHE ,EHET,DHET/3.35,34.6,1.98E+06/
      REAL KHET
      AHET= 10.0**AHE
       RGH= 1000.0*DP
C
C     FOR A SPHERE.
      IF(NSPH.EQ.1) SAV= 6.0/DP
      IF(NSPH.EQ.-1) SAV= 4./DP*(1.-THI)/THI
C
      IF(NSPH.EQ.0) SAV=4.0*(1.-ALPHA+BETA)/DP/(1.-ALPHA)/BETA
      RR= 1.98E-03
      DO 1 J=1,NR
      DO 1 K=1,N
      PF= PFI/(1.0+ XC(J,K,3))
      TT= (XC(J,K,3) + 1.0)*T
      KHET= AHET*EXP(-EHET/RR/TT)
      IF(NCONT.EQ.1) FAC=1
      IF(NCONT.EQ.0) FAC= GK/(KHET*RGH+GK)
      R(J,K,1)=SAV*XC(J,K,1)*PF*KHET
       R(J,K,1)= R(J,K,1)*RGH
      IF(NCONT.EQ.0) R(J,K,1)= R(J,K,1)*FAC
      R(J,K,2)=0.0
      R(J,K,3)=DHET*R(J,K,1) /T
      R(J,K,1)=-R(J,K,1)
    1 CONTINUE
      RETURN
      END
C
C
C
      SUBROUTINEDERAF1(XC,R,DRT,NSPEC,NR,NZ,NT)
C
C     NITROUS OXIDE  OXIDATION
C
C     HETEROGENEOUS DERIVATIVE TERM
C
C     SPECIES.....
C
C     1 = NITROUS OXIDE(N2O)
C
C     2 = NITROGEN DIOXIDE(NO2)
C
C     3 = TEMPERATURE
C
C     RATE  EVALUATED ON KG/M3/SEC / MASS FRACTION BASIS
C
      DIMENSION DRA(10)
      DIMENSION XC(NR,NZ,NSPEC)
      DIMENSION R(NR,NZ,NSPEC),DRT(NR)
      COMMON/SYSTEM/DP,DT,AL,GS,THI
       COMMON/FIL2/NCONT,GK
      COMMON/TEMP2/T,P,X,NSP,PFI
      COMMON/SHAPE/NSPH
      COMMON/PELL2/PR,SH,AKS,SET,BETA,ALPHA
      DIMENSION X(10),SH(5)
      REAL KHET,KA
      DATA AHE ,EHET,DHET/3.35,34.6,1.98E+06/
      AHET= 10.0**AHE
       RGH= 1000.0*DP
      RR= 1.98E-03
C     FOR A SPHERE
      IF(NSPH.EQ.1) SAV= 6.0/DP
C
      IF(NSPH.EQ.0) SAV=4.0*(1.-ALPHA+BETA)/DP/(1.-ALPHA)/BETA
      DO 1 JR=1,NR
      DO 1 JZ= 1,NZ
      TT= (XC(JR,JZ,3) + 1.0)*T
        TA= (XC(JR,JZ,3)+1.01+1.01)*T
       IF(XC(JR,JZ,3).EQ.0.0) TA= TT+1.001
      AA= TA/T
      KHET= AHET*EXP(-EHET/RR/TT)
      IF(NCONT.EQ.0) FAC= GK/(KHET*RGH+GK)
      IF(NCONT.EQ.1) FAC=1
      KA= AHET*EXP(-EHET/RR/TA)
      PF= PFI/(1.0+XC(JR,JZ,3))
```

```
      PFA= PFI/AA
      R(JR,JZ,1)= KNET*PF*XC(JR,JZ,1)*SAV*RGH
      RA= RA+PFA*XC(JR,JZ,1)*SAV *RGH
       IF(NCONT.EQ.0) RA= RA*FAC
       IF(NCONT.EQ.0) R(JR,JZ,1)= R(JR,JZ,1)*FAC
      R(JR,JZ,3)=QNET*R(JR,JZ,1)
      RA= QNET*RA
      QRT(JR)= (RA-R(JR,JZ,3))/(TA-TT)
      R(JR,JZ,3)= R(JR,JZ,3)/T
       DKDT= AMET*EXP(-EMET/RR/TT)*EMET/RR/TT**2
       DRA(JR)= DKDT*PF*XC(JR,JZ,1)*SAV*QNET*RGH
       IF(NCONT.EQ.0) DRA(JR)= DRA(JR)*FAC
    1 CONTINUE
       DO 200 JR= 1,NR
       QRT(JR)= DRA(JR)
  200 CONTINUE
      RETURN
      END
C
C
C
      SUBROUTINE RAGAS1(XC,RG,NSPEC,NR,N)
C
C     NITROUS  OXIDE OXIDATION
C
C     HOMOGENEOUS TERMS
C
C     SPECIES..
C
C     1 = NITROUS OXIDE(N2O)
C
C     2 = NITROGEN DIOXIDE(NO2)
C
C     3 = TEMPERATURE
C
C     RATE  EVALUATED ON KG/M3/SEC / MASS FRACTION BASIS
C
      DIMENSION RG(NR,N,NSPEC),XC(NR,N,NSPEC)
      COMMON/SYSTEM/DP,DT,AL,GS,TIT
      COMMON/PROPS/CP,AMU,AKF
      COMMON/TRIM2/T,P,X,NSP,PFI
      DIMENSION X(10)
      DATA AHOM ,AHOM A,AHOMB/16.48,6.99,13.88/
      DATA EHOM1,EHOM1A,EHOM2/41.8,28.4,72.4/
      DATA DHOM1,DHOM2/1.98E+06,1.05E+06/
      REAL KHOM1,KHOM1A,KHOM2
      AHOM1= 10.0**AHOM
      AHOM1A= 10.0**AHOMA
      AHOM2=10.0**AHOMB
      RR= 1.98E-03
      DO 1 J=1,NR
      DO 1 K=1,N
      PF= PFI/(1.0+ XC(J,K,3))
      TT= (XC(J,K,3) + 1.0)*T
      KHOM1= AHOM1*EXP(-EHOM1/RR/TT)
      KHOM1A= AHOM1A*EXP(-EHOM1A/RR/TT)
      KHOM2= AHOM2*EXP(-EHOM2/RR/TT)
      RG(J,K,1)=KHOM1*(PF*XC(J,K,1))**2/(1.+KHOM1A*PF*XC(J,K,1))+KHOM2*
     1(PF*XC(J,K,1))**2
      RG(J,K,2)=KHOM2*(PF*XC(J,K,1))**2
      RG(J,K,3)=RG(J,K,2)*DHOM2+(RG(J,K,1)-RG(J,K,2))*DHOM1
      RG(J,K,1)=-RG(J,K,1)
      RG(J,K,3)= RG(J,K,3)/T
    1 CONTINUE
      RETURN
      END
```

```
      SUBROUTINE HTMT(NSPH)
C
C      PROVIDES HEAT TRANSPORT PARAMETERS TO MODELS
C
      DIMENSION X(10)
      DIMENSION SH(5)
      COMMON/TEIM2/T,P,X,NSP,PFI
      COMMON/PELL2/ PR,SH,AKS,SET,BETA,ALPHA
      COMMON/SYSTEM/DP,DT,AL,GS,THI
      COMMON/CONT/ALC,PMR,U,ALPHAC
      COMMON/PHASE2/ALS,ALF,HVAV,PMR2,ALPHAS,ALPHAF
      COMMON/PROPS/CP,AMU,AKF
C
C      HP,B,GAM,THE FROM YAGII+KUNII/DEWASCH+FROMENT
C
C      HP IS CONTACT COEFF.(W/M2/K)
C
C      NSPH=1,SPHERICAL PELLETS
C
C      DP= PELLET DIAMETER
C
C      DPP= EQUIVALENT SPHERE DIAMETER
C
      E= 0.5
      IF(NSPH.EQ.1) GO TO3
      AV= (1.0-ALPHA + BETA)*4.0/(1.0-ALPHA)/DP/BETA
      DPP= 6.0/AV
    3 CONTINUE
      HP= 23.2
      B=1.0
      IF(ALPHA.NE.0.0) B=0.72
      GAM= 1.0-ALPHA
      THE= 0.050
      PR= CP*AMU/AKF
      SIG= 2.2HE-07
      REP=DP*GS/AMU
C     RADIAL PELLET NUMBER
      PMR=4.0*(19.4*(DP/DT)**2+1.0)
      V=REP**0.333*PR**0.333
      Y=REP**0.80*PR**0.40
C       CONTINUOUS MODEL WALL HEAT TRANSFER COEFF.
      IF(NSPH.EQ.1) GO TO 1
C     CYLINDERS
      ALPHAC= AKF*(2.58*V+0.094*Y)/DP
      REP= REP*DPP/DP
      GO TO 2
    1 CONTINUE
C     SPHERES
      AV= 6.0/DP
      ALPHAC= AKF*(0.203*V+0.22*Y)/DP
      DPP= DP
    2 CONTINUE
      V=DPP*THI/(1.0-THI)/AKF
      REP=REP*THI/(1.0-THI)
C     SOLID/FLUID FILM HEAT TRANSFER
      HV=(0.5*REP**0.5 +0.2*REP**0.667)*PR/V
      T3=T**3
       V=CP*GS*DP/PMR
       V= V/THI
      Y=SIG*T3/(1.0+THI/(1.-THI)/2.0*(1.-E)/E)
C     EFFECTIVE FLUID RADIAL CONDUCTIVITY
      ALF= THI*(AKF*V+Y*B*DP)
      ARS=E*T3*SIG/(2.0-E)
C     EFFECTIVE SOLID RADIAL CONDUCTIVITY
      ALS=B*(1.-THI)/(GAM/AKS+1./11./THE*HP*DP/AKF+ARS*DP/AKF))
      ALC= ALF+ALS
      PMR2= PMR
      U= 1.0/(1.0/ALPHAC + DT/8.0/ALC)
      HVAV= HV*AV*(1.0-THI)
C       2-PHASE PARAMETERS AFTER DEWASCH+FROMENT(1971)
      ALPHAS= ALS/ALC*ALPHAC
      ALPHAF= ALF/ALC*ALPHAC
      RETURN
      END
```

```
      SUBROUTINE PROPS(T,P,X,NSP)
C
C     EVALUATES PHSYICAL PROPERTIES AT INLET CONDITIONS
C
C     THIS ROUTINE ASSUMES THAT FEED IS MIXTURE OF NITROGEN AND
C     STEAM
C     X(I) IS MOLE FRACTION OF   I
C
C     X(1) = NITROGEN
C
C     X(2)= H2O(VAPOUR)
C
C     METHOD...
C     CP FROM HOUGEN+ RAGATZ POLYNOMIALS.
C      VISCOSITY CORRELATED BY SUTHERLAND EQN. USING DATA OF PERRY
C     KF=ASSUMES PRANDTL NO. IS NOT FIT)
C
C     MIXTURE RULES.....
C     CP= CP(I)*X(I)+ CP(J)*X(J)+
C     VISCOSITY-  WILKE EQUATION
C     KF=  BROMLEY EQUATION
C           REFERENCE...REID+SHERWOOD
C
C     NOTE... IN BROMLEY EQN. AI IS ASSUMED INVARIAT WITH T
C
C     UNITS......
C     CP= J/KG/K
C     AMU= KG/M/SEC
C     AKF= W/M/SEC
C
C     NOTE....
C     HOLTON(1975) USED
C     KF=0.04    ,CP= 1000.0
C     AMU=1.05E-05 + 3.08E-08*T
C     AND THIS GIVES PR= 0.5625 AT 400K
C
      DIMENSION X(NSP)
      DIMENSION ACP(2),KF(2),U(2)
      REAL KF
      COMMON/PROPS/ CP,AMU,AKF
      S1= 211.48
      S2= 888.50
      PR1= 0.74
      PR2= 0.78
      A12= 1.053493
      A21= 0.87343
      TT= T**1.5
      ACP(1)= 6.903-0.3753E-03*T+0.1930E-05*T**2
      ACP(2)= 7.70+0.4594E-03*T+0.2521E-05*T**2
      CP= (ACP(1)*X(1) +ACP(2)*X(2))/(28.0*X(1)+18.0*X(2))*4.184*1000.0
      ACP(1)= ACP(1)*1000.0*4.184/28.0
      ACP(2)= ACP(2)*1000.0*4.184/18.0
      U(1)= 0.1702E-05*TT/(S1+T)
      U(2)= 0.2189E-05*TT/(S2+T)
      KF(1)= ACP(1)*U(1)/PR1
      KF(2)= ACP(2)*U(2)/PR2
      IF(X(1).EQ.1.0) GO TO 1
      AKF= KF(1)/(1.0+A12*X(2)/X(1)) + KF(2)/(1.0+A21*X(1)/X(2))
      TH12= (1.+SQRT(U(1)/U(2))*0.895424)**2/4.521555
      TH21= TH12*U(2)/U(1)*1.5556
      AMU= U(1)/(1.+X(2)*TH12/X(1))+U(2)/(1.+X(1)*TH21/X(2))
      GO TO 2
    1 CONTINUE
      AMU= U(1)
      AKF= KF(1)
    2 CONTINUE
      RETURN
      END
```

```
      SUBROUTINE RATE7(XC,R,NSP1,NR,N)
C
C     HETEROGENEOUS RATE FOR FULL BUTENE-BUTADIENE SYSTEM
C
C     PELLET MODEL WITHOUT FILM EFFECTS
C     PELLET IS ISOTHERMAL
C
      DIMENSION XB(7),RAV(7),SH(5)
      DIMENSION XC(NR,N,NSP1),R(NR,1,NSP1)
      DIMENSION X(10)
      DIMENSION AM(7)
      DIMENSION XCP(2,2,7),RT(2,2,7),ST(2,2,7),STO(2,2,7)
      DIMENSION ANETA(7),NSTART(2,2),F(1),DIR(2,2,7),RP(2,2)
      COMMON/ACC/ACC2,ACC3
      COMMON/SOLVE/IDIAG
      COMMON/REACT/ICO,INETA
      COMMON/TEMP/TT
      COMMON/DIFF/SETT
      COMMON/PELL/PRR,DPP,ALT
      COMMON/IDIV2/T,P,X,NSP,PEI
      COMMON/SYSTEM/DP,DT,AL,GS,THI
      COMMON/PELL2/ PP,SH,AKS,SET,BETA,ALPHAP
      COMMON/PROPS/CP,AMU,AKF
      COMMON/NEWT/ALPHA,ALPHA1
      COMMON/CC/ARS(2,2),AZS(2,2),BZS(2,2),BRS(2,2),XRS(2),WRS(2),WZS(2)
     1,PER(1,1)
      COMMON/DIFF2/ASH(7),DIR(7)
      DATA/AM/32.0,56.0,54.0,1.0,28.0,56.0,56.0/
      IDIAG= 0
      NSPEC= NSP1
      ALPHA= 0.4
      ALPHA1= 0.7
      NRP=2
      NZP=2
      NRPZ=1
      ICO=1
      INETA= 0
      ALT= BETA*DP/2.0
      ACC2= 0.7
      ACC3= 0.4
      SETT=SET
      NSTART(1,1)=1
      NSTART(1,2)= NRP-1
      NSTART(2,1)= 1
      NSTART(2,2)= NZP-1
      DPP= DP*(1.0-ALPHAP)
      PRR=PP
      DO 11 NS= 1,5
   11 ASH(NS)= SH(NS)
      ASH(6)= SH(2)
      ASH(7)= SH(2)
      DO 1 JJ= 1,NR
      TT= T*(1.0+XC(JJ,1,4))
C     DIFFUSIVITIES
      DIR(1)= 0.33E-06*SQRT(TT/32.0)
      DIR(2)= 0.42E-06*SQRT(TT/56.0)
      DIR(3)= 0.42E-06*SQRT(TT/56.0)
      DIR(4)= 0.952E-04 * 0.44E-06*TT
      DIR(5)= 0.33E-06*SQRT(TT/28.0)
      DIR(6)= DIR(2)
      DIR(7)= DIR(2)
C
C     CONVERSION OF WEIGHT FRACTION TO CONCENTRATION(KMOL/M3) AS USED
C     IN  PELLET MODEL
C     ASSUME AN2 (RESIDUAL) HAS A MOL. WT. OF 26.0(N2/H2O)
C
      VM= 22.4*TT/273.0/P
      AN2= 1.0-XC(JJ,1,1)-XC(JJ,1,2)-XC(JJ,1,3)-XC(JJ,1,5)
     1-XC(JJ,1,6)-XC(JJ,1,7)
      SUM= AN2/26.0+XC(JJ,1,1)/AM(1)+XC(JJ,1,2)/AM(2)+XC(JJ,1,3)/AM(3)
     1 + XC(JJ,1,5)/AM(5)+XC(JJ,1,6)/AM(6)+XC(JJ,1,7)/AM(7)
      DO 2 KK= 1,NSP1
    2 XB(KK)= XC(JJ,1,KK)/VM/AM(KK) /SUM
      XB(4)= TT/T-1.
      DO 6 J= 1,NRP
      DO 6 K= 1,NZP
      DO  6 NS= 1,NSP1
    6 XC(JJ,K,NS)= XB(NS)
      DO 12 J= 1,NRP
      DO 12 K= 1,NZP
      DO 12 NS= 1,NSP1
   12 ST(J,K,NS)= 0.0
      CALL PELL3(DER,XB,ANETA,NSPEC,ARS,BRS,AZS,BZS,XRS,NRP,NZP,NRPZ,RAV
     1,WRS,WZS,F,DR,RP,XCP,RT,ST,NSTART,NSP1,STO)
      DO 3 K= 1,NSP1
    3 R(JJ,1,K)= RAV(K)*AM(K)
    1 CONTINUE
      RETURN
      END
```

```
      SUBROUTINE PELL3(DER,XR,ANETA,NSPEC,ARS,BRS,AZS,BZS,XRS,NR,NZ,NRNZ
     1 ,RAV,WRS,WZS,F,DR,R,XC,RT,ST,NSTART,NSP1,STO)
      DIMENSION STO(NR,NZ,NSPEC)
C
C      O.C.  2D PELLET MODEL -GENERAL KINETICS.
C      WITHOUT FILM EFFECTS
C      SEVEN SPECIES
C
      DIMENSION ARS(NR,NR),BRS(NR,NR),WRS(NR),XRS(NR)
      DIMENSION AZS(NZ,NZ),BZS(NZ,NZ),WZS(NZ)
      DIMENSION DER(NRNZ,NRNZ)
      DIMENSION F(NRNZ)
      DIMENSION DR(NR,NZ,NSPEC),RT(NR,NZ,NSP1 ),XC(NR,NZ,NSP1)
      DIMENSION R(NR,NZ)
      DIMENSION XR(NSP1),ANETA(NSP1)
      DIMENSION RAV(NSP1)
      DIMENSION DD(3)
      DIMENSION ST(NR,NZ,NSPEC)
      DIMENSION NSTART(2,2)
      DIMENSION RS(1,1,7),XCS(1,1,7)
      COMMON/PELL/PB,DP,AL
      COMMON/DIFF/SET
      COMMON/TIME/T
      COMMON/REACT/ICO,INETA
      COMMON/SOLVE/IDIAG
      COMMON/TRANS/ALT,AM(7),TH
      COMMON/DIFF2/SH(7),DIR(7)
      COMMON/NEWT/ALPHA,ALPHA1
      COMMON/ACC/ACC2,ACC3
      COMMON/BUTD/AKBD(6),HBD(6)
      COMMON/TOUT/AKT(7),POWT(6),HRT(7)
      COMMON/COUT/AKC(7),POWC(6),HRC(7)
      COMMON/BUT1/AK1(7),POW1(6),HR1(7)
      COMMON/AISOM/AKIS(6),HIS(6)
      EXTERNAL RADER1,RADER2,RADER3
       EXTERNAL RADER6,RADER7
C     NSPEC=7
C      NSP1=7
      NS= NSP1
      IDER=0
      ACC= 0.01
      ALT= DP/AL
      ALT2=ALT**2
      DO 8 N=1,NSPEC
      XCS(1,1,N)= XR(N)
      AM(N)=DP/SQRT(DIR(N))/2.0
    8 CONTINUE
      NT= 4
      TH= SET*ALT2
C
C      SUBROUTINE SETUP(T) EVALUATES INFORMATION IN THE FOLLOWING
C     COMMON BLOCKS
C     /BUTD/
C     /TEUT/
C     /CEUT/
C     /BUT1/
C     /AISOM/
C
      CALL SETUP(T)
       NCOUNT=0
       NTOP= 15
   17 CONTINUE
       NCOUNT= NCOUNT+1
C
C     SOLUTION OF SET OF EQUATIONS FOR EACH SPECIES IN TURN
C
      TEST=0.0
      CALL AIPREW(RADER1,1,DER ,ARS,BRS,AZS,BZS,XRS,NR,NZ,F,NRNZ,XC,DR,D
     1D,NSPEC,TEST,R,XR,ST,NSTART,NSP1,STO)
      CALL BOUND3(1,XC,XR,ARS,AZS,NR,NZ,NSP1)
      CALL AIPREW(RADER2,2,DER ,ARS,BRS,AZS,BZS,XRS,NR,NZ,F,NRNZ,XC,DR,D
     1D,NSPEC,TEST,R,XR,ST,NSTART,NSP1,STO)
      CALL BOUND3(2,XC,XR,ARS,AZS,NR,NZ,NSP1)
      CALL AIPREW(RADER3,3,DER ,ARS,BRS,AZS,BZS,XRS,NR,NZ,F,NRNZ,XC,DR,D
     1D,NSPEC,TEST,R,XR,ST,NSTART,NSP1,STO)
      CALL BOUND3(3,XC,XR,ARS,AZS,NR,NZ,NSP1)
      CALL AIPREW(RADER6,6,DER ,ARS,BRS,AZS,BZS,XRS,NR,NZ,F,NRNZ,XC,DR,D
     1D,NSPEC,TEST,R,XR,ST,NSTART,NSP1,STO)
      CALL BOUND3(6,XC,XR,ARS,AZS,NR,NZ,NSP1)
      CALL AIPREW(RADER7,7,DER ,ARS,BRS,AZS,BZS,XRS,NR,NZ,F,NRNZ,XC,DR,D
     1D,NSPEC,TEST,R,XR,ST,NSTART,NSP1,STO)
      CALL BOUND3(7,XC,XR,ARS,AZS,NR,NZ,NSP1)
      IF(IDIAG.EQ.0) GOTO 100
C     DIAGNOSTIC PRINTOUT
      PRINT,ALPHA
      DO 101 N= 1,NSPEC
```

```
      IF(N.EQ.4) GO TO 102
      IF(N.EQ.5) GO TO 102
      PRINT,(XC(J,K,N),K= 1,NZ)
       PRINT,(XC(J,1,N),J= 1,NR)
  102 CONTINUE
  101 CONTINUE
  100 CONTINUE
      IF(TEST.LT.ACC2) ALPHA= ALPHA1
      IF(TEST.LT.ACC3) ALPHA= 1.0
C     CONVERGENCE TEST
       IF(TEST.LT.ACC) GO TO 18
       IF(NCOUNT.LT.NTOP) GO TO 17
C      APPLICATION OF BISECTION RULE
        DO 19 N= 1,NSPEC
       IF(N.EQ.4) GO TO 20
       IF(N.EQ.5) GO TO 20
      DO 19 J= NSTART(1,1),NSTART(1,2)
       DO 19 K= NSTART(2,1),NSTART(2,2)
        XC(J,K,N)= XC(J,K,N)+STO(J,K,N)/2.0
   19 IF(XC(J,K,N).LT.0.0) XC(J,K,N)= 0.0
   20 CONTINUE
       WRITE(6,200)
  200 FORMAT(11X,'BISECTION RULE OPERATED')
   18 CONTINUE
      NSTART(1,1)= 1
      NSTART(1,2)= 1
      NSTART(2,1)= 1
      NSTART(2,2)= 1
C
C     EVALUATION OF EFFECTIVENESS FACTOR
C     USE QUADRATURE FORMULA TO OBTAIN AVERAGE RATE
C
      CALL RATES(RS,XCS,NSPEC,1,1    ,NSP1,NSTART)
      NSTART(1,2)= NR
      NSTART(2,2)= NZ
      CALL RATES(RT,XC,NSPEC,NR,NZ    ,NSP1,NSTART)
      DO 30 N= 1,NS
   30 RS(1,1,N)= RS(1,1,N)*PB
      RS(1,1,4)= RS(1,1,4)/T
       DO 23 J= 1,NR
       DO 23 K= 1,NZ
      DO 22 N= 1,NS
   22 RT(J,K,N)= RT(J,K,N)*PB
   23 RT(J,K,4)= RT(J,K,4)/T
      DO 27 N= 1,NS
      H= 0.0
      DO29 K= 1,NZ
      G= 0.0
      DO 28 J= 1,NR
   28 G= G + RT(J,K,N)*WRS(J)
   29 H= H+ G*WZS(K)
      RAV(N)= H
      IF(INETA.EQ.1) GO TO 27
      ANETA(N)= RAV(N)/RS(1,1,N)
   27 CONTINUE
      RETURN
      END


      SUBROUTINE F2ISO (F,AZS,BZS,ARS,BRS,XRS,XC,R,NR,NZ,NSPEC,N,NRNZ,XB
C
C     SETS UP FUNCTION VECTOR FOR EACH SPECIES,FOR NEWTON PROCEDURE
C
     1,NSTART,NSP1)
      DIMENSION F(NRNZ),ARS(NR,NR),BRS(NR,NR),AZS(NZ,NZ),BZS(NZ,NZ)
      DIMENSION XRS(NR)
      DIMENSION XC(NR,NZ,NSP1 ),R(NR,NZ),XB(NSP1)
      DIMENSION NSTART(2,2)
      COMMON/TRANS/ALT,AM(7),TH
      COMMON/DIFF2/SH(7),DIR(7)
      DO 3 J= NSTART(1,1),NSTART(1,2)
      DO 3 K= NSTART(2,1),NSTART(2,2)
      L= (J-NSTART(1,1)+1)+(K-NSTART(2,1))*(NSTART(1,2)-NSTART(1,1)+1)
      RA= XRS(J)
      F(L)= AM(N)**2*R(J,K)
      DO 6 KZ=1,NZ
    6 F(L)=F(L)+TH    *BZS(K,KZ)*XC(J,KZ,N)
      DO 7 JR=1,NR
    7 F(L)= F(L)+BRS(J,JR)*XC(JR,K,N)
    3 CONTINUE
      RETURN
      END
      SUBROUTINE BOUND3(N,XC,XB,ARS,AZS,NR,NZ,NSP1)
C
C     BOUNDARY CONDITIONS
C
      DIMENSION XC(NR,NZ,NSP1),XB(NSP1),AZS(NZ,NZ),ARS(NR,NR)
      DO 32 K= 1,NZ
   32 XC(NR,K,N)= XB(N)
      DO 33 J= 1,NR
   33 XC(J,NZ,N)= XB(N)
       RETURN
      END
```

```
C
C
      SUBROUTINE AIMPNEW(RADER,N,DERI,ARS,BRS,AZS,BZS,XRS,NR,NZ,F,NRNZ,XC
     1,DR,DD,NSPEC,TEST,R,XB,ST,NSTART,NSP1,STO)
C
C     CARRIES OUT SPLIT NEWTON ITERATION PROCEDURE
C
      DIMENSION STO(NR,NZ,NSPEC)
      DIMENSION ST(NR,NZ,NSPEC),NSTART(2,2)
      DIMENSION XB(NSP1),XC(NR,NZ,NSP1),R(NR,NZ)
      DIMENSION F(NRNZ),DERI(NRNZ,NRNZ),DD(NRNZ)
      DIMENSION DR(NR,NZ,NSPEC),XRS(NR),ARS(NR,NR),BRS(NR,NR),AZS(NZ,NZ
     1),BZS(NZ,NZ)
      COMMON/TRANS/ALT,AR(7),TH
      COMMON/DIFF2/SH(7),DIR(7)
      COMMON/AISOM/AKIS(6),HIS(6)
      COMMON/BUT1/AK1(7),POW1(6),HR1(7)
      COMMON/CHUT/AKC(7),POWC(6),HRC(7)
      COMMON/THUT/AKT(7),POWT(6),HRT(7)
      COMMON/BUTO/AKBO(6),HBO(6)
      COMMON/TEMP/T
      COMMON/PELL/PR,DP,AL
      COMMON/NEWT/ALPHA,ALPHA1
C
C     CALL OF KINETIC AND FUNCTION EVALUATION ROUTINES
C
       CALL RADER(R,DR,XC,NSPEC,NR,NZ   ,NSP1,NSTART)
      CALL F2ISO (F,AZS,BZS,ARS,BRS,XRS,XC,R,NR,NZ,NSPEC,N,NRNZ,XB,NSTAR
     1T,NSP1)
      DO 1 J= NSTART(1,1),NSTART(1,2)
      DO1 K= NSTART(2,1),NSTART(2,2)
      JIT= (J-NSTART(1,1)+1)+(K-NSTART(2,1))*(NSTART(2,2)-NSTART(2,1)+1)
      DD(JIT)= F(JIT)
      DO 2NT=1,NSPEC
    2 DD(JIT)=DD(JIT)-DR(J,K,NT)*ST(J,K,NT)
    1 CONTINUE
      DO 3 J= NSTART(1,1),NSTART(1,2)
      DO3 K= NSTART(2,1),NSTART(2,2)
      KIT= (J-NSTART(1,1)+1)+(K-NSTART(2,1))*(NSTART(2,2)-NSTART(2,1)+1)
      DEL= 0.0
      DO 4J2= NSTART(1,1),NSTART(1,2)
      DO4K2= NSTART(2,1),NSTART(2,2)
      JIT= (J2-NSTART(1,1)+1)+(K2-NSTART(2,1))*(NSTART(2,2)-NSTART(2,1)+
     11)
    4 DEL= DD(JIT)*DERI(KIT,JIT) + DEL
      XC(J,K,N)= XC(J,K,N)-DEL*ALPHA
      IF(XC(J,K,N).LT.0.0) XC(J,K,N)= 0.0
      STO(J,K,N)= DEL*ALPHA
      IF(XC(J,K,N).EQ.0.0) GO TO 3
       Y=ABS(DEL/XC(J,K,N))
      IF(Y.GT.TEST) TEST=Y
    3 CONTINUE
      RETURN
      END
```

A.5.2 Coding for multiplicity analysis

Only the coding of the main search routine and one example subroutine are presented. The logic of the search routine should be clear from the flow diagram (Fig. A.5.3) and list of important variables (Table 5.3). The example subroutine was written for one of the simplest models used but illustrates the general approach.

Table A.5.3 - List of variables for multiplicity models

Computer Variable	Definition	Equivalent in text
AF	Pre exponential factor for each reaction	α_f
AS		α_s
BF	Adiabatic temperature rises for each reaction	β_f
BS		β_s
GF	Activation energies for fluid and solid phases	γ_f
GS		γ_s
H	Film heat transport group	H
AK	Film mass transport group	K
ET	Voidage	ε
AL	External cooling group	A
ZO	Product inlet concentration	Z_f^o
YS	Solid phase temperature	Y_s
YF	Fluid phase temperature	Y_f
XS	Solid phase concentration (reactant)	X_s
XF	Fluid phase concentration (reactant)	X_f
ZS	Solid phase concentration (product)	Z_s
ZF	Fluid phase concentration (product)	Z_f
YO	Coolant temperature	Y_o

All parameters are dimensionless

Fig A.5.3 - Logic diagram for multiplicity search coding

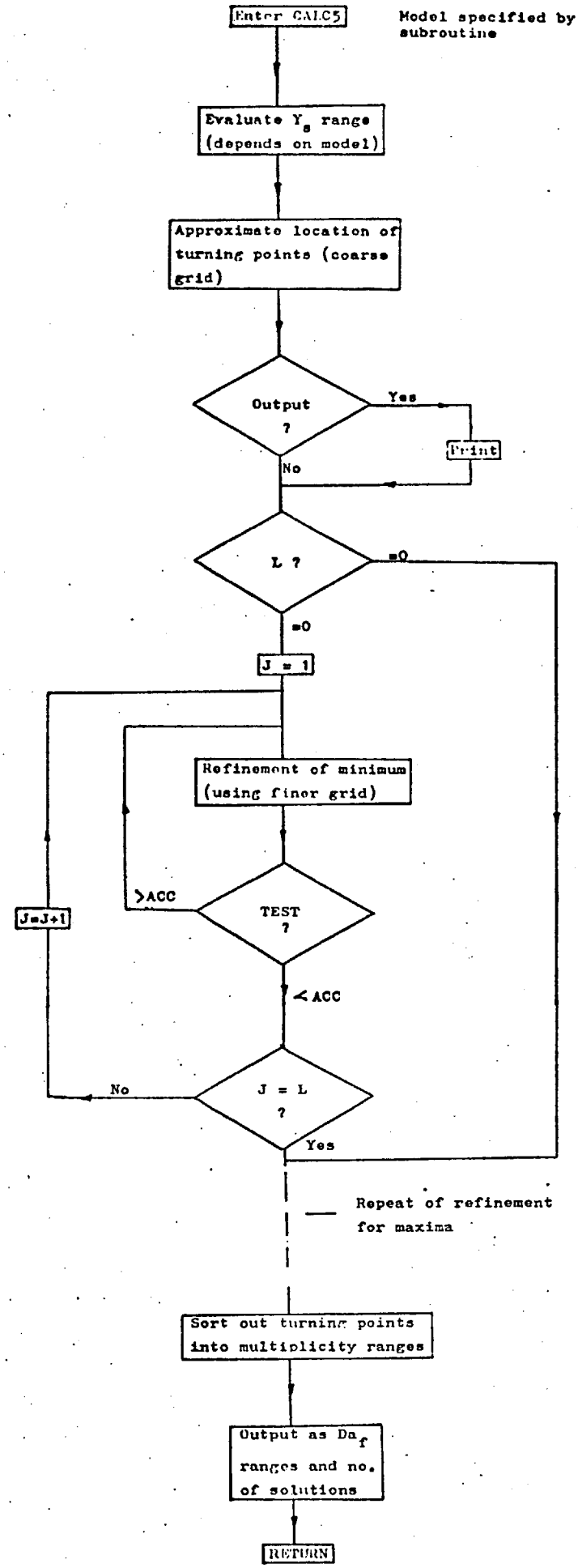

```
C
C*****F*****F*****F*****F*****F*****F*****F*****F*****F*****F*****F*****F**
C
C        NOTE
C     ALL CALC ROUTINES USE PARAMETERS DEFINED ON A 2 PHASE BASIS
C      I.E.  VOIDAGE IS AN EXPLICIT PARAMETER FOR EVEN ONE PHASE
C      MODELS.
C      TO CONVERT  AS(1-PHASE)= AS(2-PHASE)*(1.ET)
C        AF(1-PHASE)= AF(2-PHASE)*ET
C*****F*****F*****F*****F*****F*****F*****F*****F*****F*****F*****F*****F**
      SUBROUTINE CALC5(CALC2)
C
C     MULTIPLICITY SEARCH PROGRAM
C
C     USES CALC2 TO EVALUATE AF = F(YS), THEN SEARCHES FOR TURNING
C     POINTS IN THIS FUNCTION
      COMMON/FAIL/ NFAIL,IFAIL,CRIT
      COMMON/CONT/ICO
      COMMON/AXIAL/AF
      COMMON/FLOW/DELT,YI,YI
      COMMON/CONT/IDIAG
      COMMON/HELP/DADY
      COMMON/OUT/AS,GS,AK,BS,BF,N,Z0,ET,GF,AL,YO
      COMMON/CALC/NCALC
      COMMON/RUN/MJ,DAMIN,DAMAX
      COMMON/ATTACK/ADRD(20),M,N
      COMMON/START/NSTART
      DIMENSION AA(10)
      DIMENSION ST(4,50),AT(4,50)
      DIMENSION NC(10),TS(10)
      DIMENSION QT(2,50),PT(2,50)
      EXTERNAL CALC2
      NSTART=1
      ACC= 0.01
      M=0
      NST=4
      NCO=0
       L=0
       MT=0
      NI=0
      MX= MJ**4/10
     BMAX= BF
C
C     EVALUATION OF YS RANGE FOR SEARCH
C
      IF(NCALC.EQ.16) YGO=1.0
      IF(NCALC.EQ.16) BINC= -0.999
       IF(NCALC.EQ.16) AINC= BINC/FLOAT(MJ-1)
       IF(NCALC.EQ.16) GO TO 800
       IF(BS.GT.BF) BMAX= BS
      BINC= BMAX
       AINC= BMAX/FLOAT(MJ-1)
       IF(NCALC.EQ.4) GO TO 53
       IF(NCALC.EQ.12)GO TO 52
       IF(NCALC.EQ.4) GO TO 52
      AINC= (BF+BS)/FLOAT(MJ-1)
       BINC= BS*AK/N/(1.+(1.-ET)*AK)+(Z0*BF+AK*(1.-ET)*(BS+BF)/(1.+(1.-E
     1T)*AK)+AL*ET+YO+1.)/(AL*ET+1.)-1.0
   53 CONTINUE
       BST= BINC
      YCOR= 1.0+ BINC/2.0
      YS= 1.0+BINC
      CINC= BINC/10.0
   50 CONTINUE
      YS= YS-CINC
      CALL CALC2(YS,AF)
       IF(NFAIL.EQ.1) GO TO 1000
      IF(YS.LT.YCOR) BINC= BST
      IF(YS.LT.YCOR) GO TO 51
      IF(CINC.LT.0.001*BINC) GO TO 51
      I F(AF.LT.0.0) GO TO 50
       IF(AF.GT.0.0) YS= YS+ CINC
       IF(AF.GT.0.0) CINC= CINC/10.0
       IF(AF.GT.0.0) GO TO 50
   51 CONTINUE
      BINC= YS-1.0
      AINC= BINC/FLOAT(MJ-1)
   52 CONTINUE
     NSTART=0
     YGO= 1.0
     IF(BF.LT.0.0.AND.BS.LT.0.0) GO TO 800
     IF(BF.LT.0.0) YGO= 1.+BF
     IF(BF.LT.0.0) AINC= AINC-BF/FLOAT(MJ-1)
     IF(BS.LT.0.0) YGO= 1.+BS
     IF(BS.LT.0.0) AINC= AINC-BS/FLOAT(MJ-1)
  800 CONTINUE
C
C     COMMENCE SEARCH PROCEDURE
C
      DO 1 J= 1,MJ
       YS= YGO+ FLOAT(J-1)*AINC
       IF(J.EQ.1) GO TO 7
       AFS= AF
    7 CONTINUE
      CALL CALC2(YS,AF)
      IF(NFAIL.EQ.1) GO TO 1000
```

```
      IF(J.EQ.1) GOTO 8
       IF(J.EQ.2) GO TO 9
       D1=D2
       P3=P2
    9 D2=AF-A1
       P2=P1
    8 A1=AF
       P1= DADY
      IF(J.EQ.1) GO TO 1
      IF(J.EQ.2) GO TO 1
       ZZ= P1/P2
       ZZ= P1/P3
       IF(AF .LT.0.0.AND.J.GT.MM) GO TO 18
       IF(AFS.LT.0.0) GO TO 35
      IF(D1.GT.0.0.AND.D2.LT.0.0.AND.ZZ.LT.0.0) M= M+1
C     TURNING POINTS = MAXIMUMS
      IF(D1.GT.0.0.AND.D2.LT.0.0.AND.ZZ.LT.0.0) AT(2,M)= AFS
      IF(D1.GT.0.0.AND.D2.LT.0.0.AND.ZZ.LT.0.0) ST(2,M)= YS-AINC
      IF(D1.GT.0.0.AND.D2.LT.0.0.AND.ZZ.GE.0.0) GO TO34
       GO TO 35
   34 CONTINUE
       MT= MT+1
       AT(3,MT)= 1.0E+06*EXP(GF)
       ST(3,MT)= YS-AINC
   35 CONTINUE
C     TURNING POINTS = MINIMUMS
       IF(D1.LT.0.0.AND.D2.GT.0.0.AND.ZZ.LT.0.0) L= L+1
       IF(D1.LT.0.0.AND.D2.GT.0.0.AND.ZZ.LT.0.0) AT(1,L)= AFS
       IF(D1.LT.0.0.AND.D2.GT.0.0.AND.ZZ.LT.0.0) ST(1,L)= YS-AINC
       IF(D1.LT.0.0.AND.D2.GT.0.0.AND.ZZ.GE.0.0) GO TO 37
       GO TO 36
   37 CONTINUE
       NT= NT+1
       AT(4,NT)= -1.0E06*EXP(GF)
       ST(4,NT)= YS-AINC
   36 CONTINUE
    1 CONTINUE
   18 CONTINUE
       NMT= MT+ MT
       IF(L.EQ.0.OR.M.EQ.0.AND.NMT.EQ.0) DAMAX= -1.0
       IF(L.EQ.0.OR.M.EQ.0.AND.NMT.EQ.0) WRITE(6,100)
  100 FORMAT(' UNIQUE SOLUTIONS ')
C     DIAGNOSTIC PRINTOUT
       PRINT,M,L,MT,NT
       IF(IDIAG.EQ.0) GO TO 310
      IF(L.EQ.0) GO TO 300
       PRINT,((ST(1,LA),AT(1,LA) ),LA= 1,L)
  300 CONTINUE
      IF(M.EQ.0) GO TO 301
       PRINT,((ST(2,LA),AT(2,LA) ),LA= 1,M)
  301 CONTINUE
       IF(MT.EQ.0) GO TO 302
       PRINT,((ST(3,LA),AT(3,LA) ),LA= 1,MT)
  302 CONTINUE
       IF(NT.EQ.0) GO TO 303
       PRINT,((ST(4,LA),AT(4,LA) ),LA= 1,NT)
  303 CONTINUE
  310 CONTINUE
       IF(L.EQ.0.OR.M.EQ.0.AND.NMT.EQ.0) GO TO 2
   30 CONTINUE
      SINC= AINC
C
C     REFINEMENT OF TURNING POINTS, USING FINER GRID
C
       IF(L.EQ.0) GO TO 307
C     MINIMUMS
       DO 20 LA= 1,L
      NCO=0
      AINC= SINC
       IF(AT(1,LA).LT.0.0) GOTO 20
  500 DINC= AINC/10.0
      NCO = NCO+1
       YY= ST(1,LA)-AINC
       YST= YY
       CALL CALC2(YY,AFST)
        IF(NFAIL.EQ.1) GO TO 1000
      DO 21 JL= 1,20
       YY= YY+ DINC
       CALL CALC2(YY,AF)
      IF(NFAIL.EQ.1) GO TO 1000
       IF(AF.LT.AFST) YST= YY
       IF(AF.LT.AFST) AFST= AF
   21 CONTINUE
       DIFF= ABS((AFST-AT(1,LA))/AT(1,LA))
      ST(1,LA)= YST
       AT(1,LA)= AFST
       IF(NCO.GE.10) GO TO 20
C     CONVERGENCE TEST
      IF(DIFF.GT.ACC) GO TO 500
   20 CONTINUE
  307 CONTINUE
   22 CONTINUE
       IF(M.EQ.0) GO TO 306
C     MAXIMUMS
       DO 23 MM= 1,M
      NCO=0
      AINC= SINC
       IF(AT(2,MM).LT.0.0) GOTO 23
  501 DINC= AINC/10.0
```

```
      NCO= NCO+1
       YY= ST(2,MM)-AINC
       YST= YY
       CALL CALC2(YY,AFST)
        IF(NFAIL.EQ.1) GO TO 1000
       DO 24 J= 1,20
       YY= YY+ DINC
       CALL CALC2(YY,AF)
      IF(NFAIL.EQ.1) GO TO 1000
       IF(AF.GT.AFST) YST= YY
       IF(AF.GT.AFST) AFST= AF
   24 CONTINUE
       DIFF= ABS((AFST-AT(2,MM))/AT(2,MM))
      ST(2,MM)= YST
      AT(2,MM)= AFST
       IF(NCO.GE.NST) GO TO 23
C     CONVERGENCE TEST
      IF(DIFF.GT.ACC) GO TO 501
   23 CONTINUE
  306 CONTINUE
S
C     COMPLETION OF SEARCH
C
C
C     SORTING OF TURNING POINTS INTO MULTIPLICITY ZONES
C
       IF(M.EQ.0) GO TO 48
       AMAX= AT(2,1)
       IF(M.EQ.1) GO TO 48
      DO 19 NB= 2,M
      IF(AT(2,NB).GT.AMAX) AMAX=AT(2,NB)
   19 CONTINUE
       DO 11 NB= 1,M
      IF(AT(2,NB).GT.0.0) GO TO 12
       DO 13 KM= NB,M-1
       ST(2,KM)= ST(2,KM+1)
   13 AT(2,KM)= AT(2,KM+1)
       M= M-1
   12 CONTINUE
   11 CONTINUE
   48 CONTINUE
      LN=0
      DO 10 NB= 1,L
       IF(AT(1,NB).LT.0.0) LN= LN+1
       IF(AT(1,NB).LT.0.0) NC(LN)= NB
       IF(AT(1,NB).LT.0.0) TS(LN)= ST(1,NB)
   10  IF(AT(1,NB).LT.0.0) AT(1,NB)= 0.0
      IF(LN.EQ.0.OR.LN.EQ.1) GO TO 16
       IF(M.EQ.0) GO TO 40
      DO 40 NL= 1,LN-1
      LC= 0
      DO 14 NB= 1,M
      IF(ST(2,NB).GT.TS(NL).AND.ST(2,NB).LT.TS(NL+1)) LC=LC+1
   14 CONTINUE
      IF(LC.EQ.1) GO TO 40
      DO 15 J= NC(NL),L-1
      ST(1,J)= ST(1,J+1)
   15 AT(1,J)= AT(1,J+1)
      L= L-1
   40 CONTINUE
   16 CONTINUE
       NS= M+L
       DO 41 J= 1,L
   41 AA(J)= AT(1,J)
       IF(M.EQ.0) GO TO 308
       DO 42 J= 1,M
   42 AA(J+L)= AT(2,J)
  308 CONTINUE
       NMAX= NT
       IF(NT.GT.NMAX) NMAX= NT
       NT= NMAX
        IF(NT.EQ.0) GO TO 200
      IF(NT.EQ.1) IFAIL=1
        IF(NT.EQ.1) WRITE(6,101)
  101 FORMAT(9 ERROR - NT=18)
       IF(NT.EQ.1.AND.ICO.EQ.0) GO TO 200
       NS= NS+1
       AA(NS)= 1.0E+06 *EXP(GF)
       M= M+1
  200 CONTINUE
       NS= M+L
       NM= NS
       NS= NS+1
       N= 1
   43 CONTINUE
       NST=1
       AORD(N)= AA(1)
       IF(NN.EQ.1) GO TO 46
       DO 44 J= 2,NN
       IF(AA(J).LT.AORD(N)) NST= J
       IF(AA(J).LT.AORD(N)) AORD(N)= AA(J)
   44 CONTINUE
       IF(NST.EQ.NN) GO TO 47
       DO 45 J= NST,NM-1
   45 AA(J)= AA(J+1)
   46 CONTINUE
   47 NN= NN-1
       N= N+1
        IF(NN.NE.0) GO TO 43
```

```
    2 CONTINUE
 1000 CONTINUE
      RETURN
      END
C
      SUBROUTINE CALC2(YS,AF)
C     SIMPLE TWO TANKS MODEL FOR A TO B TO C
C     OBTAINS AF AND DADY FOR GIVEN YS
      COMMON/OUT/AS,GS,AK,BS,BF,H,ZO,ET,GF,AL,YO
      COMMON/FLUID/ZF,YF,ZS
       COMMON/HELP/DADY
       ZO= ZO
      P= AS*EXP(-GS/YS)
      XX= (H/AK*(1.+(1.-ET)*AK)*P+H)*YS-BS*P
      YY= H/AK*(1.+(1.-ET)*AK)*P+H
      YF= XX/YY
      XX= YS*(1.-ET)*H-YF*(1.+(1.-ET)*H)+1.0
      YY= YF*((1.-ET)*H*BF/BS+1.+(1.-ET)*H)-YS*(1.-ET)*H*(BF/BS+1.)-1.-Z
     10*HF
       XX= XX- AL*ET*YF+AL*ET*YO
       YY= YY-AL*ET*YO+AL*ET*YF
      ZF= -YY/HF
      Q= XX/YY
      AF= Q*EXP(GF/YF)/ET
       DP= AS*EXP(-GS/YS)*GS/YS**2
       XX= H/AK*(1.+(1.-ET)*AK)*P+H
       YY= XX+YS*H/AK*(1.+(1.-ET)*AK)*DP-BS*DP-YF*(H/AK*(1.+(1.-ET)*AK)*
     1DP)
       DYF= YY/XX
      YY= DYF*(1.+(1.-ET)*H+(1.-ET)*H*BF/BS*Q+(1.-ET)*H*Q+AL*ET*Q+AL*ET*
     1Q)-
     1(1.-ET)*H-Q*(1.-ET)*H*BF/BS-Q*(1.-ET)*H
      XX=YS*(1.-ET)*H*(BF/BS+1.)+AL*ET*YO+1.+ZO*GF-YF*((1.-ET)*H*(BF/BS+
     11.)+1.+AL*ET)
       DQ= YY/XX
       DADY= (DQ-DYF*AF*ET*EXP(-GF/YF)*GF/YF**2)/ET/EXP(-GF/YF)
      XS= H*(YF-YS)*(1.+(1.-ET)*AK)/BS/AK+1.0
      ZS= ZF*(1.-XS)/(1.+(1.-ET)*AK)
       RETURN
      END
```

REFERENCES

Aiba, S., A.E. Humphrey and N.F. Millis (1973),
'Biochemical Engineering ' (2nd Edition), Academic Press (New York).

Argo, W.B. and J.M. Smith (1953),
Chem. Eng. Prog., 49, p.443.

Aris, R. (1965),
'Introduction to the analysis of chemical reactors', Prentice-Hall (Englewood Cliffs, N.J.).

Barker, J.J. (1965),
Ind. Eng. Chem., 57, (4), p.43.

Beek, J. (1962), in
'Advances in Chemical Engineering', 3, (Ed: T.B. Drew and J.W. Hoopes) Academic Press (New York).

Benson, S.W. (1968),
'Thermochemical kinetics', J. Wiley (New York).

Bernard, R.A. and R.H. Wilhelm (1950),
Chem. Eng. Progr., 46, p.233.

Beskov, V.S., V.N. Bibin, O.A. Malnovskay and B.I. Popov (1972),
Kinetics and Catalysis, 13, p.1176.

Bhattacharyya, D., and D.C.T. Pei (1975),
Chem. Eng. Sci., 30, p.293.

Bibin, V.N. and B.I. Popov (1969),
Kinetics and Catalysis, 10, p.1091.

Blundell, A. and G. Skirrow (1958),
Proc. Roy. Soc., A244, p.331.

Calderbank, P.H. and L.A. Pogorski (1957),
Trans. Inst. Chem. Engrs., 35, p.195.

Carberry, J.J. (1976),
'Chemical and Catalytic Reaction Engineering', Mc.Graw Hill (New York).

Carberry, J.J. and M.W. Wendel (1963),
A.I.Ch.E.J., 9, p.129.

Carey, G.F. and B.A. Finlayson (1975),
Chem. Eng. Sci., 30, p.587.

Carnham, B., H.A. Luther and J.O. Wilkes (1969),
'Applied Numerical Methods', J. Wiley (New York).

Cartlidge, J., L. McGarth and S.H. Wilson (1975),
Trans. Inst. Chem. Engrs., 53, p.117.

Corrie, J. (1972),
Ph.D. Thesis, Imperial College.

Coulson, J.M. and J.F. Richardson (1968),
'Chemical Engineering - Vol.2' 2nd Edition, Pergamon (Oxford).

Denbigh, K.G. and J.C.R. Turner (1971),
'Chemical Reactor Theory' (2nd Edition), Cambridge Univ.Press (Cambridge).

DeWasch, A.P. and G.F. Froment (1971),
Chem. Eng. Sci., 26, p.629.

DeWasch, A.P. and G.F. Froment (1972),
Ibid., 27, p.567.

Edwards, W.M., F.L. Worley and D. Luss (1973),
Chem. Eng. Sci., 28, p.1479.

Eigenburger, G. (1972),
Chem. Eng. Sci., 27, p.1909.

Elanashie, S.S. (1975),
Chem. Eng. Sci., 30, p.1297.

Enga, F. (1976),
Johnson-Mathey Limited, Private Communication.

England, R. and D.J. Gunn (1970),
Trans. Inst. Chem. Engrs., 48, T265.

Fahien, R.W. and J.M. Smith (1955),
A.I.Ch.E.J., 1, p.28.

Ferguson, N.B. and B.A. Finlayson (1972),
A.I.Ch.E.J., 18, p.1053.

Finlayson, B.A. (1974),
'Methods of weighted residuals and collocation priciples'
Academic Press (New York).

Firth, J.G. and H.B. Holland (1969),
Trans. Farad. Soc., 65, p.1121.

Friedly, J.C. (1972),
'Dynamic behaviour of processes', Prentice Hall (Englewood Cliffs, N.J.).

Froment, G.F. (1967),
Ind. Eng. Chem., 59, (2), p.18.

Froment, G.F. (1972),
Proc. 2nd. Int. Symp. on Chem. Reaction Eng. (Amsterdam).

Gabbay, D.S. (1969),
Ph.D. Thesis, Imperial College.

Gorliek, A.G., N.V. Kandralenko and V.I. Trofimov (1973),
Chem. Eng. Sci., 28, p.1358.

Gunn, D.J. (1969),
Trans. Inst. Chem. Engrs., 47, T351.

Halladay, J.B. and R.V. Marazek (1973),
J. Cat., 28, p.221.

Hanratty, T. (1954),
Chem. Eng. Sci., 3, p.209.

Harriot, P. (1975),
Chem. Eng. J., 10, p.65.

Hessam, K. (1971),
Ph.D. Thesis, London University.

Hlavacek, V. (1970),
Ind. Eng. Chem., 62, (7), p.8.

Hlavacek, V., M. Kubicek and K. Visnak (1972),
Chem. Eng. Sci., 27, p.719.

Hochstim, A.R. (1969),
'Bibliography of Chemical Kinetics and Collision Processes',
Plenum Press (New York).

Holton, R.D. (1975),
Ph.D. Thesis, Imperial College.

Hougen, O.A., K.M. Watson and R.A. Ragatz (1954),
'Chemical process principles - part 2', J. Wiley (New York).

Kern, D.Q. (1950),
'Process Heat Transfer', McGraw Hill (New York).

Kerr, J.A. and E. Ratajack (1972),
'Second supplementary tables of bimolecular gas reactions',
Univ. of Birmingham - O.S.T.I.

Keulks, G.W. and C. Daniel (1972),
J. Cat., 24, p.529.

Keulks, G.W., J.P. Monnier and C. Daniel (1973),
J. Cat. 31, p.360.

Kirk - Othmer (1967),
'Encylopedia of Chemical Technology' 2nd Edition, (Ed: A. Standen),
J. Wiley (New York).

Kúnii, D. and T. Furusawa (1972),
Chem. Eng. J., 4, p.268.

Kuo, J.C.W., C.R. Morgan and H.G. Lassen (1971),
Soc. Auto. Engrs. Trans. No. 710289.

La Cava, A.I. (1977),
Ph.D. Thesis, Imperial College.

Lam, C.W. (1975),
M.Sc. Report, Imperial College.

Levenspiel, O. (1962),
'Chemical Reactor Engineering', Wiley (New York).

Lewis, B. and G. Von Elbe (1961),
'Combustion, flames and explosions of gases', Academic Press (New York).

Liu, S.L. and N.R. Amundson (1962),
Ind. Eng. Chem. (Fund), 1, p.200.

Lord, H.A., E.A. Sondreal, R.H. Kadlec and D.J. Patterson (1973),
Soc. Auto. Engrs. Trans. No. 730203.

Lozano, F.J. (1973),
M.Sc. Report, Imperial College.

Luss, D. and G.T. Chen (1975),
Chem. Eng. Sci., 30, p.1483.

Luss, D., J.S.Y. Ding and S. Sharma (1974),
Ind. Eng. Chem. (Fund), 13, p.76.

Mann, R.S. and K.W. Hahn (1969),
J. Cat. 15, p.329.

Mann, R.S. and M.K. Dosi (1973),
Ibid, 28, p.282.

Matsuura, T. and M. Kato (1967),
Chem. Eng. Sci., 22, p.171.

Mears, D.E. (1971),
J. Cat., 20, p.127.

Mears, D.E. (1976),
Ind. Eng. Chem. (Fund), 15, p.20.

McAdams, W.H. (1954),
'Heat Transmission', 3rd Edition, McGraw Hill (New York).

McCain, C.C. and G.W. Godin (1964),
Nature, 202, p.692.

McCain, C.C. (1976), Private communication
(B.P. Chemicals).

McGreavy, C., and D.L. Cresswell (1969),
Canad. J. Chem. Eng., 47, p.583.

McGreavy, C. and J.M. Thornton (1970),
Canad. J. Chem. Eng., 48, p.187.

McGuire, M.L. and L. Lapidus (1965),
A.I.Ch.E.J., 11, p.85.

Mulchahy, M.F.R. (1973),
'Gas Kinetics', Nelson (London).

Olbrich, W.E. (1970),
Proc. 'Chemica 70'. Sect. 6A, p.101, Butterworths (London).

Olbrich, W.E. and O.E. Potter (1972),
Chem. Eng. Sci., 27, p.1723.

O'Neil, S.P., M.D. Lilly and P.N. Rowe (1971),
Chem. Eng. Sci., 26, p.173.

Orhon, M., J. Corrie and D.L. Trimm (1973),
Chem. Eng. J., 6, p.74.

Paterson, W.R. and D.L. Cresswell (1971),
Chem. Eng. Sci., 26, p.605.

Perry, J.H. (1963),
'Chemical Engineers Handbook' 4th Edition, McGraw Hill (New York).

Ratajack, E. and A.F. Trotman-Dickenson (1967),
'Tables of bimolecular gas reactions', N.B.S.-N.R.D.C. (New York).

Ratajack, E. and A.F. Trotman-Dickenson (1969),
'Supplementary Tables of bimolecular gas reactions' U.W.I.S.T.-O.S.T.I.

Ray, W.H., A. Uppal and A.B. Poore (1974),
Chem. Eng. Sci., 29, p.1330.

Reid, R.C. and T.K. Sherwood (1966),
'The properties of gases and liquids : their estimation and correlation',
2nd Edition, McGraw Hill (New York).

Rhee, H.K., P.R. Lewis and N.R. Amundson (1974),
Ind. Eng. Chem. (Fund), 13, p.317.

Satterfield, C.N. (1970),
'Mass transfer in Heterogeneous Catalysis', M.I.T. Press (Cambridge).

Schmitz, R.A. (1975), in
'Advances in Chemistry Series', No. 148, p.156, A.C.S. (New York).

Schmitz, R.A. and N.R. Amundson (1963),
Chem. Eng. Sci., 18, p.265, 391, 415.

Schmitz, R.A. and S.A. Vejtasa (1970),
A.I.Ch.E.J., 16, p.410.

Schulmann, T.W. and V. Voss (1934),
Fuel, 13, p.249.

Shah, M. and D. Roberts (1974), in
'Advances in Chemistry Series' No. 133, p.259 A.C.S. (New York).

Shtern, V. Ya. (1964),
'The gas phase oxidation of hydrocarbons', Pergamon (Oxford).

Smith, J.M. (1970),
'Chemical Engineering Kinetics', 2nd Edition, McGraw Hill (New York).

Smith, J.M. (1973),
Chem. Eng. J., 5, p.103.

Sorenson, J.P., E.W. Guertin and W.E. Stewart (1973),
A.I.Ch.E.J., 19, p.969.

Uppal, A., W.H. Ray and A.B. Poore (1974),
Chem. Eng. Sci., 29, p.967.

Valstar, J.M., P.J. Van den Berg and J. Oyserman (1975),
Chem. Eng. Sci., 30, p.723.

Van den Bosch, B. and D. Luss (1977),
Chem. Eng. Sci., 32, p.203.

Vardanyan, I.A., G.A. Sachyan and A.B. Nabbandyan (1974),
Comb. Flame, 22, p.153.

Ibid. (1971), 17, p.315.

Villadsen, J.V. and W.E. Stewart (1967),
Chem. Eng. Sci., 22, p.1483.

Wei, J. (1975), in
'Advances in Chemistry Series' no. 148, p.1, A.C.S. (New York).

Weisz, P.B. and J.S. Hicks (1962),
Chem. Eng. Sci., 17, p.265.

Whitaker, S. (1972),
A.I.Ch.E.J., 18, p.361.

Yagii, S. and D. Kunii (1957),
A.I.Ch.E.J., 3, p.373.

Yagii, S. and N. Wakao (1959),
Ibid, 5, p.79.

Yagii, S. and D. Kunii (1960),
Ibid, 6, p.97.

Yeung, S.K. (1976),
M.Sc. Report, Imperial College.

Young, L.C. and B.A. Finlayson (1973),
Ind. Eng. Chem. (Fund), 12, p.412.